THESIS

LIBRARY
Michigan State
University

This is to certify that the

dissertation entitled

POWER CONTROL AND INTERFERENCE MANAGEMENT IN A
SPREAD-SPECTRUM CELLULAR MOBILE RADIO SYSTEM

presented by

Hossein Alavi

has been accepted towards fulfillment
of the requirements for

Doctor of Philosophy degree in Electrical Engineering

R W Nutter
Major professor

Date March 19, 1984

MSU is an Affirmative Action/Equal Opportunity Institution

O-12771

MSU
LIBRARIES

RETURNING MATERIALS:
Place in book drop to remove this checkout from your record. FINES will be charged if book is returned after the date stamped below.

POWER CONTROL AND INTERFERENCE MANAGEMENT IN A
SPREAD-SPECTRUM CELLULAR MOBILE RADIO SYSTEM

By

Hossein Alavi

A DISSERTATION

Submitted to
Michigan State University
in partial fulfillment of the requirements
for the degree of

DOCTOR OF PHILOSOPHY

Department of Electrical Engineering and Systems Science

1984

ABSTRACT

POWER CONTROL AND INTERFERENCE MANAGEMENT IN A SPREAD-SPECTRUM CELLULAR MOBILE RADIO SYSTEM

By

Hossein Alavi

Spread-spectrum multiple-access systems usually require some form of power control when the terminals are mobile, in order to prevent signals from nearby units from swamping out more distant signals. Power control is even more essential when the system is a cellular one, due to the interference from cell to cell. Here we report on a power control system that permits the signal-to-interference ratio of every signal to be equalized within each cell and, optionally, from cell to cell throughout the system, for both upstream (mobile to base station) and downstream (base station to mobile) signals. The method is introduced mathematically and results of a computer simulation are presented. Downstream balancing eliminates the so-called "corner effect", and upstream balancing eliminates the so-called "near-far effect".

We conclude that in-cell balancing is essential for the efficient operation of the system, and is mathematically easy to accomplish. By comparison, cell-to-cell balancing has a more marginal effect on the

system efficiency and is more difficult to perform; but its use may still be advisable in systems where the traffic load is distinctly nonuniform from cell to cell.

Results show that when practical implementations are considered, the downstream balancing can easily be accomplished with full dynamic range. Upstream balancing, however, may be very hard to implement due to very high values of dynamic range required of the mobile transmitters, to battle the severe results of the near-far effect. Truncation of the upstream dynamic range would result in an "outage" phenomenon akin to the outage due to shadow fading that occurs with narrowband systems. In the spread-specrum case, however, outage is less probable due to power control.

ACKNOWLEDGMENT

I wish to express my greatful appreciation to my parents for their continued support and encouragement throughout my studies. To my wife, Shakiba, I offer sincere thanks for her continuous patience, help and encouragement. To Dr. Ray W. Nettleton, my advisor, I express my deep gratitude for his guidance throughout this project. This work was supported by the National Science Foundation under Grant no. ECS-81 oo692.

TABLE OF CONTENTS

	Page
LIST OF TABLES	v
LIST OF FIGURES	vi
CHAPTER 1: INTRODUCTION	1
1.1 Statement of Problem	1
1.2 Outline of Contents	5
CHAPTER 2: BACKGROUND	7
2.1 Characteristics of the Channel	7
2.1.1 Rayleigh Fading	7
2.1.2 Shadow Fading	8
2.2 Cellular Land-Mobile Radio Systems	10
2.3 Narrow Band Systems	15
CHAPTER 3: DESCRIPTION OF THE SPREAD-SPECTRUM SYSTEM	19
3.1 Overview	19
3.2 Spread-Spectrum Performance Limitations	20
3.3 Code Division Multiple Access	21
3.3.1 CDMA Limitations	22
3.4 Principle Features of a Spread-Spectrum System	25
3.4.1 Advantages	28
3.4.2 Disadvantages	29
CHAPTER 4: POWER CONTROL	31
4.1 General Remarks	31
4.2 Assumptions	33
4.3 Power Balancing Algorithms	37
4.3.1 Upstream	38
4.3.2 Downstream	39
4.4 Existence and Uniqueness of the Solution	43
CHAPTER 5: SIMULATION	46
5.1 Geometry	47
5.1.1 Base Station and Load Distribution	47
5.1.2 Fading	49
5.2 Power Distribution and Interference	52
5.2.1 No Power Balancing	52
5.2.2 In-Cell Balancing	54
5.2.3 Cell-to-Cell Balancing	56

CHAPTER 6: RESULTS 60
6.1 Load Distribution and Environmental Parameters 60
6.2 Upstream Results 67
6.2.1 Denial Statistics 67
6.2.2 Dynamic Ranges of Transmitted Powers . . 84
6.3 Downstream Results 93
6.3.1 Denial Statistics 93
6.3.2 Dynamic Ranges of Transmitted Powers . . 109
6.4 Signal-to-Interference Ratio 118

CHAPTER 7: CONCLUDING REMARKS 122
7.1 Conclusions 122
7.2 Recommendations for Further Study 123
7.2.1 Restricted Power Control 124
7.2.2 Fading Model 124
7.2.3 Interference Modeling 125

LIST OF REFERENCES 126

LIST OF TABLES

Table page
1.1 Frequency allocations in "900 MHz" band 2

6.1 Ratios of the load in different cells as α/σ varies 66

6.2 Power control dynamic ranges required at full system capacity for the upstream link 92

6.3 Power control dynamic ranges required at full system capacity for the downstream link 116

LIST OF FIGURES

Figure		Page
2.1	Principle of the cellular land-mobile radio system	12
2.2	A cellular system in which cell sizes vary with user density	14
2.3	A narrowband/frequency-reuse system with L=4	16
3.1	Spread-spectrum connecting system	26
4.1	Interference geometry	36
5.1	Base station distribution in the 19 cell simulated system	48
5.2	Geometry used in simulating the shadow fading	51
5.3	Power Method for solving an eigenvalue problem	59
6.1	Geometry for load distribution analysis	62
6.2	$\Pr\{d^{ef} > R\}$ values versus the ratio d/R for different α/σ values	64
6.3	Denial statistics for the center cell, $\alpha = 3.0$, uniform traffic distribution, upstream	68
6.4	Denial statistics for the center cell, $\alpha = 3.5$, uniform traffic distribution, upstream	69
6.5	Denial statistics for the center cell, $\alpha = 4.0$, uniform traffic distribution, upstream	70
6.6	Denial statistics for the center cell, $\alpha = 3.0$, tapered traffic distribution, upstream	71
6.7	Denial statistics for the center cell, $\alpha = 3.5$, tapered traffic distribution, upstream	72
6.8	Denial statistics for the center cell, $\alpha = 4.0$, tapered traffic distribution, upstream	73

6.9 Denial statistics for the total system, $\alpha = 3.0$, uniform traffic distribution, upstream 74

6.10 Denial statistics for the total system, $\alpha = 3.5$, uniform traffic distribution, upstream 75

6.11 Denial statistics for the total system, $\alpha = 4.0$, uniform traffic distribution, upstream 76

6.12 Denial statistics for the total system, $\alpha = 3.0$, tapered traffic distribution, upstream 77

6.13 Denial statistics for the total system, $\alpha = 3.5$, tapered traffic distribution, upstream 78

6.14 Denial statistics for the total system, $\alpha = 4.0$, tapered traffic distribution, upstream 79

6.15 Average power control dynamic ranges required for upstream link balance, $\alpha = 3.0$, uniform traffic 85

6.16 Average power control dynamic ranges required for upstream link balance, $\alpha = 3.5$, uniform traffic 86

6.17 Average power control dynamic ranges required for upstream link balance, $\alpha = 4.0$, uniform traffic 87

6.18 Average power control dynamic ranges required for upstream link balance, $\alpha = 3.0$, tapered traffic 88

6.19 Average power control dynamic ranges required for upstream link balance, $\alpha = 3.5$, tapered traffic 89

6.20 Average power control dynamic ranges required for upstream link balance, $\alpha = 4.0$, tapered traffic 90

6.21 Denial statistics for the center cell, $\alpha = 3.0$, uniform traffic distribution, downstream 94

6.22 Denial statistics for the center cell, $\alpha = 3.5$, uniform traffic distribution, downstream 95

6.23 Denial statistics for the center cell, $\alpha = 4.0$, uniform traffic distribution, downstream 96

6.24 Denial statistics for the center cell, α= 3.0, tapered traffic distribution, downstream 97

6.25 Denial statistics for the center cell, α= 3.5, tapered traffic distribution, downstream 98

6.26 Denial statistics for the center cell, α= 4.0, tapered traffic distribution, downstream 99

6.27 Denial statistics for the total system, α= 3.0, uniform traffic distribution, downstream 100

6.28 Denial statistics for the total system, α= 3.5, uniform traffic distribution, downstream 101

6.29 Denial statistics for the total system, α= 4.0, uniform traffic distribution, downstream 102

6.30 Denial statistics for the total system, α= 3.0, tapered traffic distribution, downstream 103

6.31 Denial statistics for the total system, α= 3.5, tapered traffic distribution, downstream 104

6.32 Denial statistics for the total system, α= 4.0, tapered traffic distribution, downstream 105

6.33 Average power control dynamic ranges required for downstream link balance, α =3.0, uniform traffic 110

6.34 Average power control dynamic ranges required for downstream link balance, α=3.5, uniform traffic 111

6.35 Average power control dynamic ranges required for downstream link balance, α=4.0, uniform traffic 112

6.36 Average power control dynamic ranges required for downstream link balance, α=3.0, tapered traffic 113

6.37 Average power control dynamic ranges required for downstream link balance, α=3.5, tapered traffic 114

6.38 Average power control dynamic ranges required for downstream link balance, α=4.0, tapered traffic 115

6.39 SIR versus average load per cell, α=3.0 119

6.40 SIR versus average load per cell, α=3.5 120

6.41 SIR versus average load per cell, α=4.0 121

CHAPTER 1

INTRODUCTION

1.1 Statement of Problem

The increasing scarcity of the spectral resource in recent years, together with increasing demand for that resource, has led to much activity in the field of spectrum management and conservation [H1].

In no other application has this problem been more intensely felt than in the land mobile radio field. Recent FCC allocations in the 900 MHz band include two bands of width 20 MHz, intended for cellular land-mobile radio use (Table 1.1) [S3]. This allocation, coupled with the introduction of the cellular frequency re-use concept, promises to give temporary relief to this problem [Y1]. Cellular systems using this concept have been proposed and a number of systems are under construction or have been

Table 1.1 Frequency allocations in the "900 MHz" band.

Frequency, MHz	Allocation
806-821	Conventional systems mobile transmissions
821-825	Held in reserve
825-845	Cellular systems mobile transmissions
845-851	Held in reserve
851-866	Conventional systems base stations
866-870	Held in reserve
870-890	Cellular systems base stations
890-902	Held in reserve
902-928	Industrial,scientific and medical equipment

constructed [S3,A2,I1]. The proposed schemes, however, employ simple and traditional technologies, and the systems are likely to be outstripped by demand for more service, better quality, and diversified applications before the end of the century.

The use of spread spectrum in cellular land-mobile radio systems has been proposed and analyzed [C1,C2,N1]. Results to date have shown that spread spectrum techniques provide better quality communications and a more efficient use of the spectrum in the case of cellular systems. However these techniques require some degree of power control to reduce interference between users. Particularly, systems employing direct-sequence modulation become useless unless they use power control [T1].

The concept of power balancing to control interference between co-users of the same spectral space has been proposed and analyzed in the context of multi-beam communication satellites [A1]. The principle of power balancing may be readily extended to other interference-limited systems however [P2], and the spread-spectrum land mobile cellular radio scheme is a prime candidate.

In the upstream links (mobile to base) a significant difficulty is the so-called "near-far" effect, which permits strong interferers in the immediate vicinity of the base station to overwhelm weak signals from more distant mobiles. This effect is considerably worse for direct-sequence signalling than for frequency-hopping, since in the latter case limiters can be placed in each hopping channel to reduce the power imbalance. But in all cases some improvement can be obtained by dynamically controlling the transmitted power for every mobile transmitter so that the base station receives more-or-less the same power from each mobile. This is true whether or not the system is cellular.

In the downstream (base to mobile) case, if the system is not cellular, and if all signals are transmitted with the same power then every receiver will suffer the same signal-to-interference ratio regardless of distance, and power control is not necessary. But if the system is cellular, there is a distinct need for power control in the downstream case. A mobile that is near its base station will be almost unaware that there is any interference from outside its cell. But in the cell corners, a mobile will receive about three times the amount of interference since it is roughly equidistant from its own and two interfering base stations. Without power control, some corner mobiles would be incapacitated during periods of high communication traffic load.

This work describes schemes for balancing the signal to interference ratio of the mobile downstream and upstream links, for every mobile in a given cell and (optionally) for all mobiles in the entire system. Results are given at the receiver antenna so that they are independent of the choice of spreading function, modulation method or coding scheme. Results are also compared for the upstream and downstream links.

1.2 Outline of Contents

Chapter 2 outlines the background material which forms the basis of the work. Section 2.1 reviews the general characteristics of the urban 900 MHz channel, and a composite model, suitable for the analysis of the proposed system, is presented. Section 2.2 outlines the features of existing proposals for the solution of the problems of the land-mobile radio service.

In Chapter 3, the spread-spectrum system is outlined in general terms. The advantages and disadvantages of the operation of the system are discussed, and some comparisons with narrowband systems are drawn. The general principles of the spread spectrum cellular land-mobile radio scheme is described, without reference to any specific signal design or modulation methods.

Chapter 4 presents the theoretical results of the present work. The power balancing algorithms for both upstream and downstream links are developed and analyzed, and the existence and uniqueness of the solution to the

problem is discussed. The power balancing algorithms, for both the upstream and downstream cases, permit the signal-to interference ratio of every signal to be equalized within each cell and, optionally, from cell to cell throughout the system.

Chapter 5 discusses the considerations and assumptions used in the computer simulation of a hypothetical system. Geometrical and propagation considerations based on an assumed service area of 19 equal size cells, arranged in three concentric rings, are presented. We describe how the power control algorithms were applied to the hypothetical system.

Chapter 6 presents the results of the computer simulation of the 19 cell system. Results of the interference, load capacity and dynamic ranges of transmitted powers are presented for both upstream and downstream cases, and are compared for different path loss parameters. Results are also compared for cases where no power control is applied; power control is applied only inside each cell; and power control is applied system-wide.

Chapter 7 summarizes the work and discusses recommendations for further research in this field.

CHAPTER 2

BACKGROUND

2.1 *Characteristics of the Channel*

The new urban 900-MHz mobile radio channel has been studied in great detail in the literature [J1]. We summarize the pertinent features of the channel below.

2.1.1 *Rayleigh Fading*

The channel disperses the transmitted signal in the time domain. This results in a highly frequency-selective fading. For example, a sine-wave continuous signal will be received as the sum of a large number of sine waves with different phases. The received signal amplitude will have Rayleigh statistics that are different for different frequencies [N1]. This fading occurs over distances of about one half wavelength. Therefore, a mobile moving through the field will experience up to hundreds of fades a second at typical vehicular speeds.

The coherence bandwidth B_c of the channel is the difference between two frequencies which have a correlation coefficient of 0.5 or less. It can be shown that B_c is inversely proportional to the rms time spread of the channel impulse response [K1]. Typically, the coherence bandwidth ranges from 30 KHz to 1 MHz. Thus the frequency-selective property of the channel causes a spread-spectrum transmission to suffer different fades at different portions of its spectrum. This results in a form of <u>frequency diversity</u> which reduces the effects of fading [K1].

2.1.2 Shadow Fading

When a mobile moves around the service area, the mean strength of the signal changes slowly. This is <u>shadow fading</u> due to buildings and terrain. This imposes a non-frequency selective, slowly changing median upon the Rayleigh field statistics. This fading has a lognormal characteristic (i.e., normal if measured in dB) with standard deviation, sometimes called the dB spread, varying between 7 and 12 dB.

The mean of the overall fading distribution is a deterministic function of distance from the transmitter ranging from an inverse cubic law to an inverse fourth-power law [J1].

Consequently we may define an instantaneous attenuation factor:

$$a_{inst} = s(t)r(t) \qquad (2\text{-}1)$$

where r(t) is due to the Rayleigh fading and has a mean of unity; and s(t) is due to the combined effect of shadow fading and attenuation with distance. Thus, if

$$\xi(t) = 10 \log_{10}(s(t)) \qquad (2\text{-}2)$$

then the random variable ξ is Gaussian with probability density function:

$$f_{\underline{\underline{\xi}}}(\xi) = \frac{1}{\sqrt{2\pi}\,\sigma} \exp(-(\xi - m)^2/2\sigma^2) \qquad (2\text{-}3)$$

where σ varies between 7 and 12 dB depending on the severity of the shadow fading. The mean value m reflects the median attenuation in signal strength in the mobile environment and is given by:

$$m=10 \log_{10} (1/d^{\alpha}) \qquad (2\text{-}4)$$

where d is the distance between the mobile and the base station. The <u>path loss exponent</u> or <u>propagation parameter</u>,

α, varies between 3 and 4 ($\alpha = 2$ represents the free space situation.)

The rapid Rayleigh fading envelope, however, causes the instantaneous attenuation to fluctuate rapidly. For example, with a velocity of 30 miles/hr, a vehicle would have traveled 44 ft (about 44 wavelengths at 900 MHz) in one second and experienced that many Rayleigh fading cycles. This rapid fluctuation is averaged due to the filtering effect of the human hearing response. This time averaging is equivalent to ensemble averaging, for ergodic signals, thus we set the average attenuation factor;

$$a = E\{a_{inst}\} = s(t) \tag{2-5}$$

This is a more meaningful indicator of the attenuation for a mobile environment and is independent of the Rayleigh fading.

2.2 Cellular Land-Mobile Radio Systems

Existing mobile telephone systems can serve a limited number of users due to spectral overcrowding. One radio frequency can only be used by one user at a time in the service area in which the mobile user is allowed to operate. But a new technology called Cellular Land-Mobile Radio (CLMR) is about to change the present situation. This technology now offers better service to several hundred thousand users than was previously offered to a few hundred users [C3].

While most of the literature concerning CLMR systems have addressed the narrow band/frequency-reuse schemes [M1,S1,S2], recent publications calling for the use of spread spectrum as a more efficient technique for CLMR systems, have attracted much attention [C1,C4,N1,C3]. Despite the differences in the modulation techniques, all cellular systems have many characteristics in common which are summarized below with reference to Figure 2.1.

The geographic area is divided into small "cells" the sizes of which reflect the expected traffic load in the area. Each cell has its own base station antenna, typically located in the middle of the cell. Although the shape of the cells are typically represented as hexagons, the actual shapes are determined by the terrain, and density and locations of hills and buildings, in the service area. Thus the region served by each base station (or its cell), is the area in which the signal strength from that base station is stronger than from all other stations. However, the use of "hexagonal" cell representation has become common practice in the technical literature and will be used in the sequel with no further apologies. Each mobile communicates only with the base station serving the cell in which the mobile unit is located, and a central controller interconnects different

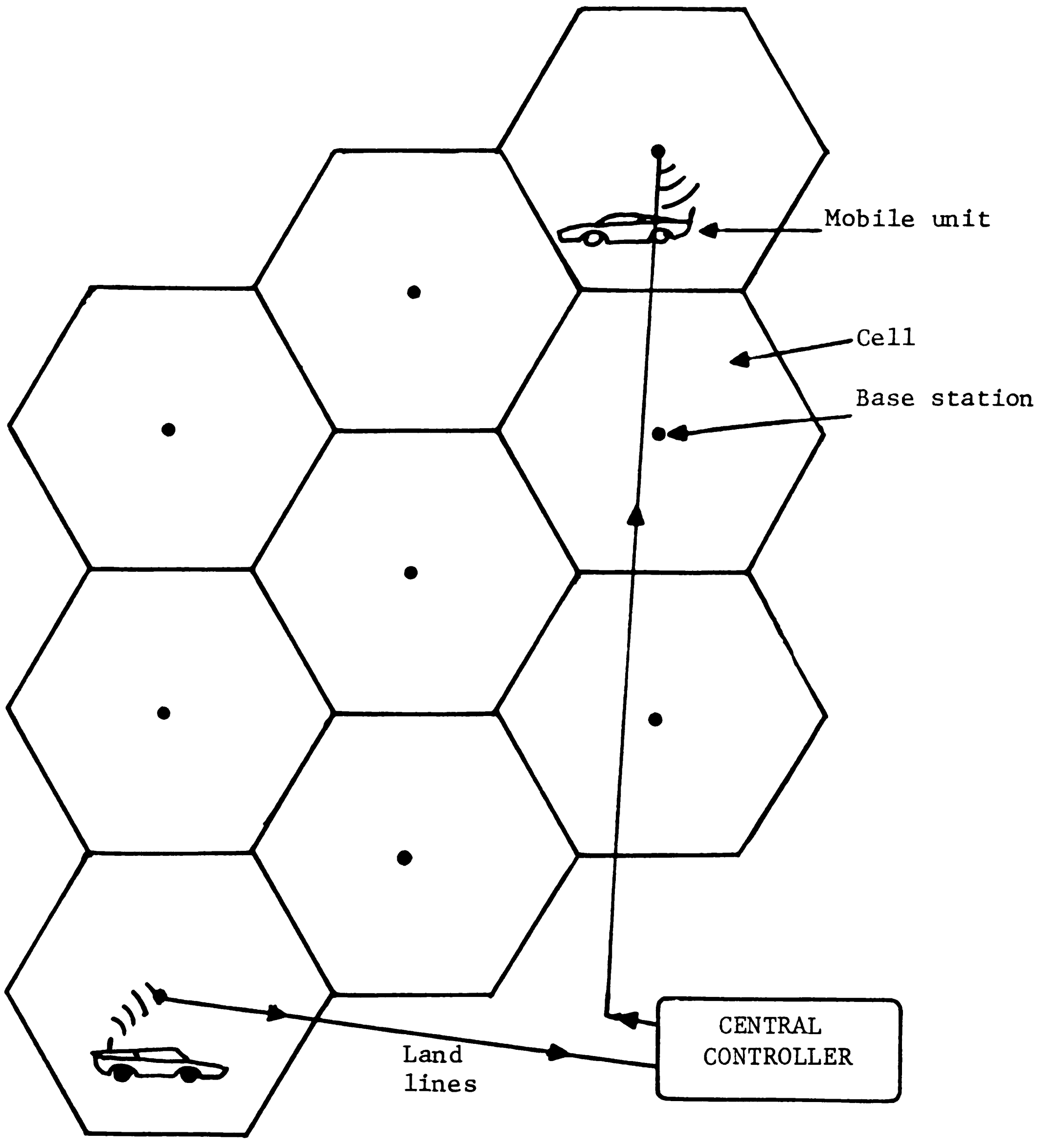

Figure 2.1 Principle of the cellular land-mobile radio system.

base stations, via a non-broadcast link, thus making communication from cell to cell possible. Therefore there is no mobile-to-mobile communication and every link is via one or two base stations, depending on whether the mobiles are located in the same or different cells. The transmitted power to and from the mobile units is limited to the amount required to communicate with satisfactory quality within the cell and at the same time to minimize the interference to neighboring cells.

The central controller also keeps track of the location of each mobile unit. When a mobile passes the boundary of a cell and enters another cell, the controller re-routes the call to the appropriate base station without any noticeable interrupt in the communications. This operation is referred to as "handoff".

Interference between simultaneous users increases as the number of users in the service area increases. System performance is then limited by interference, rather than background noise [C7]. The amount of interference is mostly a function of the number of users inside each cell, and thus the expansion of the system in order to serve more users can be accomplished by reducing the size of the cells rather than by expanding the spectral space [S2]. Figure 2.2 shows a cellular system in which the cell-size distribution reflects the non-uniform distribution of user density.

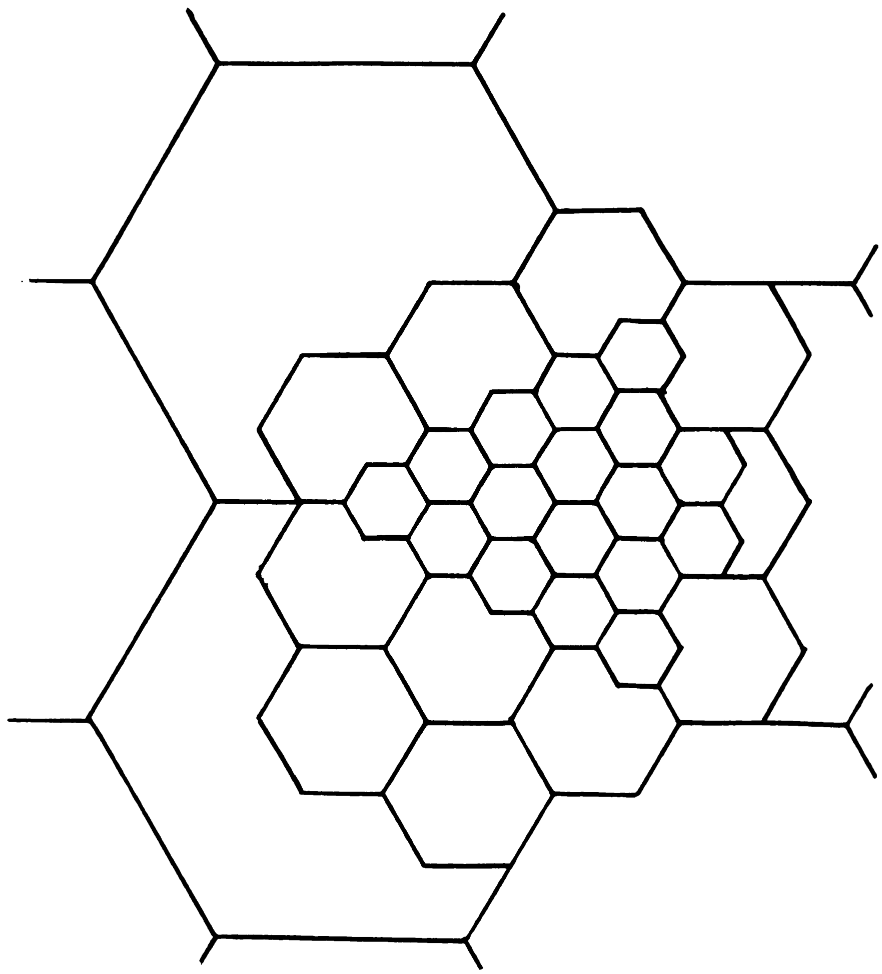

Figure 2.2 A cellular system in which cell sizes vary with user density.

Besides the above characteristics that are common between all systems, there are some additional features characterizing the narrow band/frequency-reuse scheme and the spread-spectrum scheme. We summarize some of the characteristics of the narrow band systems here, and Chapter 3 is devoted to the characteristics of the spread-spectrum system.

2.3 *Narrow Band Systems*

In the narrow band/frequency-reuse systems the available spectrum is divided into narrow band channels. The channel set is divided into L disjoint subsets, and each subset is assigned to one cell of a cluster of L cells. This is to minimize the cochannel interference that may result from the use of the same channel in the neighboring cells. The number of subsets of channels is equal to the number of cells in a cluster. The cluster is formed such that it can tesselate the plane. Figure 2.3 shows a system with a cluster size of 4 [M1]. The channel assignment, then, is repeated in the same configuration in all clusters.

In addition, each subset of channels is divided into two portions; one for base station transmissions and one for mobile unit transmissions.

When handoff occurs, in addition to re-routing the

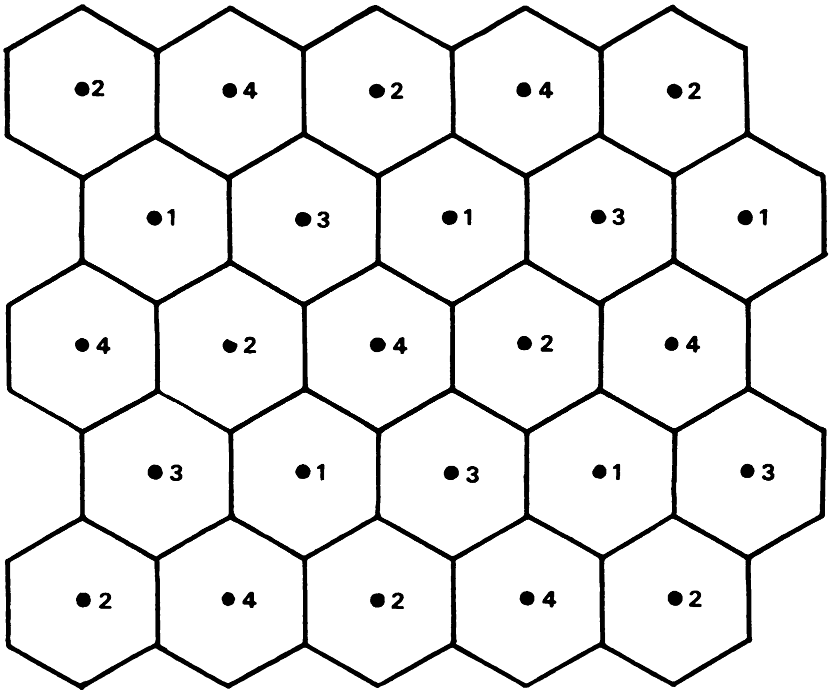

Figure 2.3 A narrowband/frequency-reuse system with L = 4.

call, the central controller must find an idle channel pair to assign to the mobile to use in the new cell. In the case where there are no channels available, the call is terminated or "blocked".

When a mobile moves around the service area, it may pass through areas in which signal-to-interference ratio is unacceptable. This is caused by shadowing due to buildings and terrain. This phenomenon is referred to as "outage".

Despite the advantage of being simple in concept and design and the availability of fully-developed technology, the narrow band/frequency-reuse scheme has many disadvantages, particularly in the case of the present FM schemes. These disadvantages include the high cost of analog circuitry and the poor quality of reception in a fading environment [P1]. In an environment where the signal strength attenuates only as the inverse cube of the distance and the standard deviation of the signal variation is as large as 10 dB, 30-40 channel sets are required to provide good service probability (on the order of 99 percent) [C8]. In addition, waste of spectrum resulting from allowing only a portion of the spectrum to be used in any given location, and the lack of privacy due to the use of simple modulation methods are among many other disadvantages that can be named. As such, it is felt that the narrow band/frequency-reuse scheme provides

a useful but necessarily temporary solution to the problem of the land-mobile radio service [N1].

CHAPTER 3

DESCRIPTION OF THE SPREAD-SPECTRUM SYSTEM

3.1 Overview

Spread-spectrum is an alternative to the narrow band schemes in multiple access systems. In systems employing spread-spectrum, different users are distinguished by different signature sequences. This technique is referred to as code division multiple access (CDMA). In such a system the base band signal is embedded into a spreading signal that has a bandwidth much greater than the data rate. This is the reason this technique is called spread-spectrum. The analysis in this chapter is more appropriate to the transmission of binary data using direct-sequence spectral spreading [W1,P3]. More careful analysis however, is needed for frequency hopped schemes.

3.2 Spread-Spectrum Performance Limitations

Generally, in any digital communication, the probability of bit error P_b must not exceed some value P_0. This restriction is satisfied if the ratio of energy per bit E_b, to the one-sided spectral density of the noise N_0, exceeds some threshold value T;

$$P_b \leq P_0 \quad \text{iff} \quad E_b/N_0 \geq T \tag{3-1}$$

Particularly, if ideal matched filters are used, P_b for a BPSK scheme is given by

$$P_b = Q[(2E_b/N_0)^{1/2}], \tag{3-2}$$

where Q(x) is the Gaussian integral function defined by

$$Q(x) = \int_x^\infty (2\pi)^{-1/2}\exp(-u^2/2)du. \tag{3-3}$$

Typically, P_0 is required to be in the range 10^{-3} - 10^{-6}. This can usually be achieved with T in the range 5 to 15 dB.

Suppose the received spread-spectrum signal has the average one-sided power spectral density of S in the band of width B. That is, if the transmitted spectrum is S(f),

$$P = SB = \int_0^\infty S(f)df \tag{3-4}$$

where P is the power of the constant envelope signal, and is equal to the product of the energy-per-bit and the bit rate R. Then (3-1) becomes

$$E_b/N_0 = P/N_0R = (S/N_0)(B/R) \geq T$$

thus, we have

$$S \geq N_0T/(B/R) \tag{3-5}$$

Note that (3-4) and (3-5) are true for any type of spreading function. The factor B/R is often called the processing gain of the spread-spectrum system.

The inequality in (3-5) suggests that for a given T, the power spectral density S of the desired signal may be less than the noise spectral density, provided that the processing gain is large enough. It is thus possible for a spread-spectrum receiver to operate even when the input signal is buried in noise. This suggests the use of a technique known as spread-spectrum multiple access (SSMA), also called code division multiple access (CDMA).

3.3 Code Division Multiple Access

Multiple access can be achieved by spread-spectrum code division using direct-sequence, frequency hopping, time hopping, or a combination of these techniques. All of these schemes use spreading signals that are minimally correlated with each other as well as with the time-shifted versions of themselves. This is to

facilitate easy recognition of the desired signal and easy synchronization of the receiver to the signal. The following discusses some analysis and performance limitations of CDMA systems that use the direct-sequence technique [W1]. Perfect synchronization of the matched filter in the receiver for the desired signal is assumed.

3.3.1 CDMA Limitations

The analysis in 3.2 also applies if the noise spectral density is replaced by a spectrum composed of thermal noise and a number of noise-like interferers. In direct-sequence techniques that use pseudonoise functions as their spreading signal, the ensemble of interferers behave like independent sources of white, Gaussian noise [P3]. Suppose that there are K interferers and the i^{th} interferer is received with power spectral density $a_i S$ Watt/Hz, where S is the power spectral density of the desired signal. Thus the total noise-plus-interference power spectral density over the transmitted bandwidth becomes

$$N = N_0 + S \sum_{i=1}^{k} a_i . \qquad (3\text{-}6)$$

Thus at the input of the receiver, the signal-to-interference ratio (SIR) is given by

$$SIR = S/N = (E_b/N)(R/B). \tag{3-7}$$

But B is much greater than R, so E_b/N can be in an acceptable range (about 10) even when SIR is very small. For example, for a processing gain of 30 dB, and E_b/N of 10 dB, SIR is as small as 0.01. Therefore if the effect of the thermal noise is neglected and all signals are received with equal powers, 100 interferers can be present in the same band, and the performance of the receiver will still stay within the acceptable range.

Combining (3-5) and (3-6) we have

$$S \geq \frac{N_0}{(B/R)/T - \sum_{i=1}^{k} a_i}, \tag{3-8}$$

It is clear that in order to have equal reception quality for all users in the system, the received power must be the same for every signal. Thus the value of the coefficient "a" must be unity for all i. (In order to achieve equal received power from users with different path lengths, some sort of power control is required. This is discussed further in the next chapter.) This will also maximize the traffic capacity of the system. In that case

$$\sum_{i=1}^{k} a_i = K \tag{3-9}$$

and (3-8) becomes

$$S \geq \frac{N_0}{(B/R)/T - K}. \tag{3-10}$$

Note that if $K \geq (B/R)/T$ there is no value of S that will lead to the required probability of error P_0. This leads to the fundamental limit for the traffic capacity of a CDMA channel with equal power interferers;

$$K \leq (B/R)/T \tag{3-11}$$

However, the capacity bound for a TDMA or FDMA scheme using binary antipodal signaling is $K \leq B/R$. Thus in general, the fundamental bound on the capacity of a system employing CDMA is less than the bound on both TDMA and FDMA by the factor T, provided that they have the same amount of available bandwidth. This, however, is not true in the case of the cellular land-mobile radio systems. In order to combat interference, in narrow band frequency/re-use systems, the available channel set is divided into many subsets, each of which is assigned to one cell in a cluster. Then, if the cluster size is L, the available bandwidth in each cell is reduced to B/L and the capacity bound is reduced by a factor of L. Thus we have

$$K \leq (B/R)/L \tag{3-12}$$

In cellular systems using CDMA, however, no clustering is required and all of the available band can be assigned to every cell. Thus for the cases where $T < L$, a CDMA scheme can have larger capacity than TDMA or FDMA schemes. This condition is expected to be true in many cases, since for good service probabilities in the frequency/re-use systems cluster size must be as large as 30-40 [C8].

3.4 Principle Features of a Spread-Spectrum System

The spread-spectrum cellular land-mobile radio system has been described in detail in the literature [C1,C2]. A suggested layout for the connecting system of such a system is shown in Figure 3.1. The overall features of this system are summarized below:

1. The available spectrum is divided into two segments, one for upstream and one for downstream. All mobiles and all base stations use the appropriate segment in its entirety for communication. The bandwidth of the signals might be in the tens of megahertz.

2. Interference between users is controlled by

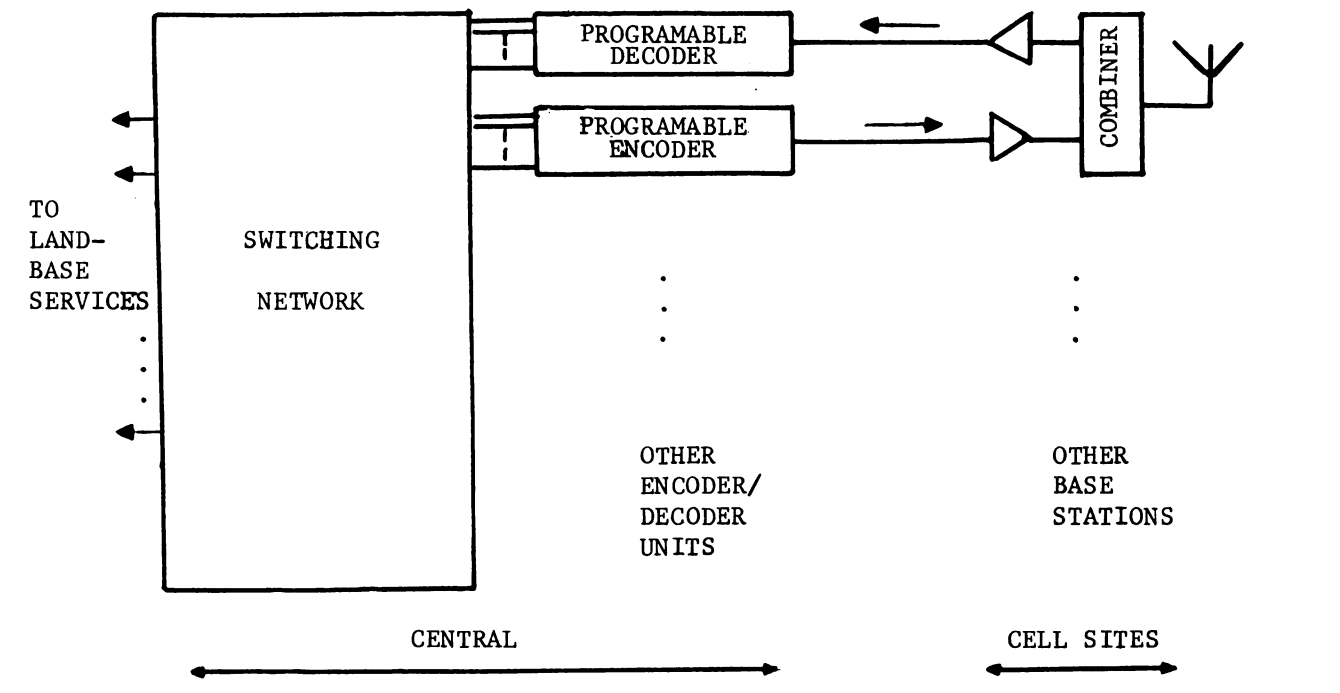

Figure 3.1 Spread-spectrum connecting system

signal design, using the large processing gain which results from transmitting a narrowband message embedded into a broadband signal [D2]. The set of signals is large enough to assign one signal uniquely to every mobile unit. No attempt is made to synchronize the mobile transmitters.

3. The "local" cell of a mobile is the cell of the base station which receives the most power from the mobile. This definition changes as the mobile moves, and "handoff" occurs when the mobile crosses a boundary from one cell to another.

4. The quality of the message is degraded by increasing interference levels, i.e. as the traffic load in the vicinity builds up. The switching network may fail to connect a call for one of two reasons: first, if there is no communication path through the system (due to hardware limitation), the call is "blocked" in the classic sense of the telephone traffic literature [B1]. Second, if the system senses that the addition of another call will result in excessive degradation of quality for all local calls, the connection will be refused by the

system. The latter failure will be referred to in the sequel as "Denial" to distinguish it from blocking.

3.4.1 Advantages

In addition to increased user-density that is possible in a small-cell system employing CDMA, many more advantages result from the use of spread-spectrum in such systems, some of which are summarized below:

The use of bandwidths that are much greater than the coherence bandwidth of the channel in such systems results in a form of frequency diversity which reduces the effects of frequency selective rapid fading significantly.

Every user is assigned a unique signal that is not used by any other user (at least locally.) This results in several advantages. First, any user can access the system at any time without having to wait for a free channel. Thus, there are no "blocked" calls in the usual sense, other than those caused by hardware limitation. The second advantage is message privacy with respect to the casual listener. Of course, this does not refer to message interception by a properly equipped receiver. Finally, the third advantage of this is that there is no channel switching or address change when the user moves from one cell to another. Therefore, there is no "forced termination", which occurs in the narrow band systems due to unavailability of channels.

When the number of simultaneous users in the service area increases, the result is degradation in the quality of the communication for all users, due to increased interference. This is usually referred to as "graceful degradation". Therefore, there is no hard limit on the number of users that can be active simultaneously. However, the switching network may fail to connect a call, if the system senses that the addition of another call will result in excessive degradation of quality for all local calls (denial).

Other advantages that can be named are; identical user hardware; easy accommodation of priority messages by increasing the power level or the time-bandwidth product of the priority signal; and finally the possibility of co-existence with other narrow band systems in the same frequency band without excessive mutual interference.

3.4.2 Disadvantages

Despite all of the significant advantages mentioned, the spread-spectrum approach has some disadvantages also, some of which are summarized below:

In the first place, the cost to start up such a

system is higher than that of the narrow band system. This is due to the more complex technology, as well as the fact that the base stations must have the initial capability for handling any of the possible sequences. In other words, the base station design must start with a mature system rather than grow as demand builds.

A second disadvantage is the need for an effective power control, to achieve the greatest system capacity. It may also be desirable to balance power among cells with different user densities. A set of solutions to this problem are reported and analyzed in the following chapters.

Another disadvantage is the requirement of a mobile locator technique, to determine the base station with which each mobile must communicate. This is also needed for the power control, to combat the near-far effect. However, such facility is required by all proposed small cell schemes whether narrowband or spread-spectrum.

CHAPTER 4

POWER CONTROL

4.1 General Remarks

Power control is essential for the efficient operation of the proposed spread-spectrum cellular system. In the upstream link, every mobile located in each cell must adjust its transmitter power, such that the base station of that cell receives the signal from each mobile with equal strength. This is to overcome the significant difficulty in the upstream link called the "near-far" effect. In the downstream link, the signal power to each mobile must be adjusted such that the signal-to-interference ratio (SIR) at every mobile receiver is the same. This is to overcome the difficulty that occurs for mobiles located at or near the cell corners.

The "near-far" effect permits strong interferers in the immediate vicinity of the base station to overwhelm weak signals from more distant mobiles. This problem is common to most spread-spectrum systems. In frequency-hopping systems, however, limiters can be placed in each hopping channel to reduce the power imbalance. This can eliminate much of the interference between users [C6]. But in the cases where direct-sequence signalling is used, the near-far effect is considerably worse. In all cases, however, some improvement can be obtained by dynamically controlling the transmitted power for every mobile, whether or not the system is cellular.

In the downstream case, the near-far effect is not a problem. For a non-cellular system, where all of the signals are transmitted with the same power, every receiver suffers the same signal-to-interference ratio regardless of distance. But if the system is cellular, some degree of power control may become necessary. A mobile that is near its base station will be almost unaware that there is any interference from outside the cell. But a mobile located in the cell corner is roughly equidistant from its own and two interfering base stations and thus, it receives three times the amount of interference. So if there is no power control in a heavily loaded system, some corner mobiles may receive too much interference and become incapacitated.

Also, in both upstream and downstream cases, when the load is not uniform from cell to cell, the amount of interference inside a heavily loaded cell can be reduced by controlling the interference from the neighboring cells. In other words, a lightly loaded cell can take more interference from outside, while a heavily loaded one is able to tolerate little outside interference.

This chapter presents schemes for balancing the SIR of both upstream and downstream links, for every mobile in a given cell and (optionally) for all mobiles in the entire system. Results are given at the receiver antenna so that they are independent of the choice of spreading function, modulation method or coding scheme.

4.2 Assumptions

1. The service area consists of N cells, whose boundaries coincide with the most probable location for cell-to-cell handoff. Although cells are shown as hexagons (as is usual), real cells are likely to be somewhat amorphous and may not even be simply-connected. Our analysis does not depend on cell shapes or sizes.

2. The load of the i-th cell is L_i Erlangs.

Although the general traffic model permits variations about this mean from time to time, we will use the simplifying assumption that precisely L_i users are linked to the i-th base station at a given time.

3. The i-th base station receives P_i^U Watts of power from any one mobile in the i-th cell. The power transmitted by the k-th mobile in the i-th cell is P_{ik}^U, $k=1,2,\ldots,L_i$ (the superscript U denotes upstream.)

4. Base station i transmits a total of Q_i Watts which we divide up two ways as follows: The average power per mobile, P_i^D; and the actual power to the k-th mobile, P_{ik}^D, $k=1,2,\ldots,L_i$. (The superscript D denotes downstream.) Thus

$$Q_i = \sum_{k=1}^{L_i} P_{ik}^D = L_i \; P_i^D. \qquad (4\text{-}1)$$

5. Knowledge of the propagation loss between each base station and each mobile is necessary for two distinct purposes: First for deciding which cell each mobile is located in; and second, for controlling the transmitted power to and from

each mobile. This knowledge can be acquired by direct measurement of signal strengths using a pilot signal with fixed power radiated from each station. Some caution must be exercized here, however. In a multipath environment, the reciprocity theorem is true only at a single frequency; if the upstream and downstream channels are separated by more than the coherence bandwidth, their respective path losses will be uncorrelated. However, the means of the Rayleigh fading channels will be the same for any frequency separation. Hence since the Rayleigh fading behavior is averaged out (as discussed in chapter 2) then "reciprocity in the mean" may be used in the system [N1]. The attenuation factor between the k-th mobile in the i-th cell and the base station of the j-th cell is denoted by a_{ikj} (see Figure 4.1.) Thus assuming the pilot signal is transmitted from the j-th station with the power Z_j^t and is received by the k-th mobile in the i-th cell having the power Z_{ikj}^r, the attenuation factor is given by

$$a_{ikj} = Z_j^t / Z_{ikj}^r. \tag{4-2}$$

Hence, the total power received by mobile k in cell i is given by:

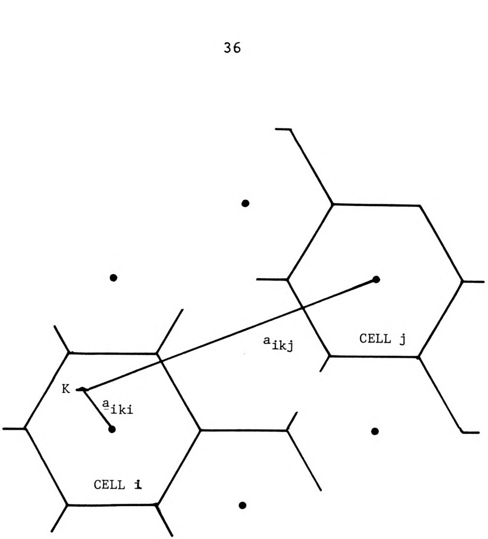

Figure 4.1 Interference geometry

$$R^{D}_{ik} = \sum_{j=1}^{N} L_j P^{D}_{j} a_{ikj}, \tag{4-3}$$

we also have:

$$P^{U}_{jk} = P^{U}_{j}/a_{ikj}. \tag{4-4}$$

And the total power received by the base station in cell i is given by:

$$R^{U}_{i} = \sum_{j=1}^{N} P^{U}_{jk} a_{jki} = \sum_{j=1}^{N} P^{U}_{j} \sum_{k=1}^{L_j} a_{jki}/a_{jkj}. \tag{4-5}$$

Since the signal from every mobile must be received with the same power.

6. The system is assigned a signal-to-interference lower limit S, determined from message-quality and service-grade requirements. This number is considerably less than unity because of the spread-spectrum processing gain. Denial occurs when the admission of a mobile requesting service would result in an SIR below the limit S.

4.3 Power Balancing Algorithms

The strengths of the transmitted signals can be adjusted such that the SIR becomes the same for all mobiles within a given cell or optionally for all mobiles in the entire system. Such a balance may be achieved for both upstream and downstream links, by means of similar algorithms.

4.3.1 *Upstream*

The total power received by the base station expressed in (4-5) contains the desired signal with power P_i^U and the interference from the other mobiles. Thus the interference from signals received by the base station of the i-th cell can be expressed as

$$I_i^U = \sum_{j=1}^{N} P_j^U \sum_{k=1}^{L_j} [a_{jki}/a_{jkj}] - P_i^U, \tag{4-6}$$

the signal from every mobile in the i-th cell thus suffers the signal-to-interference ratio

$$S_i^U = P_i^U / I_i^U. \tag{4-7}$$

Hence

$$\frac{1 + S_i^U}{S_i^U} P_i^U = \sum_{j=1}^{N} P_j^U \sum_{k=1}^{L_j} [a_{ikj}/a_{jkj}]. \tag{4-8}$$

Here, it is assumed that the received signal power from a mobile by its base station is the same for all mobiles in each cell.

This assumption results in a balance in the SIR values for each mobile in each cell. We refer to this operation as "in-cell balancing" since equalization is

done only within each cell, and different cells will in general have different SIR values. This equalization is easily accomplished using the set of estimated attenuation values by solving equation (4-4) for every mobile.

To equalize the value of SIR for all cells, we let

$$\mathbf{p}^U = [P_1^U, P_2^U, \ldots, P_N^U]^T;$$

$$B^U = [\, \beta_{ij}^U], \text{ where}$$

$$\beta_{ij}^U = \sum_{k=1}^{L_j} [a_{jki}/a_{jkj}]; \text{ and} \qquad (4\text{-}9)$$

$$S_i^U = S^U \text{ for all cells.}$$

Then we have

$$\frac{1 + S^U}{S^U}\, \mathbf{p}^U = B^U \mathbf{p}^U. \qquad (4\text{-}10)$$

This is a classic eigenvalue problem, where $\mathbf{p}^U$ is the eigenvector and the factor $(1+S^U)/S^U$ is the eigenvalue. Solving this problem together with (4-4) leads to the required upstream signal strengths P_{ik}^U that will lead to the uniform S^U for all mobile signals.

4.3.2 Downstream

The total received power expressed in (4-3) has three components; the power of the desired signal, the interference from the user's own cell, and the interference from outside. The first term is given by;

$$P_{des} = P^{D}_{ik} a_{iki}. \tag{4-11}$$

Subtracting (4-11) from (4-3) we get an expression for the interference encountered by the mobile k in cell i,

$$I^{D}_{ik} = \sum_{j=1}^{N} P^{D}_{j} L_{j} a_{ikj} - P^{D}_{ik} a_{iki}. \tag{4-12}$$

Thus this mobile suffers the signal-to-interference ratio,

$$S^{D}_{ik} = \frac{P^{D}_{ik} a_{iki}}{I^{D}_{ik}}. \tag{4-13}$$

Combining (4-12) and (4-13) and solving for the transmitted power we have:

$$P^{D}_{ik} = \frac{S^{D}_{ik}}{1 + S^{D}_{ik}} \cdot \frac{1}{a_{iki}} \sum_{j=1}^{N} P^{D}_{j} L_{j} a_{ikj}. \tag{4-14}$$

To balance the SIR values for each mobile in cell i, we set

$$S^{D}_{ik} = S^{D}_{i}; \; k=1,2,\ldots,L_{i}$$

and combining (4-13) and (4-1), we have;

$$L_{i} P^{D}_{i} = \frac{S^{D}_{i}}{1 + S^{D}_{i}} \sum_{k=1}^{L_{i}} \frac{1}{a_{iki}} \sum_{j=1}^{N} P^{D}_{j} L_{j} a_{ikj}. \tag{4-15}$$

Solving for S^{D}_{i}, we get an expression in terms of the set

of P_i^D,

$$S_i^D = \frac{L_i P_i^D}{\sum_{k=1}^{L_i} 1/a_{iki} \sum_{j=1}^{N} P_j^D L_j a_{ikj} - L_i P_i^D}, \qquad (4\text{-}16)$$

and observing that (4-14) must be true for each k in i,

$$P_{ik}^D = \frac{S_i^D}{1 + S_i^D} \cdot \frac{1}{a_{iki}} \sum_{j=1}^{N} P_j^D L_j a_{ikj}. \qquad (4\text{-}17)$$

Equations (4-16) and (4-17) are simply solved algebraically for transmitted powers, thereby balancing the downstream SIR values for all mobiles in a given cell. As in the upstream case, in general these values will be different from cell to cell, and within a given cell the SIR values will be different for the upstream and downstream links.

To balance the values of S_i^D for all cells, we construct an eigenvalue equation similar to (4-10). Setting all the S_i^D in (4-17) to S^D, and using (4-1), we have,

$$Q_i = \frac{S^D}{1 + S^D} \sum_{j=1}^{N} Q_j \sum_{k=1}^{L_j} \frac{a_{ikj}}{a_{iki}}. \qquad (4\text{-}18)$$

We now define:

$$\mathbf{q} = [Q_1, Q_2, \ldots, Q_N]^T;$$

$$\mathbf{B}^D = [\beta^D_{ij}], \text{ where } \beta^D_{ij} = \sum_{k=1}^{L_i} [a_{ikj}/a_{iki}]; \tag{4-19}$$

The eigenvalue problem then becomes

$$\frac{1 + S^D}{S^D} \mathbf{q} = \mathbf{B}^D \mathbf{q} \tag{4-20}$$

Where $\mathbf{q}$ is the eigenvector and the factor $(1+S^D)/S^D$ is the eigenvalue.

Solving the eigenvalue problem and using the Q_i values in (4-1) and (4-17) lead to proper values for the signal strengths P^D_{ik} that will result in a uniform signal-to-interference ratio S^D throughout the service area.

Comparison of the defining equations (4-9) and (4-19) reveals that

$$\mathbf{B}^U = [\mathbf{B}^D]^T, \tag{4-21}$$

so that the eigenvalue solution to (4-10) and (4-20) and hence S^U and S^D are identical [G1]. Therefore if system-wide balancing is performed, the quality of transmission will be the same for all mobiles in both the upstream and the downstream links. Therefore denials will occur in both links at the same time.

4.4 Existence and Uniqueness of the Solution

The following theorem on the property of the spectra (i.e., the eigenvalues and eigenvectors) of positive matrices is due to Perron [G1].

> Theorem: A positive matrix $\mathbf{H} = [h_{ik}]_1^n$ always has a real and positive eigenvalue r which is a simple root of the characteristic equation and exceeds the moduli of all other characteristic values. To this "maximal" eigenvalue r there corresponds an eigenvector $\mathbf{e} = (e_1, e_2, \ldots, e_n)$ of $\mathbf{H}$ with positive coordinates $e_i > 0$, $(i=1,2,\ldots,n.)$

The following two properties about r and **e** are also shown to be true [G1]:

1. A positive matrix **H** can not have two linearly independent positive eigenvectors **e**.

2. If we define w_i as the sum of the elements in the i-th row of **H**;

$$w_i = \sum_{k=1}^{n} h_{ik}; \ (i=1,2,\ldots,n), \tag{4-22}$$

and

$$w = \min w_i, \quad W = \max w_i; \; 1 \leq i \leq n \tag{4-23}$$

Then for the positive matrix ,we have

$$w \leq r \leq W, \tag{4-24}$$

and the equality sign holds when $w = W$.

Here, since r is a simple eigenvalue, the eigenvector e corresponding to it is determined uniquely within a scalar factor. Now the matrices $\mathbf{B}^D$ and $\mathbf{B}^U$ are always positive matrices since if a cell is not occupied, the size of the matrix can be reduced instead of having a zero row and column. Then there exists one and only one all positive eigenvector (within a scalar factor), the elements of which are the required transmitted powers P_i^U for the upstream matrix $\mathbf{B}^U$, or Q_i for the downstream matrix $\mathbf{B}^D$. This eigenvector corresponds to the maximal eigenvalue of the matrix $\mathbf{B}^U$ or $\mathbf{B}^D$, which is equal to $(1+S^U)/S^U$ or $(1+S^D)/S^D$.

Here, we note that the solution is acceptable only if the maximal eigenvalue r is larger than unity, since for any SIR such that $0 < (S^U,S^D) < \infty$,

$$(1 + S^U)/S^U > 1 \text{ and } (1 + S^D)/S^D > 1. \tag{4-25}$$

This can be shown to be true using the second property mentioned above. Let w_i^U and w_i^D be defined as

$$w_i^U = \sum_{j=1}^{N} \beta_{ij}^U \text{ and}$$

$$w_i^D = \sum_{j=1}^{N} \beta_{ij}^D$$

Then from (4-9) and (4-19), it is obvious that $\beta_{ij}^U > 1$ and $\beta_{ij}^D > 1$ for all i and j, and thus using (4-24), maximal eigenvalues for both upstream and downstream cases are larger than unity. Therefore the solution to the problem always exists and is unique.

Many computer methods are available for solving an eigenvalue problem, one of which is used in the solution of a simulated hypothetical system discussed in the next chapters.

CHAPTER 5

SIMULATION

To evaluate the proposed scheme, a hypothetical system has been simulated by computer. Since the system is interference limited, it is important to understand how interference varies with traffic load and mobile location. The effect of Rayleigh and shadow fading on the interference levels need to be investigated also. The probability of denial, which is an interference-dependent mechanism, its dependence on traffic levels and environmental parameters, and the effect of power control on the interference and denial mechanism also need to be investigated. A small scale computer simulation of the proposed scheme is thus undertaken to investigate the system under different load distributions and environmental parameters.

5.1 Geometry

In order to simulate the system a hypothetical geometry is used, which determines the location of the base stations, the environmental parameters, and the distribution of the users in the area. Attempts have been made to simulate a geometry which resembles a relatively realistic situation.

5.1.1 Base Station and Load Distribution

The base station distribution in an actual service area must be determined considering many factors such as the topology of the service area, the distribution of blocking objects such as tall buildings, and statistics of mobile user quantity and distribution throughout the system. Then, as mentioned in chapter 2, the cell associated with each base station is the area in which the received signal from that station is the strongest (i.e. the attenuation from that station is smallest.) However, in our simplified model, the base stations are distributed as if the service area consisted of nineteen hexagonal cells, each of equal size, arranged in three concentric rings (See Figure 5.1.) The purpose of the hexagonal shape assumption is only to determine the location of the base stations. The actual shape of a cell varies and its

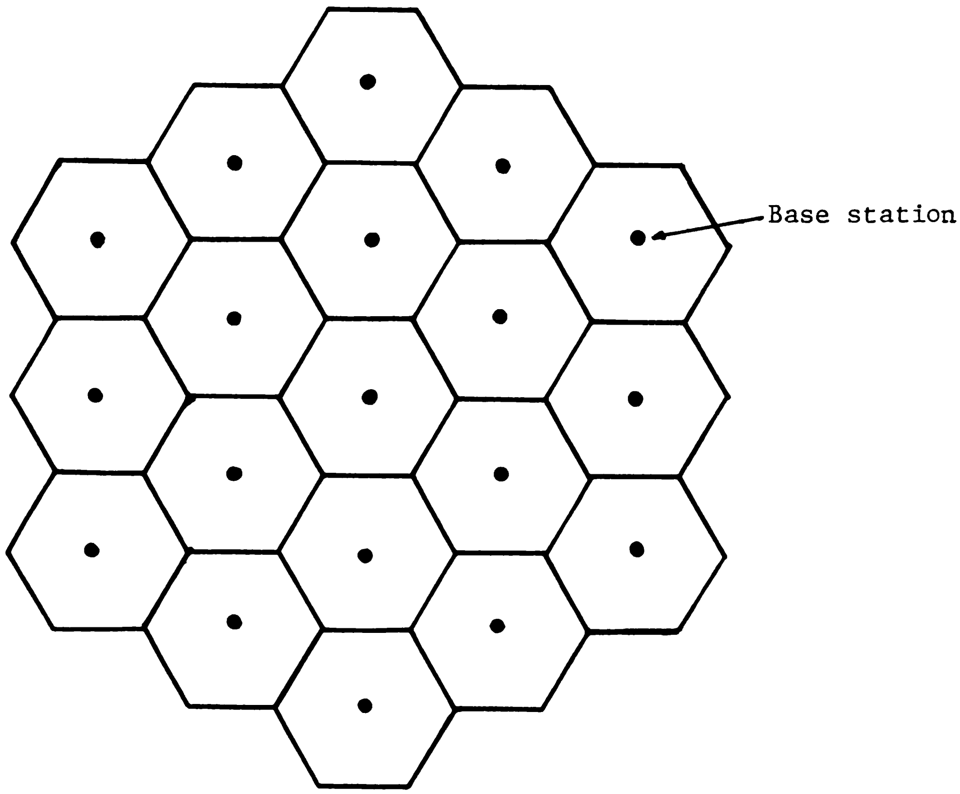

Figure 5.1 Base station distribution in the 19 cell simulated system.

parts may not even be connected.

To simulate the random positions of the mobile units, two spatial distributions were used. In the first, the mobiles were distributed randomly with "uniform" distributions so that the mean number of units in each cell was the same. In the second case, a bivariate Gaussian distribution was used, with mode at the center of the system and the variance adjusted to give the mean number of units per cell in the ratios: 7.5 for the center cell; 4 for the intermediate ring of cells; and 1 for outer ring. In the sequel this will be referred to as the "tapered" traffic distribution.

5.1.2 Fading

In section 2.1 we mentioned that in a mobile environment the received signal fluctuates very rapidly due to the rapid Rayleigh fading. We also mentioned that these fluctuations are averaged by the filtering effect of the human hearing response. Neglecting the effects that these fluctuations may have on the performance of the receiver, we have considered the attenuation to be independent of Rayleigh fading.

To simulate the distance-plus-shadowing composite attenuation factor for each mobile to each base station, the service area was divided into small squares of sides

1/5 the radius of a cell (i.e. 1/10 the distance between two base stations), each square representing, for example, a city block in a suitably scaled cell (See Figure 5.2.) Each square was then assigned a normally distributed random number as its shadow fading coefficient to each base station. Thus, each square was assigned 19 independent values corresponding to the path loss from that square to each base station. These values are denoted by ρ_{mi}; where m denotes the square and i, the corresponding base station. Thus for an initiating mobile (IM) located in the m-th square, the attenuation factor to the j-th base station b_j^{IM}, is given by;

$$10 \log_{10}(b_j^{IM}) = \sigma \rho_{mj} + 10 \log_{10}(1/d_j^{IM})^{\alpha} \tag{5-1}$$

where $\sigma \in [7,12]$,

$\alpha \in [3,4]$, and

d_j^{IM} = The distance from the initiating mobile to the j-th base station.

(Note: The attenuation factor is log-normal with variance σ and mean $10 \log_{10}(1/d)^{\alpha}$.)

The mobile "belongs" to the cell i for which the attenuation factor is smallest. Thus, if there are k-1 mobiles in the cell i prior to the arrival of the new mobile, we have:

$$a_{ikj} = b_j^{IM}, \quad j=1,\ldots,19 \tag{5-2}$$

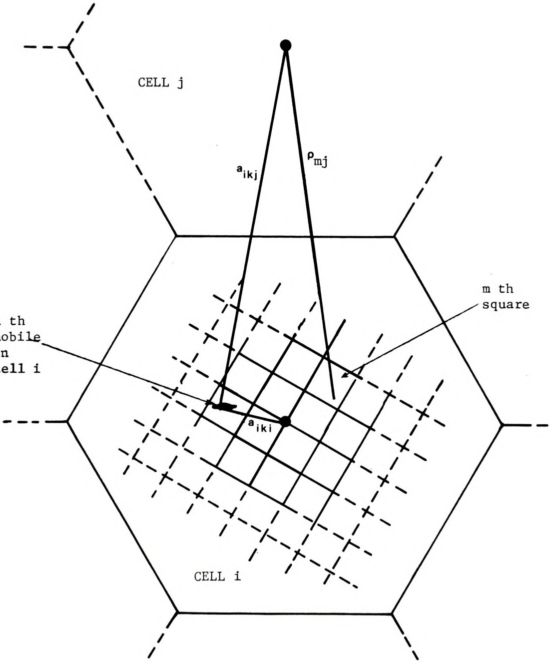

Figure 5.2 Geometry used in simulating the shadow fading.

$$a_{iki} = \min(b_j^{IM}), \quad j=1,\ldots,19 \tag{5-3}$$

The purpose of dividing the service area into small squares was to simulate a realistic urban situation in which, although the overall shadow fading has a lognormal characteristic, the mobiles located within an immediate geographic area (e.g. a city block) of each other experience the same amount of shadowing. The total amount of fading, however, is still a function of their distance ($\sim d^{\alpha}$), and different for mobiles at different locations.

5.2 Power Distribution and Interference

Results were generated for each set of mobile locations with no power balancing, for in-cell balancing only, and for in-cell plus cell-to-cell balancing. The value of SIR criterion S used in the simulation was -20 dB, which corresponds to a signalling system with a processing gain of 30-35 dB with typical coding schemes. The capacity of a power-balanced single-cell system with this SIR criterion would be 1/S=100 users.

5.2.1 No Power Balancing

To generate the results with no power control, it was assumed that the power transmitted to and from every

mobile was the same. Thus if we let $P^U_{ik} = P^U$ and $P^D_{ik} = P^D$ for all $(k=1,\ldots,L_i)$ and $(i=1,\ldots,N)$, then using (4-4) and (4-5), we have:

$$P^U_j = P^U a_{ikj},$$

$$R^U_i = \sum_{j=1}^{N}\sum_{k=1}^{L_j} P^U a_{jki},$$

and thus (4-7) becomes;

$$S^U_{ik} = \frac{a_{iki}P^U}{\sum_{j=1}^{N}\sum_{k=1}^{L_j} P^U a_{jki} - P^U a_{iki}}$$

Thus we have:

$$S^U_{ik} = \frac{1}{\sum_{j=1}^{N}\sum_{k=1}^{L_j} [a_{jki}/ a_{iki}] - 1}. \tag{5-4}$$

Also, using (4-1), we have:

$$\sum_{k=1}^{L_j} P^D = L_i P^D_i,$$

so $P^D_i = P^D_{ik} = P^D$,

and then (4-3) becomes;

$$R^D_{ik} = \sum_{j=1}^{N} L_j P^D a_{ikj}.$$

Therefore, (4-13) becomes

$$S_{ik}^{D} = \frac{a_{iki}P^{D}}{\sum_{j=1}^{N} L_j a_{ikj} P^{D} - a_{iki}P^{D}},$$

thus we have:

$$S_{ik}^{D} = \frac{1}{\sum_{j=1}^{N} L_j [a_{ikj}/a_{iki}] - 1}. \qquad (5\text{-}5)$$

(5-4) and (5-5) were used to generate the SIR's for all mobiles where no power control was applied. Some denial statistics then were produced using the SIR threshold of -20 dB.

5.2.2 In-Cell Balancing

In-cell balancing was simulated by balancing the powers within every cell, without any attempt to balance SIR's system-wide. In general these values will be different for different cells and also for the upstream and downstream links. For the upstream case, it was assumed that P_{ik}^{U} is adjusted according to (4-4) to lead to the same P_j^{U} for every mobile in a given cell. In addition, P_j^{U} was assumed to be the same for every cell. Thus we have:

$$P_j^{U} = \mathcal{P}^{U} \quad \text{for } (j=1,\ldots,N),$$

and (4-7) becomes

$$S_i^U = \frac{P^U}{\sum_{j=1}^{N} P^U \sum_{k=1}^{L_j} [a_{jki}/a_{jkj}] - P^U}.$$

So we have:

$$S_i^U = \frac{1}{\sum_{j=1}^{N} \sum_{k=1}^{L_j} [a_{jki}/a_{jkj}] - 1}. \tag{5-6}$$

For the downstream case, it is assumed that the average transmitted power P_i^D is the same for all cells. Thus we have:

$$P_i^D = P^D \quad \text{for all } (i=1,\ldots,N),$$

and (4-16) becomes

$$S_i^D = \frac{L_i P^D}{\sum_{k=1}^{L_j} \sum_{j=1}^{N} P^D L_j [a_{ikj}/a_{iki}] - L_i P^D}.$$

So, we have:

$$S_i^D = \frac{1}{\sum_{k=1}^{L_j} \sum_{j=1}^{N} [L_j/\ L_i][a_{ikj}/a_{iki}] - 1}. \tag{5-7}$$

Then (4-17) was used to compute P_{ik}^D for individual signal strengths.

(5-6) and (5-7) were used to generate the SIR's for every cell, where power control was performed to equalize the SIR for the mobiles inside each cell. Again in this case, denial statistics were produced using the SIR threshold of -20 dB.

5.2.3 Cell-To-Cell Balancing

Cell-to-cell balancing was performed on the simulated system, by solving the eigenvalue problems expressed by (4-10), for the upstream case and (4-20), for the downstream case. Then the dominant eigenvalue and its corresponding eigenvector are the accepted solutions to the problems. Many numerical techniques exist for evaluating eigenvalues and eigenvectors of various types of matrices [D1]. Here we use an iterative method called the Power Method. This method is used for determining the eigenvalue with the largest absolute value (dominant eigenvalue) and a corresponding eigenvector. The Power Method is based on the following theorem [W2].

> Theorem: Let $\mathbf{A}$ be an nxn matrix having n linearly independent eigenvectors and a dominant eigenvalue. Let $\mathbf{x}_0$ be an arbitrary chosen initial vector such that $\mathbf{Ax}_0$ exists. The sequence of vectors

$$\mathbf{x}_1=\mathbf{A}\mathbf{x}_0,\ \mathbf{x}_2=\mathbf{A}\mathbf{x}_1,\ldots,\ \mathbf{x}_k=\mathbf{A}\mathbf{x}_{k-1},\ldots,$$

as k becomes larger, will approach an eigenvector for λ_1, the dominant eigenvalue, if $\mathbf{x}_0$ has a nonzero component in the direction of an eigenvector for $\boldsymbol{\lambda}_1$.

In the cases where N is large (19 in our simulation) the probability of matrices $\mathbf{B}^U$ or $\mathbf{B}^D$, having linearly dependent rows (ranks less than N) is very small and they almost always have N linearly independent eigenvectors. Also, the chances of the arbitrary chosen initial vector $\mathbf{x}_0$ being perpendicular to the eigenvector is very remote. So this method, almost always, will lead to the correct results.

It remains to find the dominant eigenvalue. If $\boldsymbol{\lambda}$ is an eigenvalue of $\mathbf{A}$ and if $\mathbf{x}$ is its corresponding eigenvector, then

$$(\mathbf{x}.\mathbf{A}\mathbf{x})/(\mathbf{x}.\mathbf{x}) = (\mathbf{x}.\boldsymbol{\lambda}\mathbf{x})/(\mathbf{x}.\mathbf{x}) = \boldsymbol{\lambda}.$$

Thus the expression $(\mathbf{x}_i.\mathbf{A}\mathbf{x}_i)/(\mathbf{x}_i.\mathbf{x}_i)$ is computed with each approximation $\mathbf{x}_i$ to the eigenvector. The method is continued until successive approximations to every component of the eigenvector and the eigenvalue are within the required accuracy.

The components of the vectors $\mathbf{x}_1$, $\mathbf{x}_2,\ldots$ may become very large, leading to significant round- off errors. This problem is overcome by dividing each component of $\mathbf{x}_i$ by the largest component and using this vector, which is in the same direction as $\mathbf{x}_i$, in the following iteration.

This method is very accurate since any error in computation only means that a new arbitrary vector has been introduced at that stage. Therefore, the only round-off errors that occur are those arising from the matrix multipication carried out during the last iteration. A flow chart for the Power Method is shown in Figure 5.3.

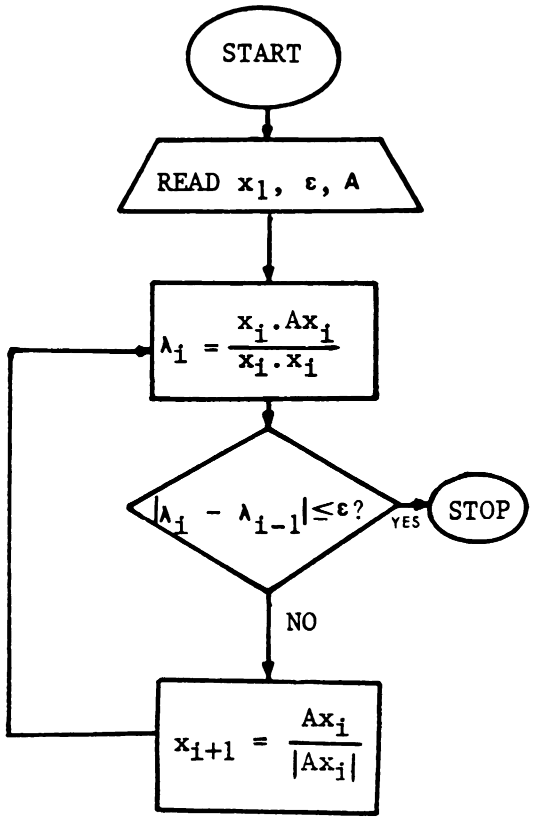

Figure 5.3 Power Method for solving an eigenvalue problem.

CHAPTER 6

RESULTS

In this chapter we present some results generated by our simulation of the system. Based on these results, we discuss the effects of power control on SIR, denial statistics and capacity of the system for both upstream and downstream links. The effects of the environmental parameters (α,σ) on the performance of the system as well as the feasibility of different degrees of power control, based on the dynamic ranges of transmitted powers are also discussed.

6.1 Load Distribution and Environmental Parameters

Distribution of load in the service area varies as the environmental parameters change. Shadow fading may cause a given mobile to receive the strongest signal from a base station that is not closest to it. The severity of this effect varies as α and σ change, since they change the mean and variance of the log-normal distribution of fading. To formulate the dependence of load distribution on α and σ, consider a mobile at distance d from a base station (See Figure 6.1.) For clarity of analysis in this section, we will refer to the geographic area closest to a base station as a "hexagon" as opposed to a "cell", which is the area receiving with the least attenuation from a base station. Hexagon would have been the shape of the cell if there was no shadow fading. Suppose that the base station is located at the center of a hexagon of radius R (R is the radius of a circle with the same area as the hexagon.) If there was no shadow fading then for $d < R$, this mobile would communicate with the base station in the same hexagon. The effect of shadow fading may be considered to be changing the effective distance between the transmitter and the receiver.

Let d^{ef} be the effective distance between the base station and the mobile due to shadowing. This means that the attenuation would have been the same if we had a mobile at distance d^{ef} from the base station and there was no shadowing. Thus we have

$$a = 1/(d^{ef})^{\alpha}, \tag{6-1}$$

where "a" is the attenuation factor. Now if $d^{ef} > R$, the

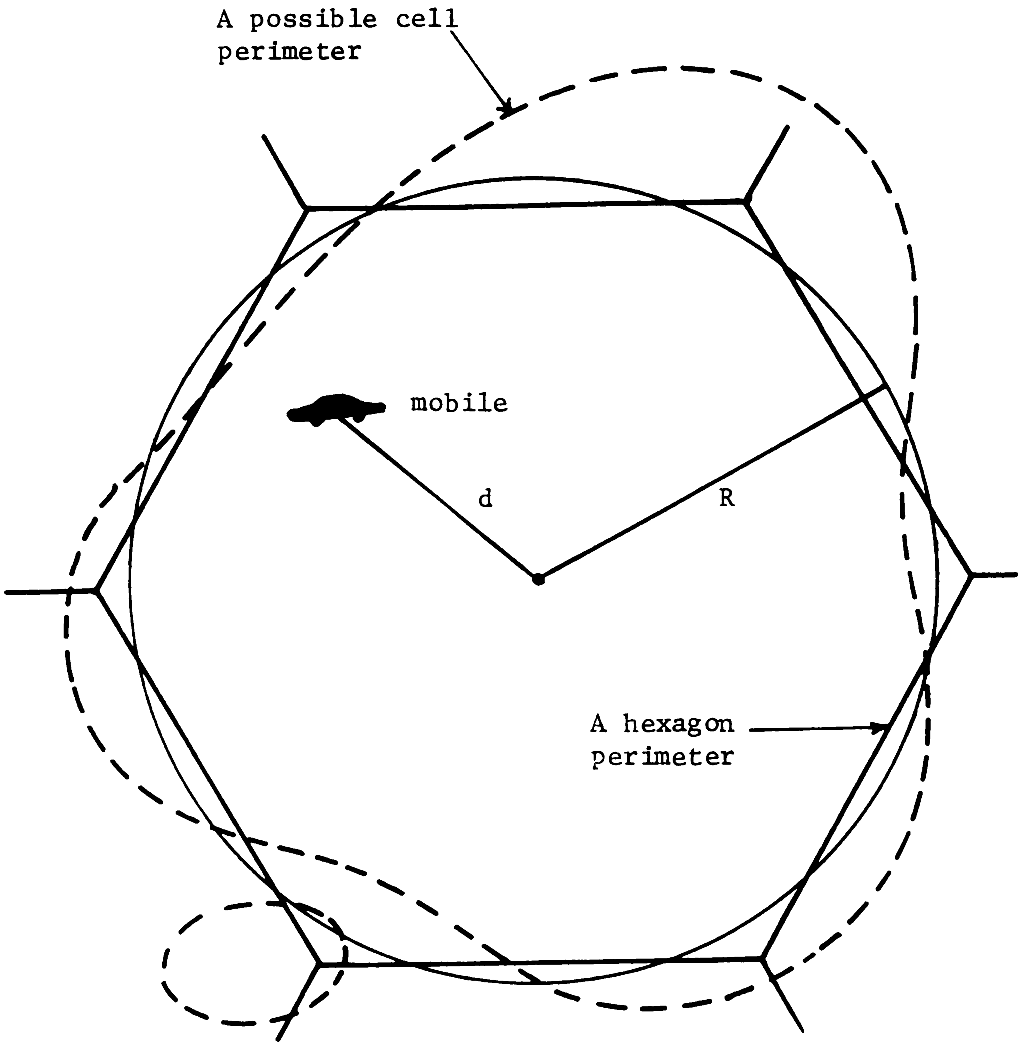

Figure 6.1 Geometry for load distribution
analysis.

mobile appears to be located outside the hexagon. The rate at which this occurs represents how load distribution may vary with shadowing. The attenuation factor a, and thus $1/(d^{ef})^{\alpha}$ have log-normal distributions with variance σ, and mean $10 \log_{10} 1/d^{\alpha}$ (See section 2.1.) So,

$$\Pr\{d^{ef} > R\} = \Pr\{10 \log_{10} 1/(d^{ef})^{\alpha} < 10 \log_{10} 1/R^{\alpha}\}$$

$$= \int_{-\infty}^{10 \log_{10} 1/R^{\alpha}} \frac{1}{\sqrt{2\pi}\,\sigma} \exp[\frac{-(t - 10 \log_{10} 1/d^{\alpha})}{2\sigma^2}] dt$$

$$= \Phi[(10 \log_{10} 1/R^{\alpha} - 10 \log_{10} 1/d^{\alpha})/\sigma].$$

Thus

$$\Pr\{d^{ef} > R\} = \Phi[\, 10\, \alpha/\sigma \log_{10} d/R \,], \qquad (6\text{-}2)$$

where $\Phi(x)$ is the normal probability distribution function of x, which is tabulated in the literature [C5] ($\Phi(x)=1-Q(x)$, where $Q(x)$ was defined in 3-3.)

Figure 6.2 shows $\Pr\{d^{ef} > R\}$ values versus the ratio d/R for different combinations of α and σ (different values of α/σ.) We observe that load distribution varies as a function of the ratio α/σ. As this ratio decreases, more mobiles appear to be located outside the hexagon. Thus a smaller α/σ causes more mobiles to link up with base stations not closest to them. As the load in a hexagon grows, the number of such mobiles also grows.

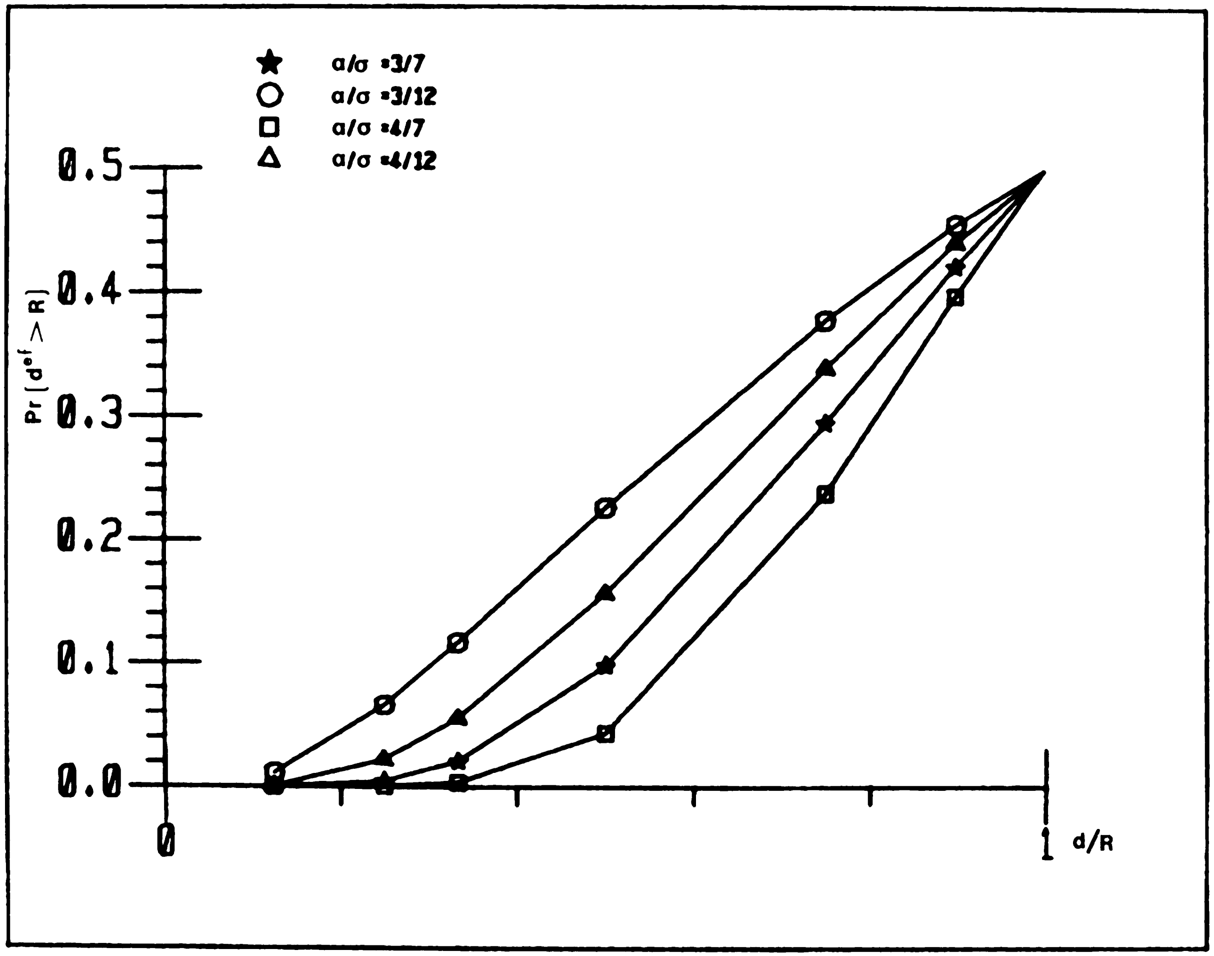

Figure 6.2 Pr{d^{ef}> R} values versus the ratio d/R for different α/σ values.

This results in a balancing effect between cells when the load is not uniform from cell to cell.

The balancing effect can be observed very clearly in our simulation results. Table 6.1 shows the ratios of the load in the center cell, cells in the intermediate ring, and cells in the outer ring. Results are shown for different load distributions (tapered and uniform), and different α/σ ratios (α = 3 or 4, σ = 7 or 12.) For the uniform load distribution, there is little change as α/σ changes. This is because with uniform load as α/σ decreases, the number of mobiles that link up to base stations of neighboring hexagons increases by approximately the same number in every hexagon. This results in about the same number of users in every cell. In the tapered load distribution case, however, variations of α/σ causes a marked change in the load distribution. It is obvious in this case that as α/σ decreases, the load distribution becomes more uniform. Table 6.1 shows that a physical load distribution of ratios 7.5, 4, and 1 in the center hexagon, hexagons in the middle ring and hexagons in the outer ring changes into a distribution of ratios 5, 2.7, and 1 as α/σ gets as small as 1/4 (α = 3, σ = 12.) It will be shown in the next sections that this effect reduces the necessity for cell-to-cell balancing, which is fortunate since it is not an easy task to perform.

Table 6.1 Ratios of the load in different cells as α/σ varies.

LOAD DISTRIBUTION	FADING	α/σ	CENTER CELL	INTERMED. CELL	OUTER CELL
UNIFORM	NO FADING	-	1	1	1
	$\alpha=4$, $\sigma=7$	4/7	1	1	1.15
	$\alpha=3$, $\sigma=7$	3/7	1	1	1.06
	$\alpha=4$, $\sigma=12$	1/3	1	1.06	1.02
	$\alpha=3$, $\sigma=12$	1/4	1.04	1.03	1
TAPERED	NO FADING	-	7.5	4	1
	$\alpha=4$, $\sigma=7$	4/7	7.1	3.8	1
	$\alpha=3$, $\sigma=7$	3/7	6.8	3.7	1
	$\alpha=4$, $\sigma=12$	1/3	6.5	3.4	1
	$\alpha=3$, $\sigma=12$	1/4	5.0	2.7	1

6.2 Upstream Results

Results were generated for the upstream case using (5-4), (5-6), and solving the eigenvalue problem in (4-10). Here we present and discuss the results for denial rates for the three cases of no balancing, in-cell balancing, and cell-to-cell balancing. Results are also discussed for dynamic ranges of the required transmitted powers for in-cell balancing, and cell-to-cell balancing. Effects of the environmental parameters on these results are also discussed.

6.2.1 Denial Statistics

Figures 6.3 to 6.8 show the denial probability values of the upstream case, versus load per cell for the <u>center</u> cell of the system; and Figures 6.9 to 6.14 show these values versus <u>average</u> load per cell throughout the system. Results are given for both the uniform, and the tapered load distributions. Typically acceptable values of blocking in a radiotelephone system are in the 1% to 2% range, so that probability of denial in the no-balancing cases are quite unacceptable except at trivially low traffic loads. The problem is very severe for the upstream case because the near-far effect is significant whenever two or more users are accessing the system.

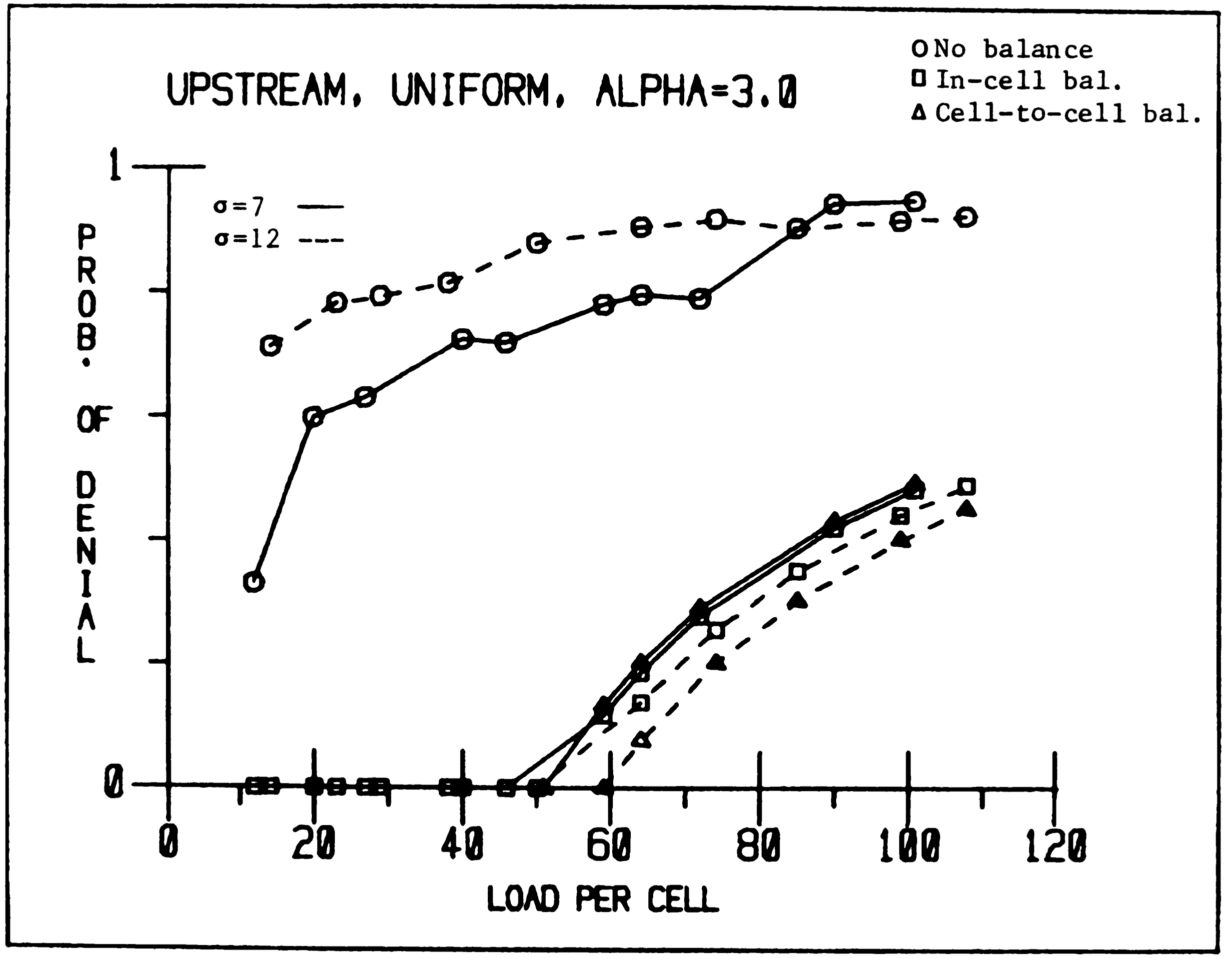

Figure 6.3 Denial statistics for the center cell, α = 3.0, uniform traffic distribution, upstream.

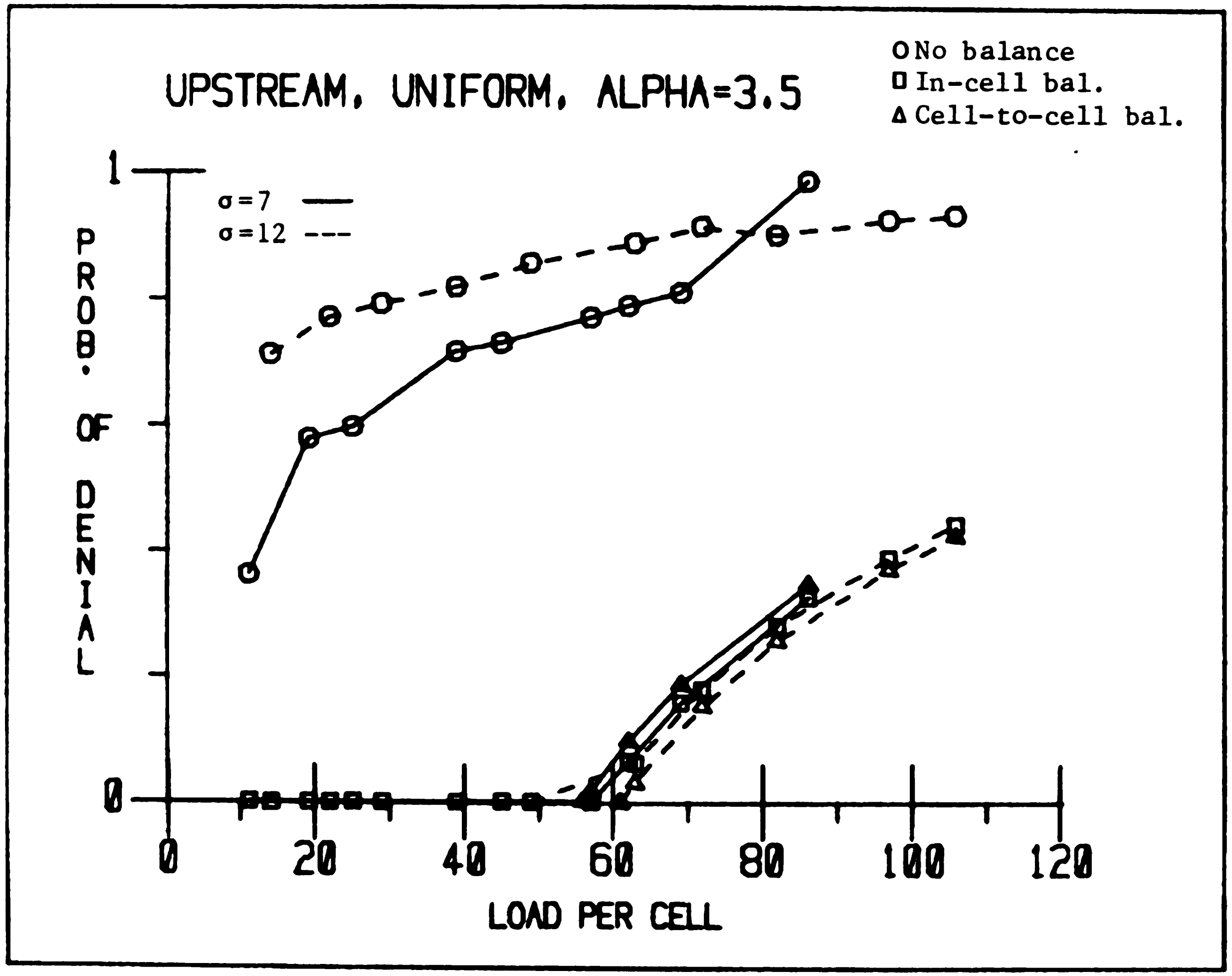

Figure 6.4 Denial statistics for the center cell, α = 3.5, uniform traffic distribution, upstream.

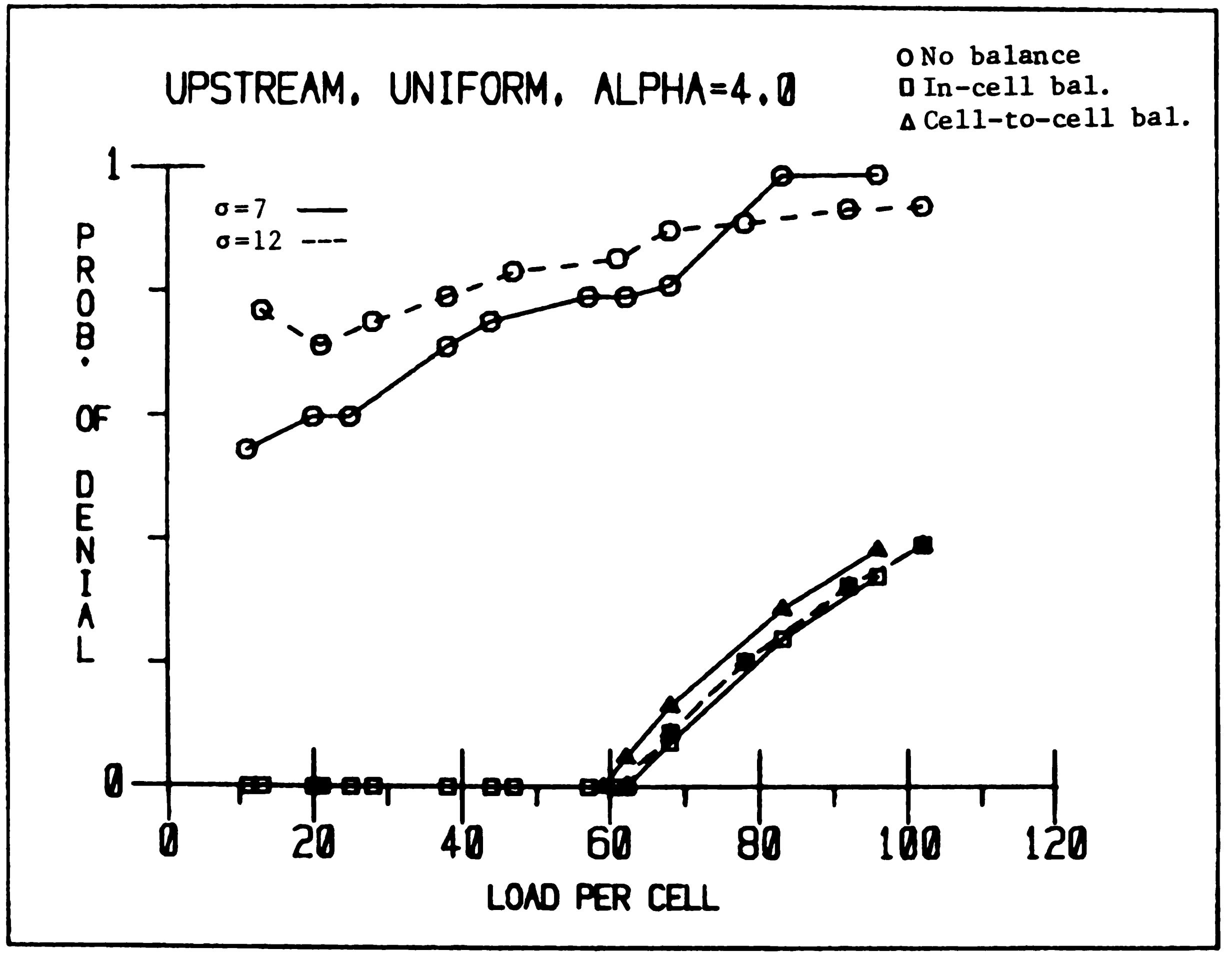

Figure 6.5 Denial statistics for the center cell, α = 4.0, uniform traffic distribution, upstream.

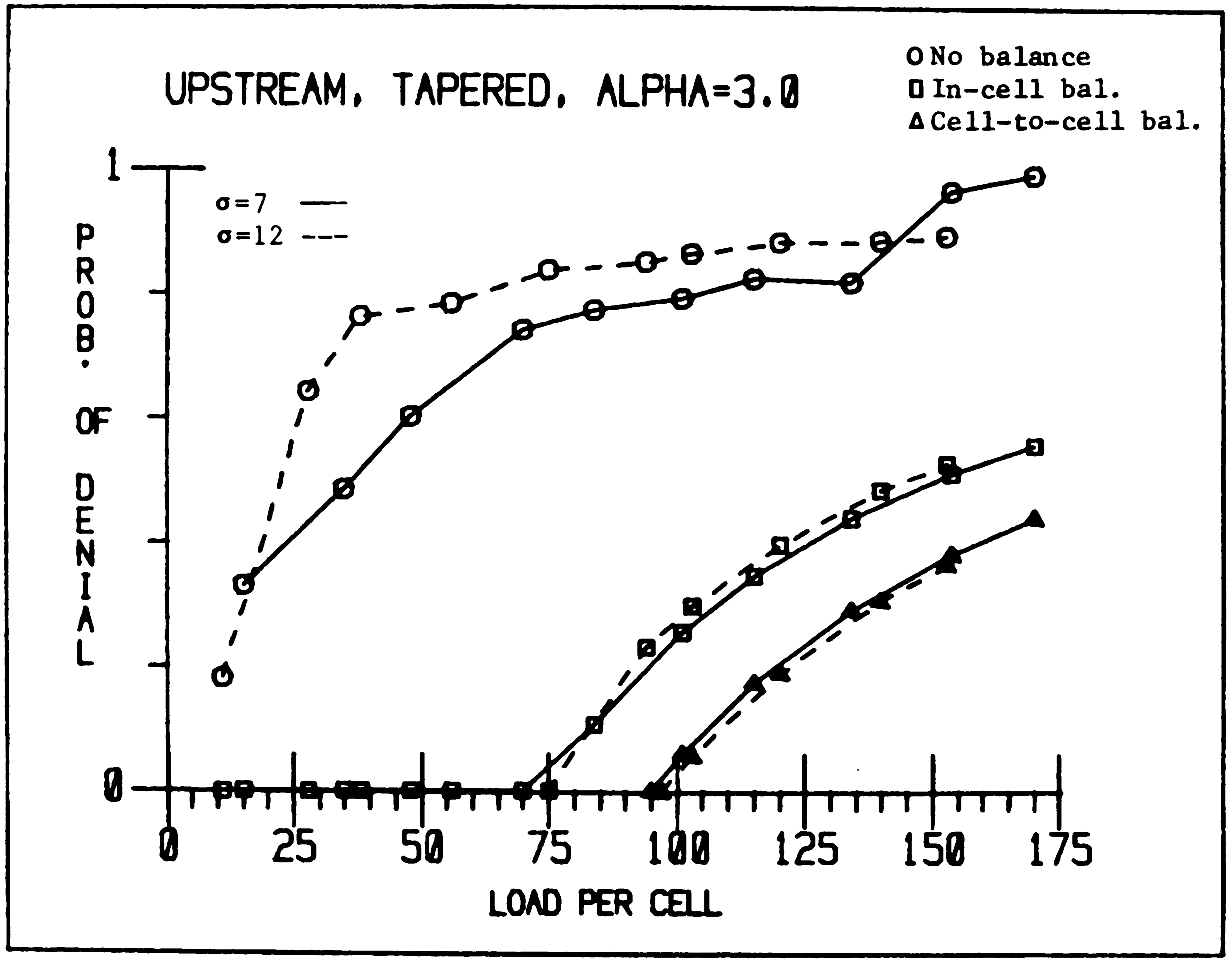

Figure 6.6 Denial statistics for the center cell, α = 3.0, tapered traffic distribution, upstream.

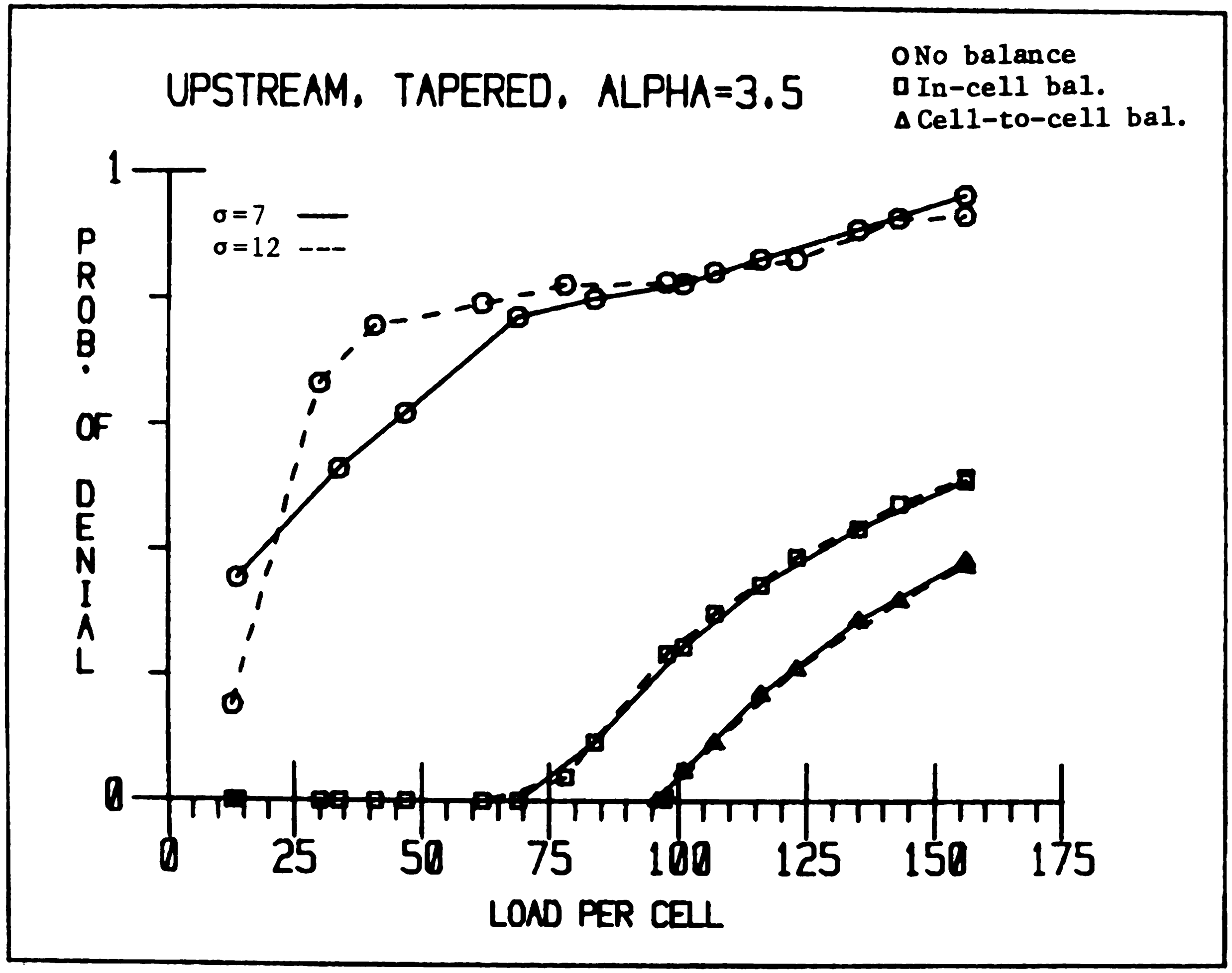

Figure 6.7 Denial statistics for the center cell, α = 3.5, tapered traffic distribution, upsream.

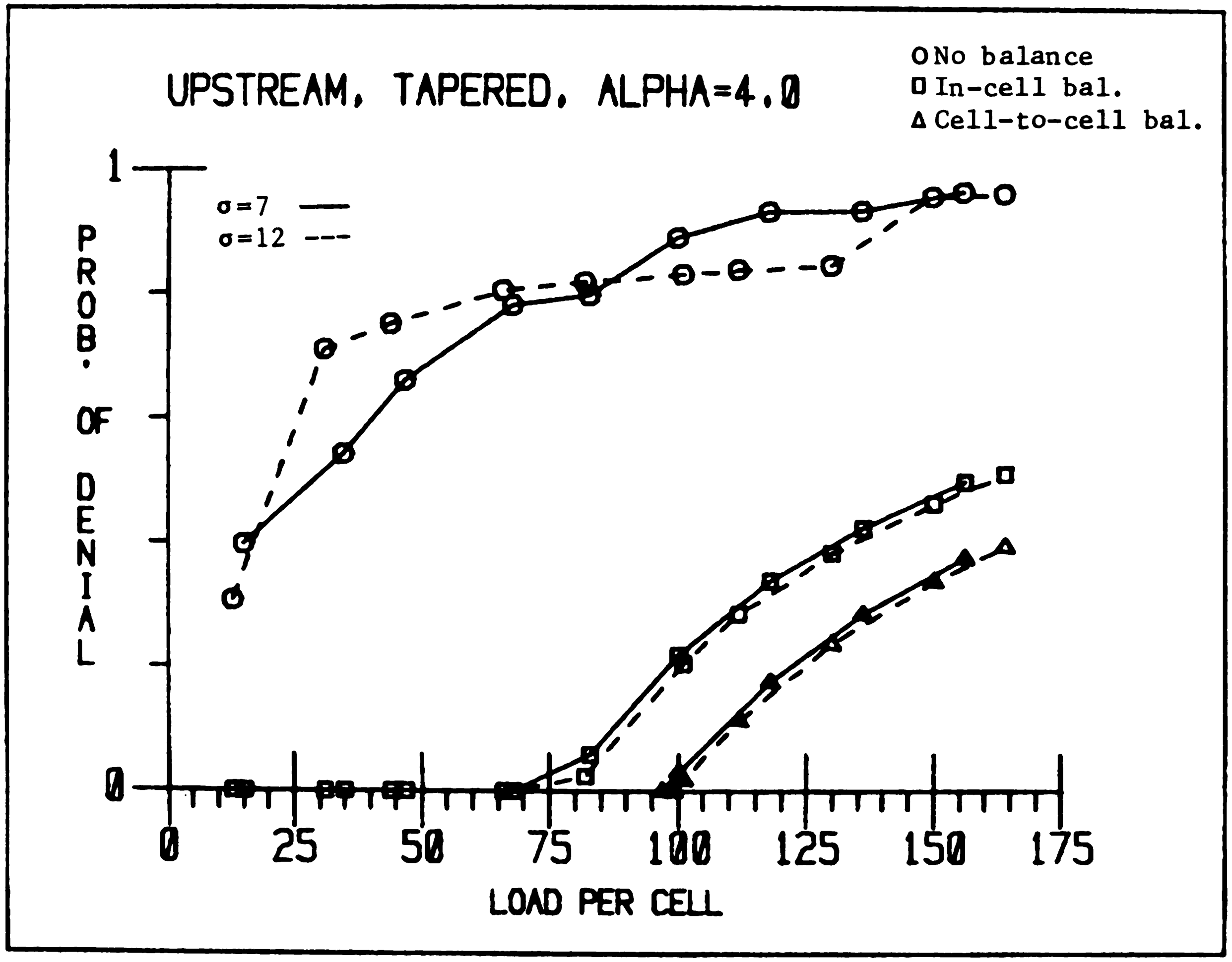

Figure 6.8 Denial statistics for the center cell, α = 4.0, tapered traffic distribution, upstream.

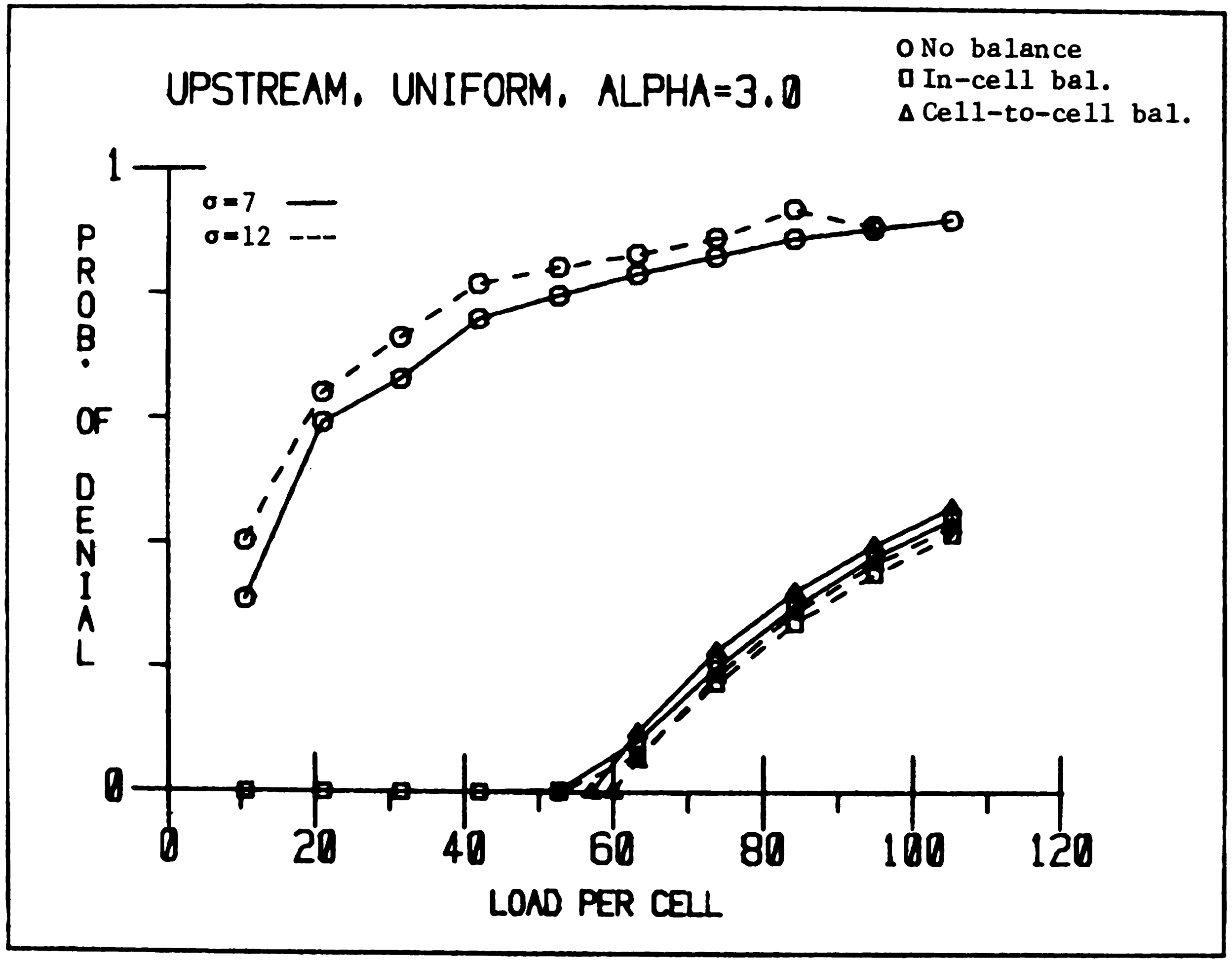

Figure 6.9 Denial statistics for the total system, α = 3.0, uniform traffic distribution, upstream.

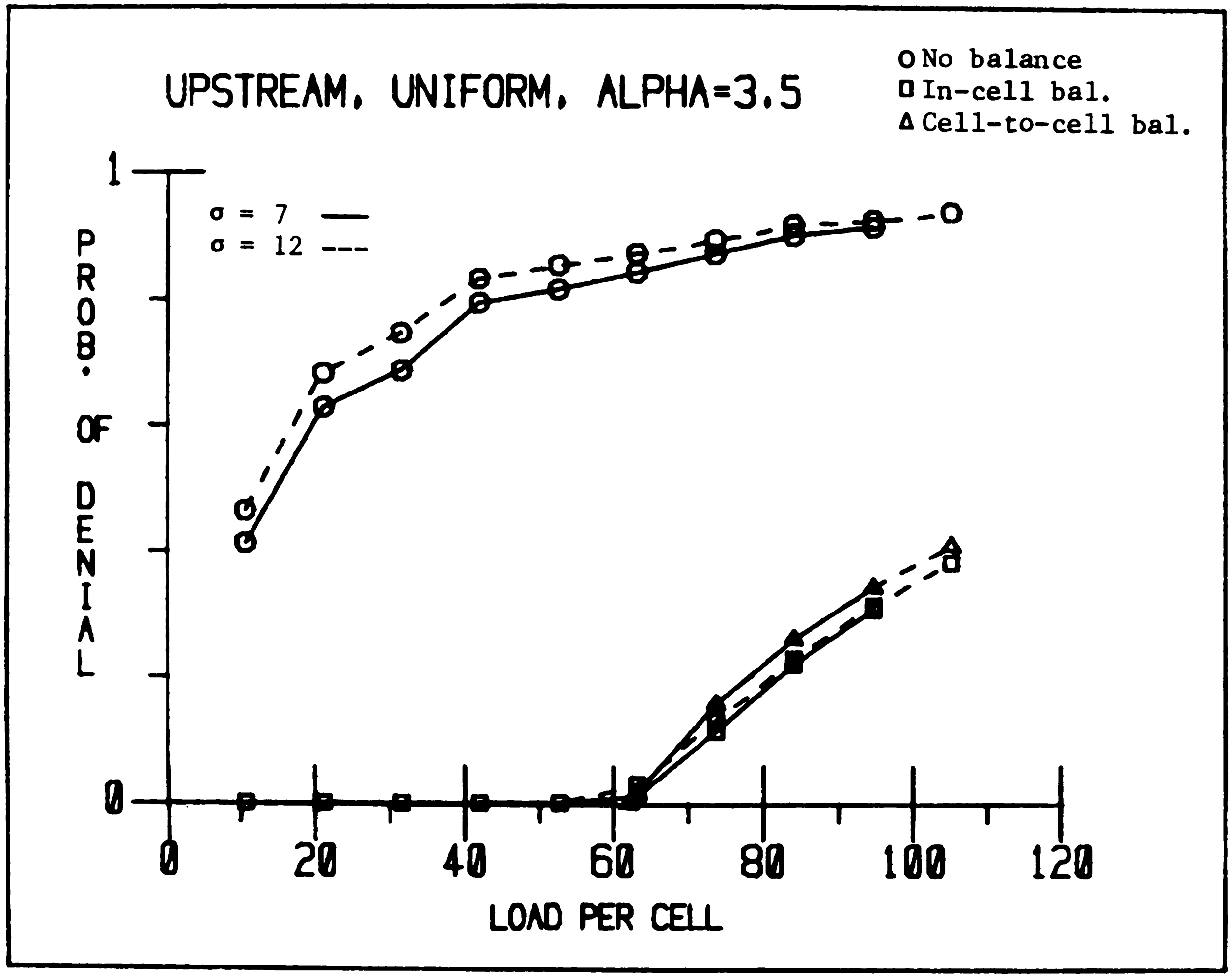

Figure 6.10 Denial statistics for the total system, $\alpha = 3.5$, uniform traffic distribution, upstream.

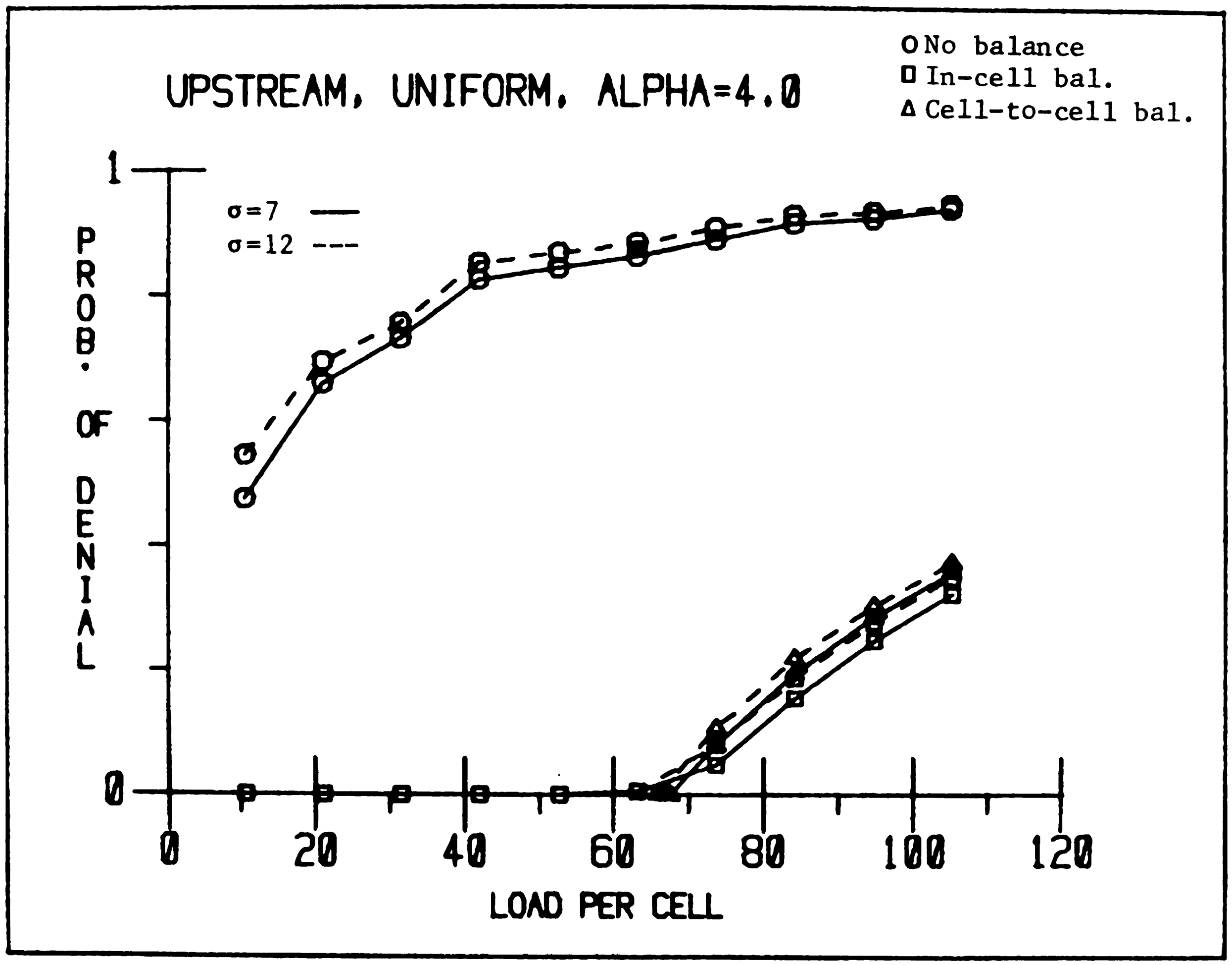

Figure 6.11 Denial statistics for the total system, α = 4.0, uniform traffic distribution, upstream.

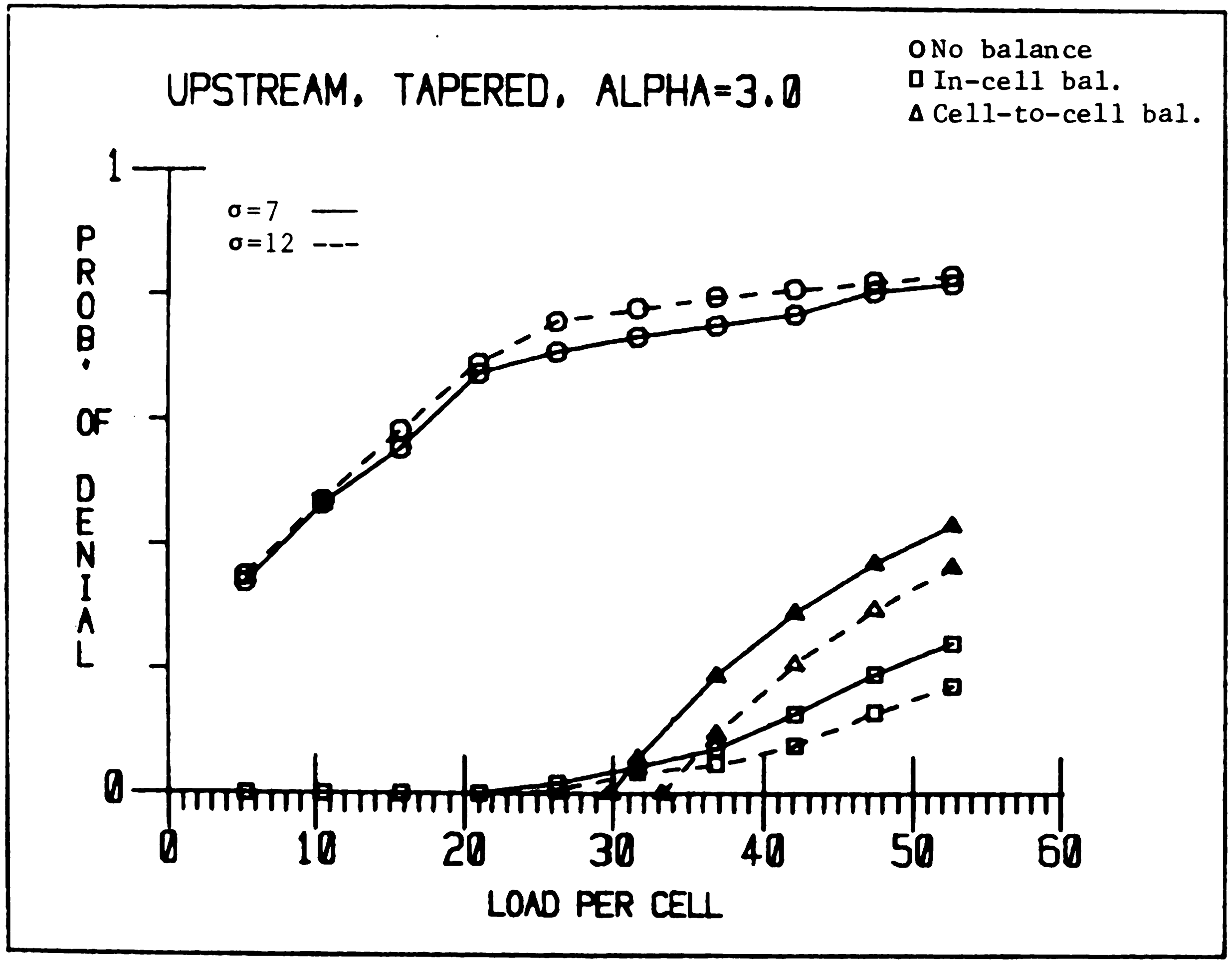

Figure 6.12 Denial statistics for the total system, α= 3.0, tapered traffic distribution, upstream.

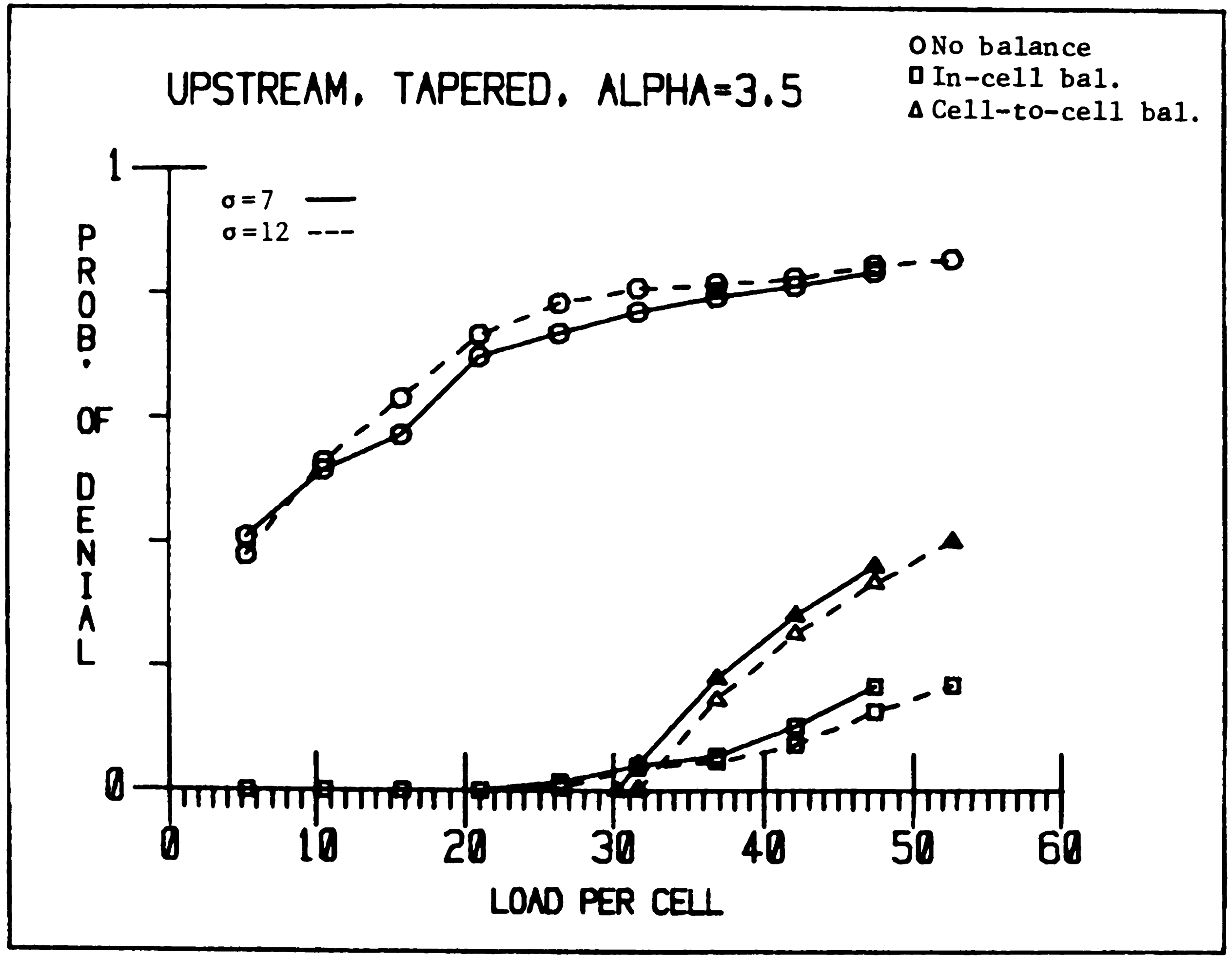

Figure 6.13 Denial statistics for the total system, α= 3.5, tapered traffic distribution, upstream.

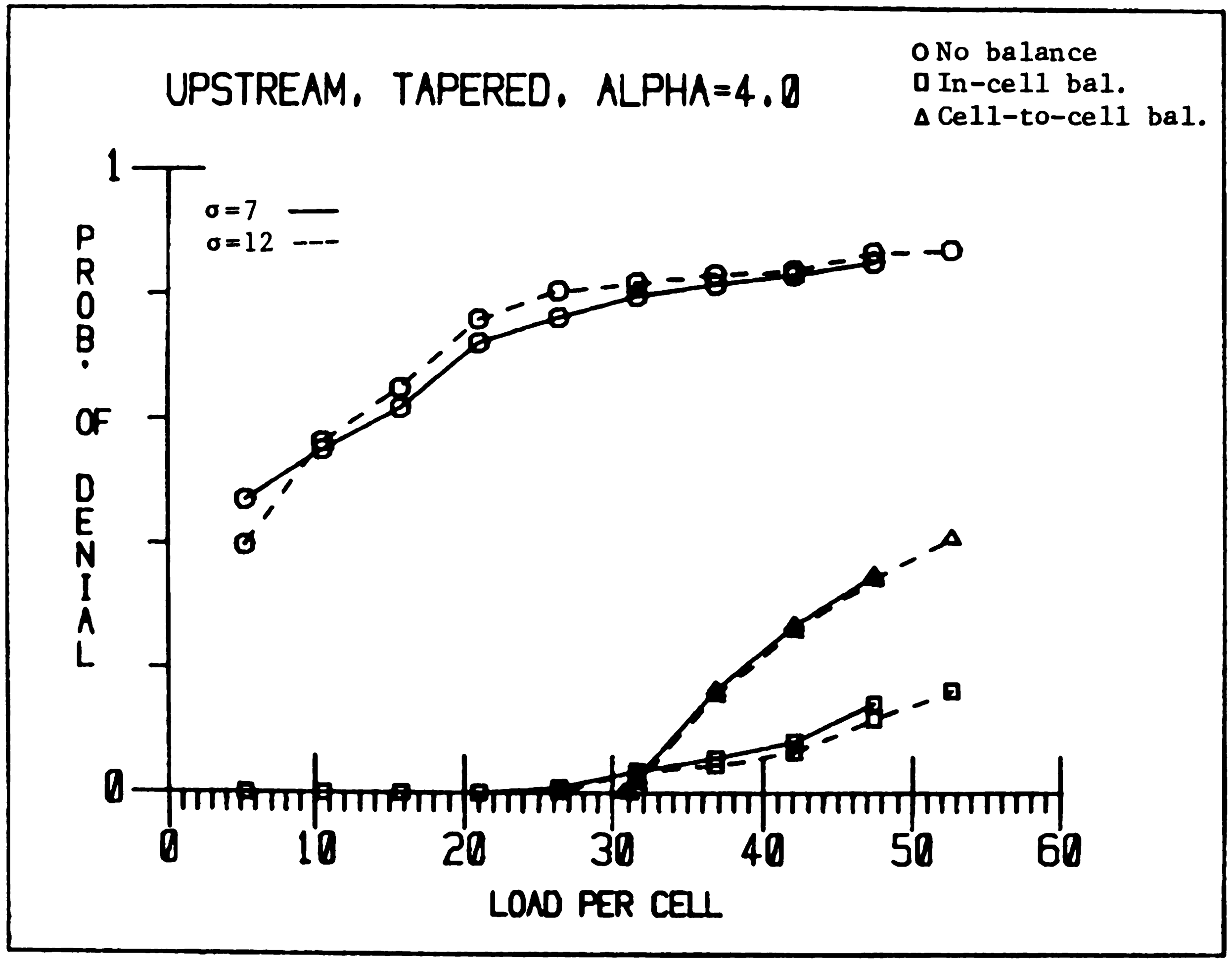

Figure 6.14 Denial statistics for the total system, α= 4.0, tapered traffic distribution, upstream.

We note also that when no balancing is used, the capacity of the system reduces as α increases from 3 to 4. This can be explained by the following: Suppose there are only two users (a and b) in a cell, transmitting the same amount of power P (i.e. no power control.) Also suppose that they are located at the effective distances of d_a^{ef} and d_b^{ef} from the base station. Neglecting the effects of the neighboring cells, the SIR experienced by the base station for the signal from a is

$$SIR_a = \frac{P/(d_a^{ef})^{\alpha}}{P/(d_b^{ef})^{\alpha} + P/(d_a^{ef})^{\alpha}} = \frac{(d_b^{ef})^{\alpha}}{(d_a^{ef})^{\alpha} + (d_b^{ef})^{\alpha}}. \quad (6\text{-}3)$$

Now, to illustrate the effect of on the near-far effect let $d_b^{ef} << d_a^{ef}$. Thus (6-3) reduces to

$$SIR_a \approx (d_b^{ef}/d_a^{ef})^{\alpha}. \quad (6\text{-}4)$$

(6-4) shows that a more rapid attenuation law (larger α) results in a worse SIR and thus a lower capacity for the system in the upstream link.

We also note that with no power control, capacity of the system increases as σ decreases from 12 to 7. This is also due to the near-far effect. A larger σ means a larger spread in the value of the effective distances of the mobiles (i.e. The ratio of the maximum effective distance to the minimum effective distance is likely to be larger.) This results in a more severe near-far effect.

Considering the balanced case results, for the uniform traffic distribution, the two types of balancing are barely distinguishable at all levels of denial, so that in the uniform traffic distribution case there appears to be little advantage, in terms of system capacity, in implementing the cell-to-cell balancing algorithm. This is due to the fact that with uniform load, there already exists some degree of balance from cell to cell, without the application of the cell-to-cell balancing algorithm. However, with in-cell balancing the increase in system capacity over the non-balanced case is very significant, though difficult to quantify at low traffic levels due to the low levels of statistical significance attached to our non-balanced results at these levels. The improvement ratios we encountered were more than 1000% for the upstream case.

For the tapered traffic distribution, our results show that in-cell balancing improves the capacity of the upstream link by about the same amount as for the uniform case. Further improvement of about 15% is obtained when cell-to-cell balancing is applied. This improvement is at all levels of denial rate for the center cell. In the total system, however, the improvement is only at the low levels of denial rate (1% to 2%). This improvement for the total system is due to the "matching" effect of the cell-to-cell balancing upon the individual cell

capacities; where the capacity of each cell is adjusted such that the ratio of the capacities match the ratio of the loads for all cells. With in-cell balancing the outer cells use only a small portion of their actual capacity. This extra capacity is sacrificed in the cell-to-cell balancing algorithm in order to increase the capacity of the heavily-loaded cells (center cell, in the tapered load distribution.) However, the effect of the capacity sacrifice of one cell on another is not very large and as the load grows throughout the system, the cells around the center cell have to give up much of their capacity to compensate for the high load in the center cell. Although the load in the outer individual cells is much smaller than the center cell, the total load in these cells gets large as the load in the system grows. Thus the denial rate of the total system in the cell-to-cell balancing case climbs above the in-cell balancing case at higher loads. This, however, occurs at denial levels that are unacceptable and a system at such levels of denial needs to be expanded (Sizes of the cells must be reduced resulting in lighter load per cell.)

Comparing the uniform and tapered load distributions, it is obvious that the capacity of the system, when balanced, is much higher for the uniform load than for the tapered one if the total system is considered (about 50%.) This higher capacity is due to the "matching" effect in

the cell-to-cell balancing case. In the in-cell balanced case, however, no such sacrifice of capacity exists between cells, and the denial rates do not increase as rapidly for the tapered case. So at higher loads, the in-cell balancing denial rate for the tapered load gets much closer to that of the uniform load case.

It can also be seen in each of these figures that upstream link capacity grows as α decreases from 4 to 3. However, the difference is very small and not more than 15% depending on the mobile distribution and traffic load. Comparing the balanced results for $\sigma = 7$ and $\sigma = 12$, the lack of sensitivity to the shadow fading dB spread is striking. The variation in capacity as σ varies from 7 to 12 is not more than 20% and contrary to the corresponding results for a narrow band frequency re-use system, these results are better for $\sigma = 12$ than for $\sigma = 7$. This can be explained by the balancing effect due to the decrease of the ratio α/σ explained in section 6.1. This effect is more obvious in the in-cell balanced results for the tapered load distribution (Figures 6.11 to 6.13) where the denial rate decreases as α/σ decreases. The effect is stronger in this case because the physical load distribution is not uniform and no attempt has been made to balance the system from cell to cell.

6.2.2 Dynamic Ranges of Transmitted Powers

Figures 6.15 to 6.20 show the average dynamic range of powers (DRP^U) required of the mobiles to transmit in order to achieve balance in the upstream link. For the upstream link these ranges are the same for the cases where only in-cell balancing is used, and cases where cell-to-cell balancing is also applied. It can be seen that these ranges are rather high and possibly impractible for some parameters, particularly at heavy loads. The high values of these ranges are results of the severity of the near-far effect. As we mentioned in section 5.2, for the upstream case in-cell balancing is accomplished by adjusting the individual transmission powers P^U_{ik} according to (4-4) such that the signal power $\mathcal{P}^U$ received by all mobiles is the same. Thus for cell i we have

$$DRP^U_i = \frac{\max\ (P^U_{ik})}{\min\ (P^U_{ik})} = \frac{\mathcal{P}^U/\min(a_{iki})}{\mathcal{P}^U/\max(a_{iki})}, \qquad (k=1,\ldots,L_i)$$

Thus

$$DRP^U_i = \frac{\max(a_{iki})}{\min(a_{iki})} = \left[\frac{\max\ d^{ef}_{iki}}{\min\ d^{ef}_{iki}}\right]^{\alpha}, \ (k=1,\ldots,L_i.) \qquad (6\text{-}5)$$

This ratio can take on arbitrary large values, and there is no limit that can be imposed on it. It is obvious from (6-5) and the results that DRP^U grows very rapidly as α

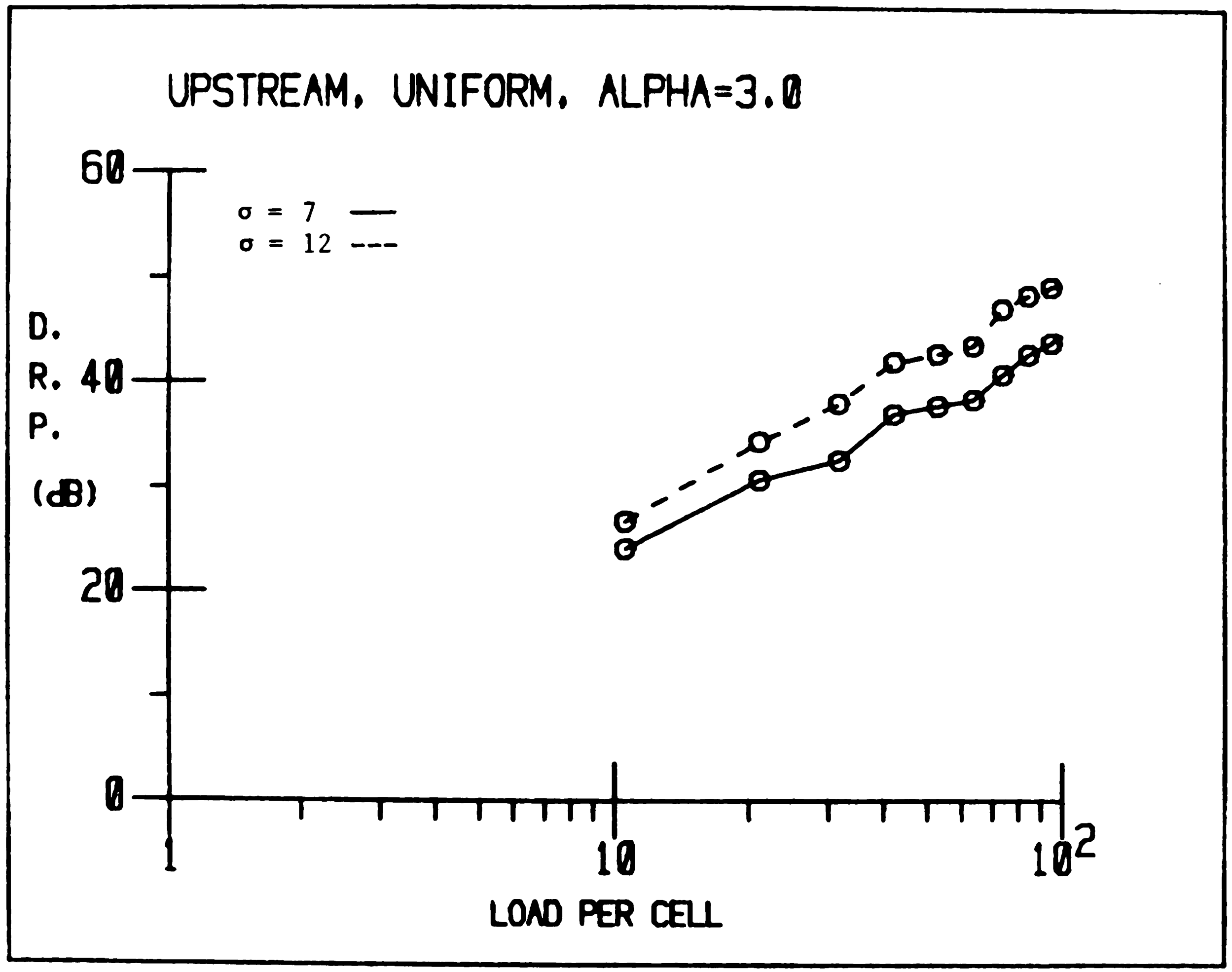

Figure 6.15 Average power control dynamic ranges required for upstream link balance, α=3.0, uniform traffic.

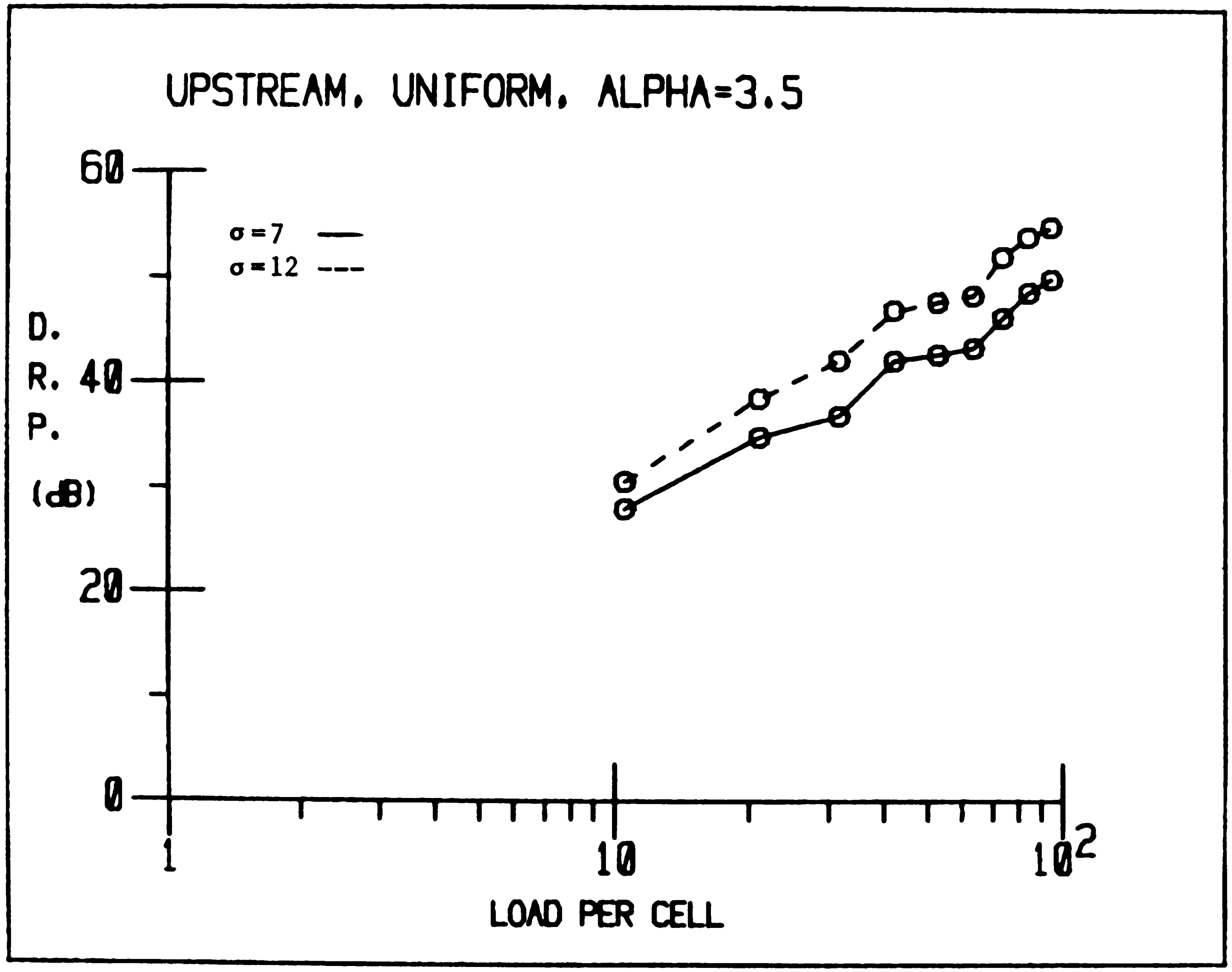

Figure 6.16 Average power control dynamic ranges required for upstream link balance, α=3.5, uniform traffic.

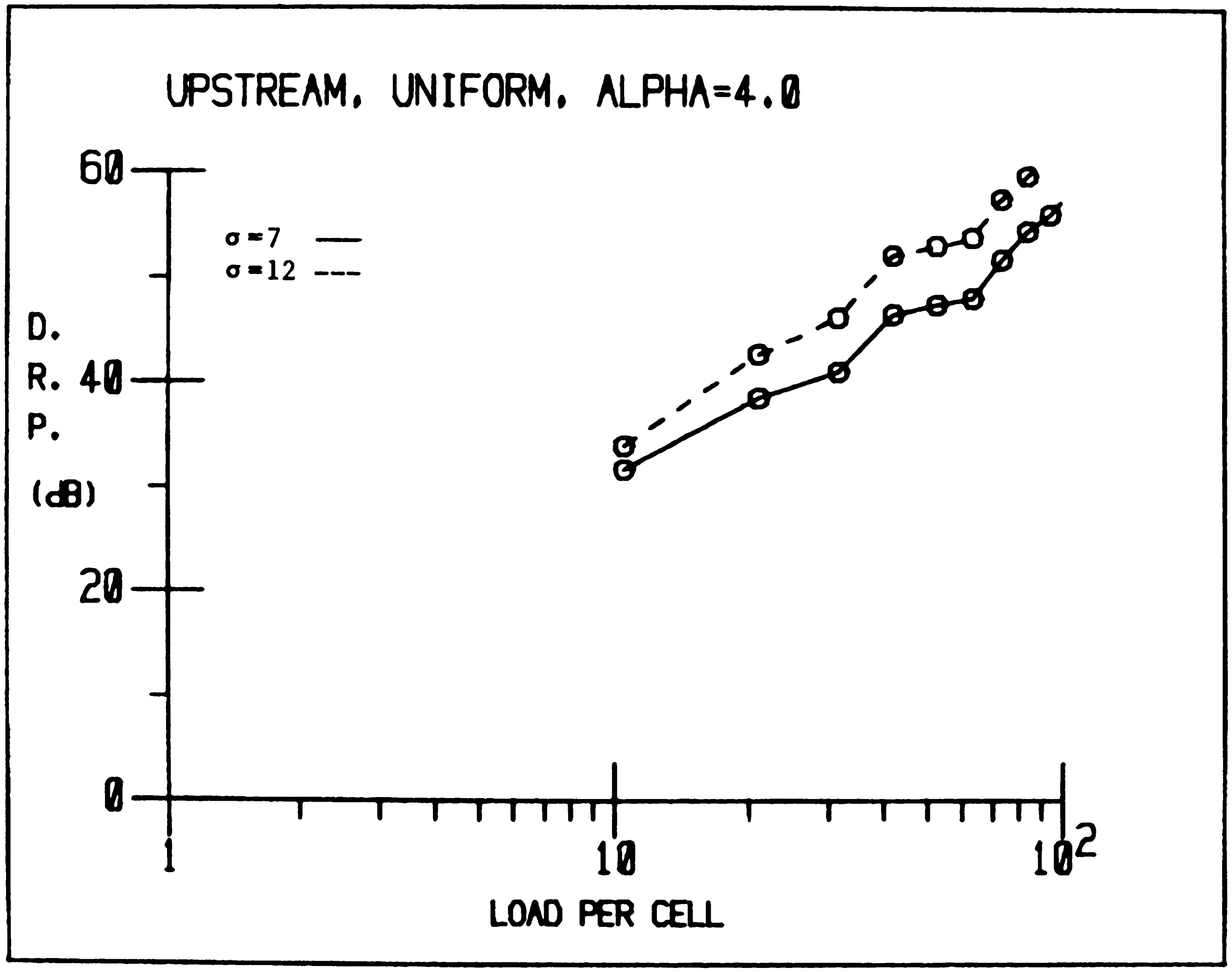

Figure 6.17 Average power control dynamic ranges required for upstream link balance, α=4.0, uniform traffic.

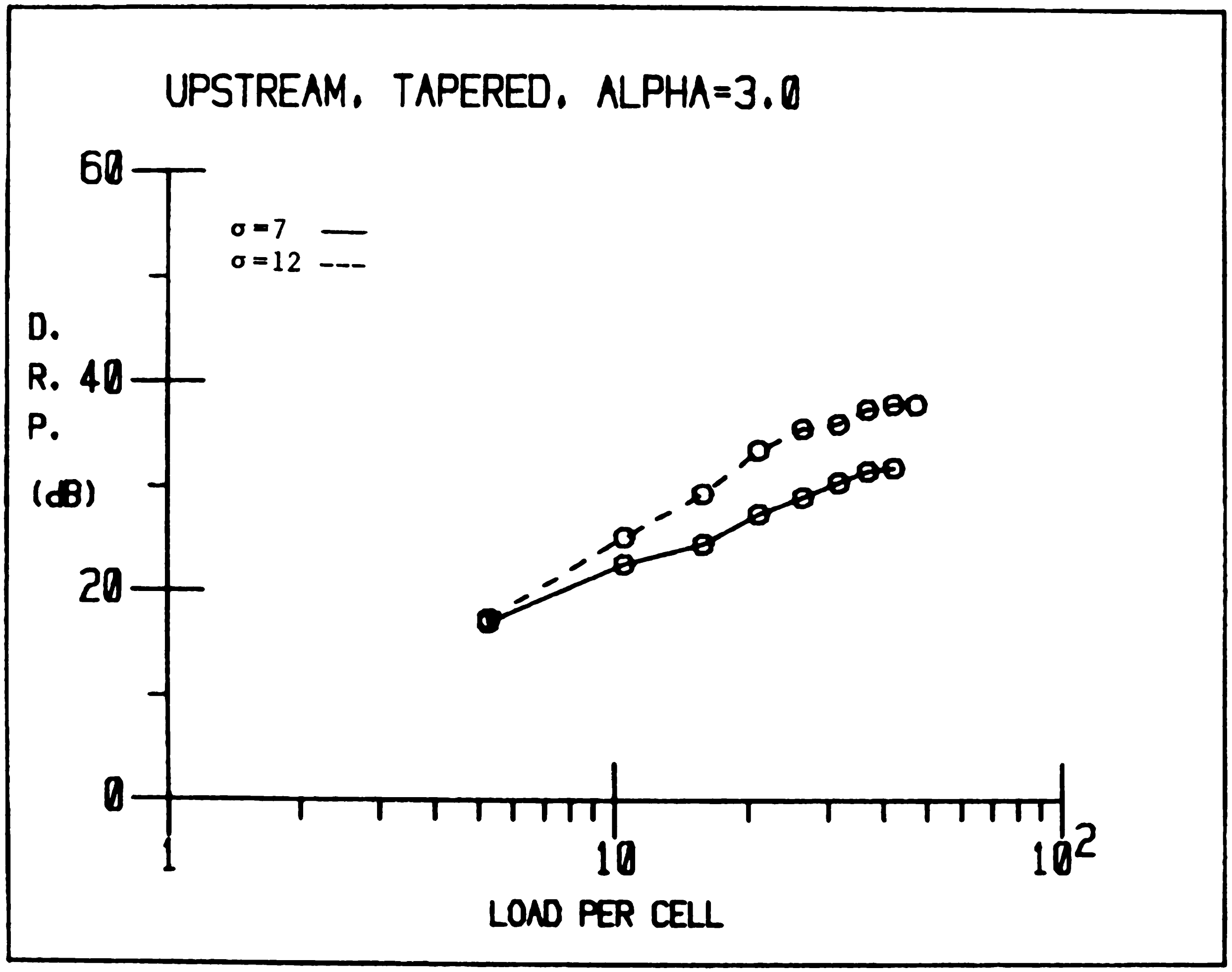

Figure 6.18 Average power control dynamic ranges required for upstream link balance, α=3.0, tapered traffic.

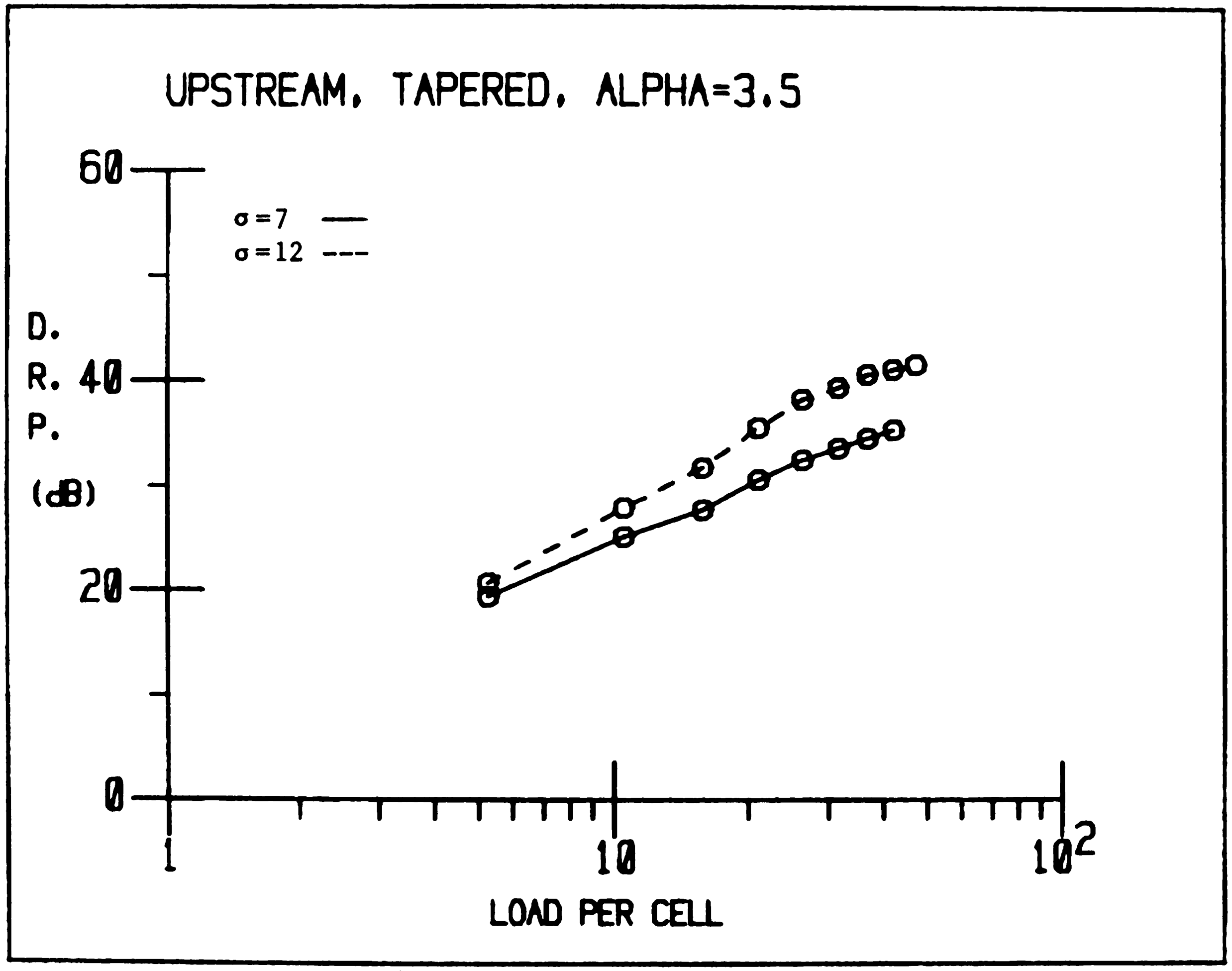

Figure 6.19 Average power control dynamic ranges required for upstream link balance, α=3.5, tapered traffic.

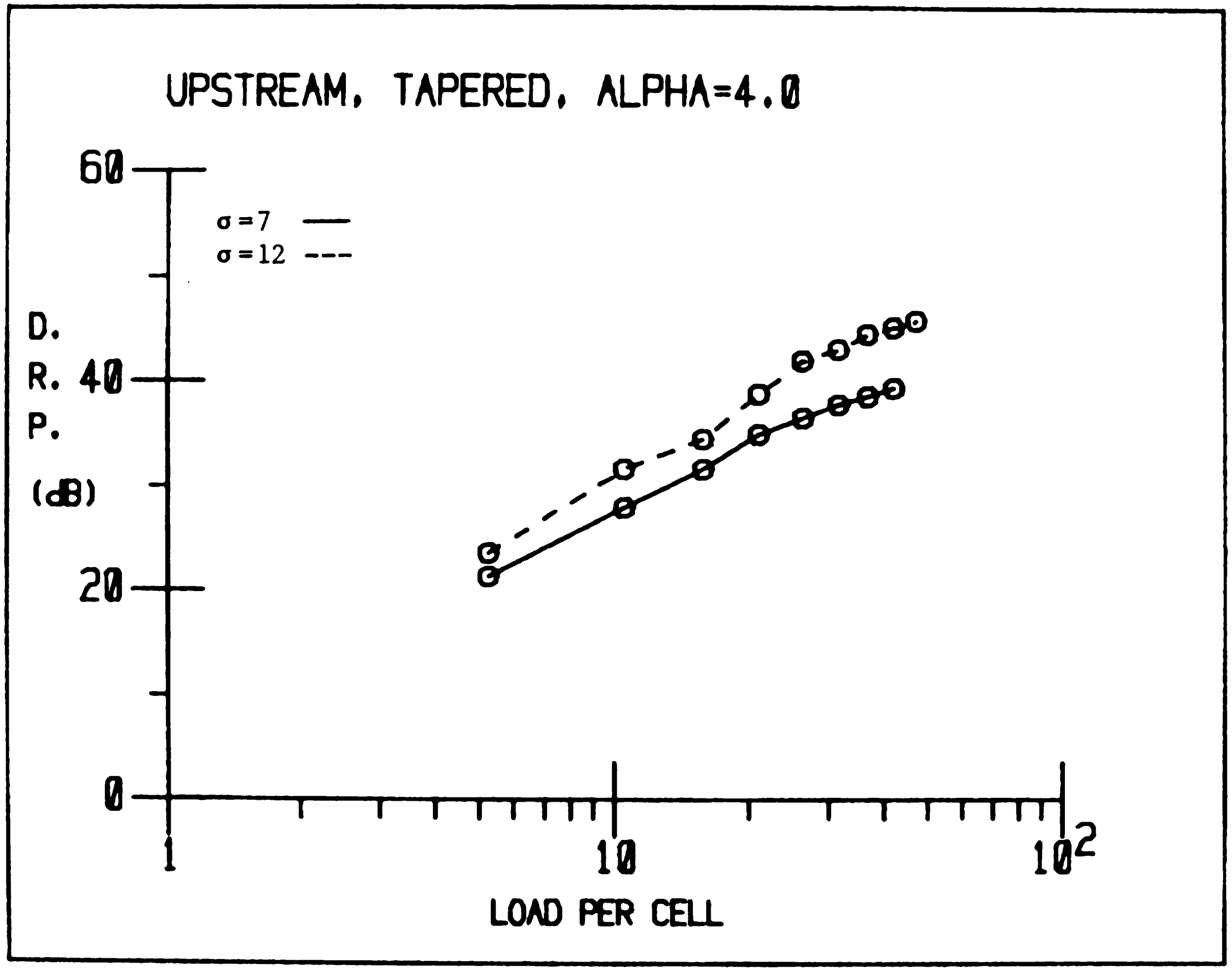

Figure 6.20 Average power control dynamic ranges required for upstream link balance, α=4.0, tapered traffic.

gets larger. Results show that as α goes from 3 to 4, the average DRP^U increases by more than 10 dB at full traffic capacity (onset of denial.) We also note that the dynamic ranges grow as σ gets larger. As σ goes from 7 to 12 the average DRP^U increases by more than 7 dB at full traffic capacity. Table 6.2 shows these values at full traffic capacity. This increase is due to the fact that larger σ causes a more severe near-far effect, by causing a larger spread in the values of the effective distances.

If a more restricted range is employed for the upstream link (i.e. if there is a fixed upper and lower limit to transmitted power) the resultant near-far effect will have some effect on system capacity and performance. Such a truncation will result in an "outage" phenomenon similar to the outage that occurs with narrowband systems due to shadowing. The degree of degradation will depend strongly on the type of modulation and its susceptability to near-far effect. Direct-Sequence (Pseudo-Noise) Signals are well known to be strongly sensitive to near-far effect, whereas frequency-hopping systems are far less sensitive. The latter is particularly true if limiters are used in each hop-frequency channel [C6]. This strongly indicates in favor of using FH rather than DS modulation for spread-spectrum cellular mobile radio.

Table 6.2 Power control dynamic ranges required at full system capacity for the upstream link.

	UNIFORM		TAPERED	
	$\sigma=7$	$\sigma=12$	$\sigma=7$	$\sigma=12$
$\alpha=3$	37.8 dB	42.8 dB	29.1 dB	36.6 dB
$\alpha=3.5$	42.8 dB	47.8 dB	33.6 dB	39.0 dB
$\alpha=4$	53.9 dB	53.9 dB	36.1 dB	42.0 dB

6.3. Downstream Results

Results were generated for the downstream link using (5-5), (5-7) and solving the eigenvalue problem in (4-20). Here we examine the results of denial rates for different degrees of power control, and the dynamic ranges of the required transmitted powers for the balanced cases. These results are also compared for different environmental parameters.

6.3.1 Denial Statistics

Figures 6.21 to 6.26 show the values of the denial rates for the downstream case versus load per cell for the center cell of the system, and Figures 6.27 to 6.32 show the denial rates versus average load per cell throughout the system. Results are given for both the uniform and the tapered load distributions. Here, although the denial rates for the unbalanced case are not as bad as the upstream case, the capacity of the system is still very low (about 15 at 1% to 2% denial rates.) The problem is less severe for the downstream case because the "corner effect" is less severe than the "near-far" effect, and requires relatively high traffic levels to become noticeable.

Also in the downstream case with no balancing,

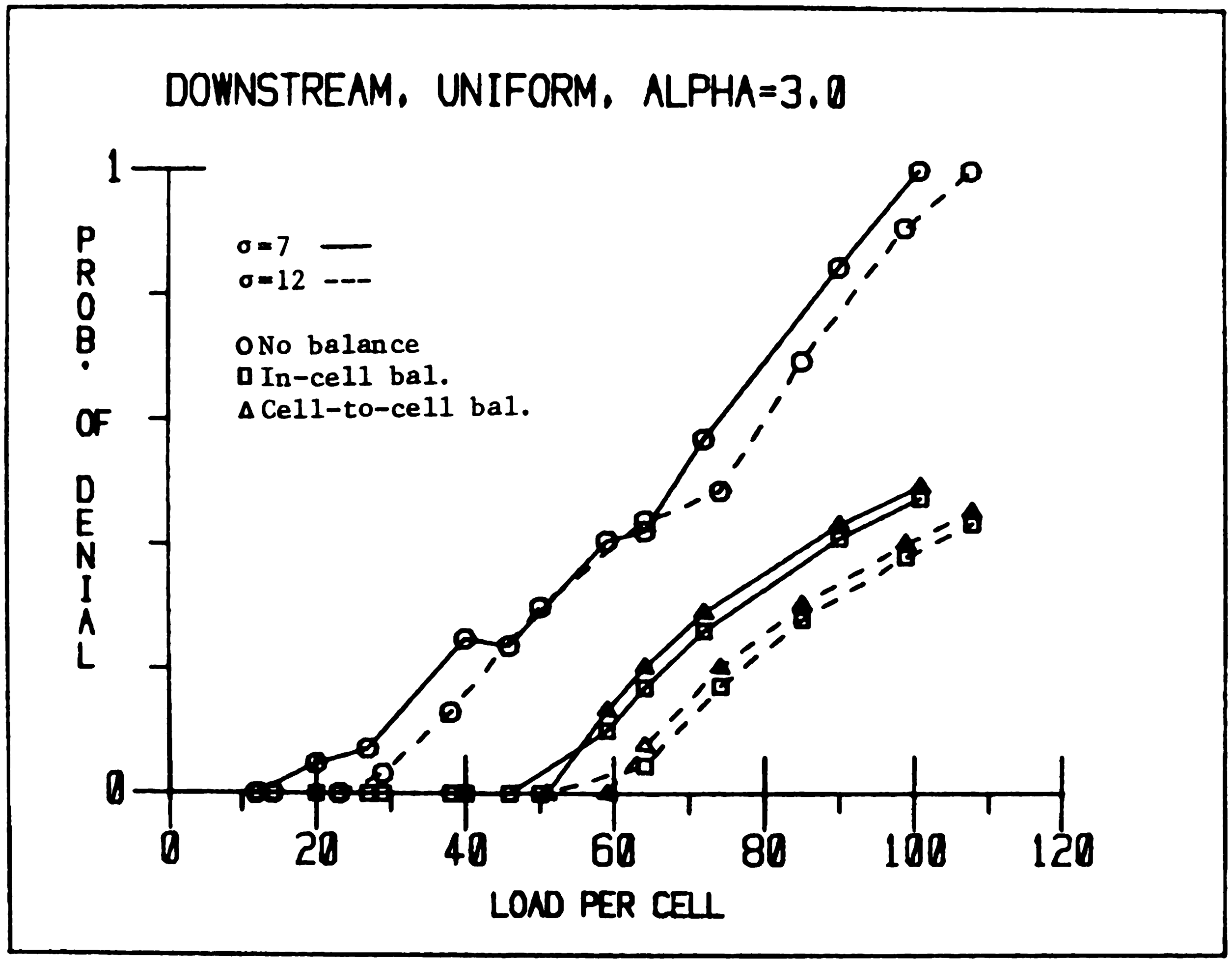

Figure 6.21 Denial statistics for the center cell, $\alpha = 3.0$, uniform traffic distribution, downstream.

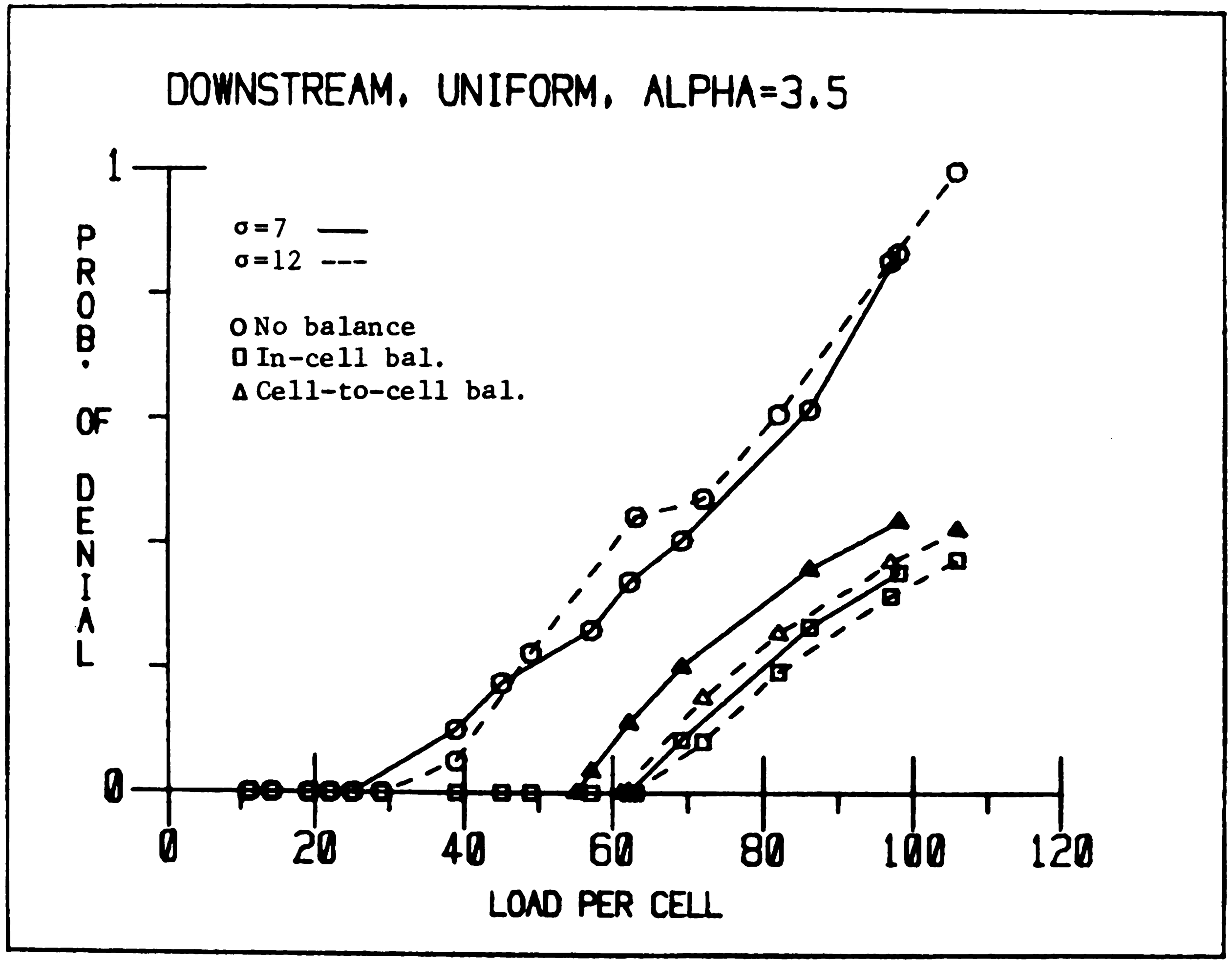

Figure 6.22 Denial statistics for the center cell, α = 3.5, uniform traffic distribution, downstream.

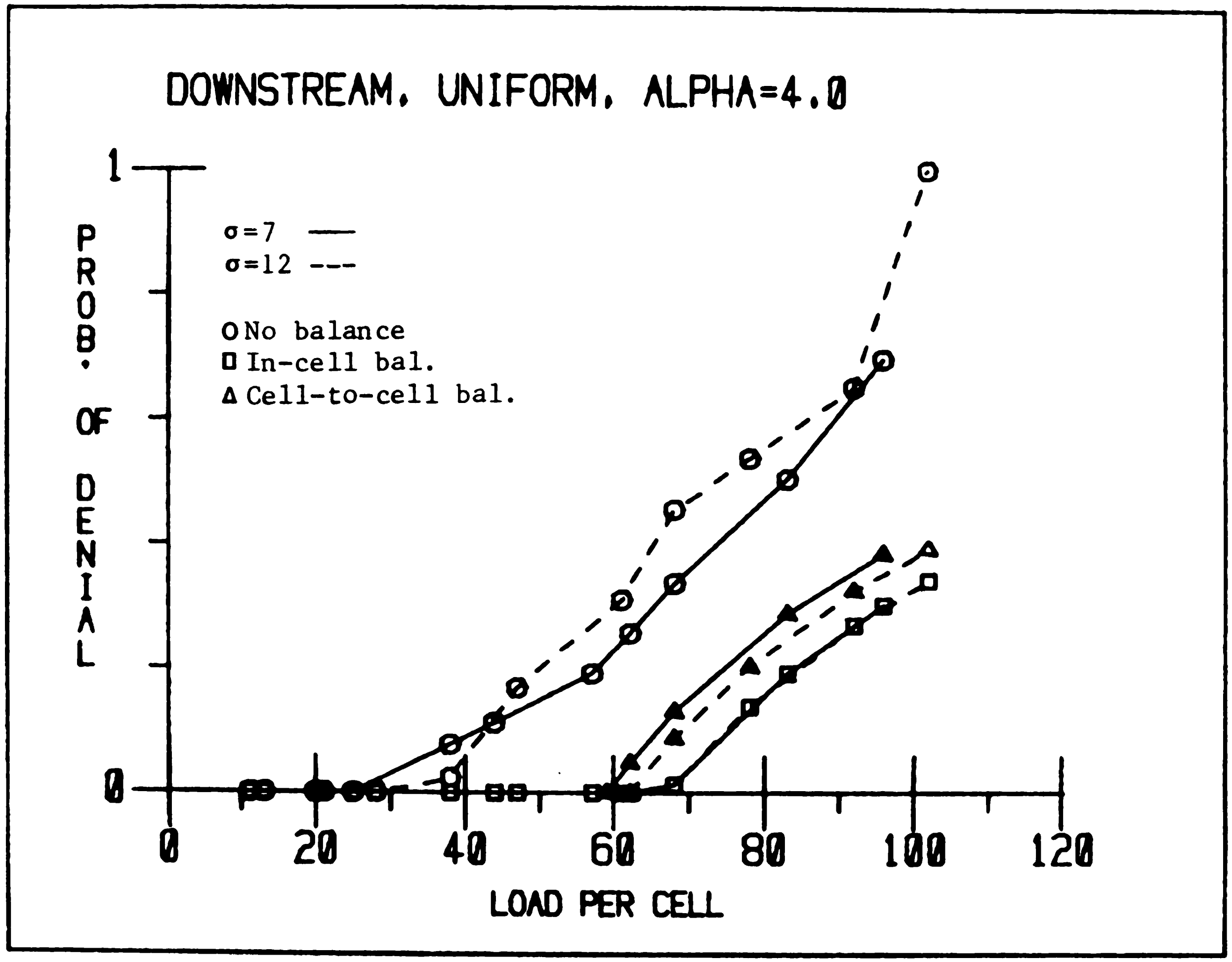

Figure 6.23 Denial statistics for the center cell, $\alpha = 4.0$, uniform traffic distribution, downstream.

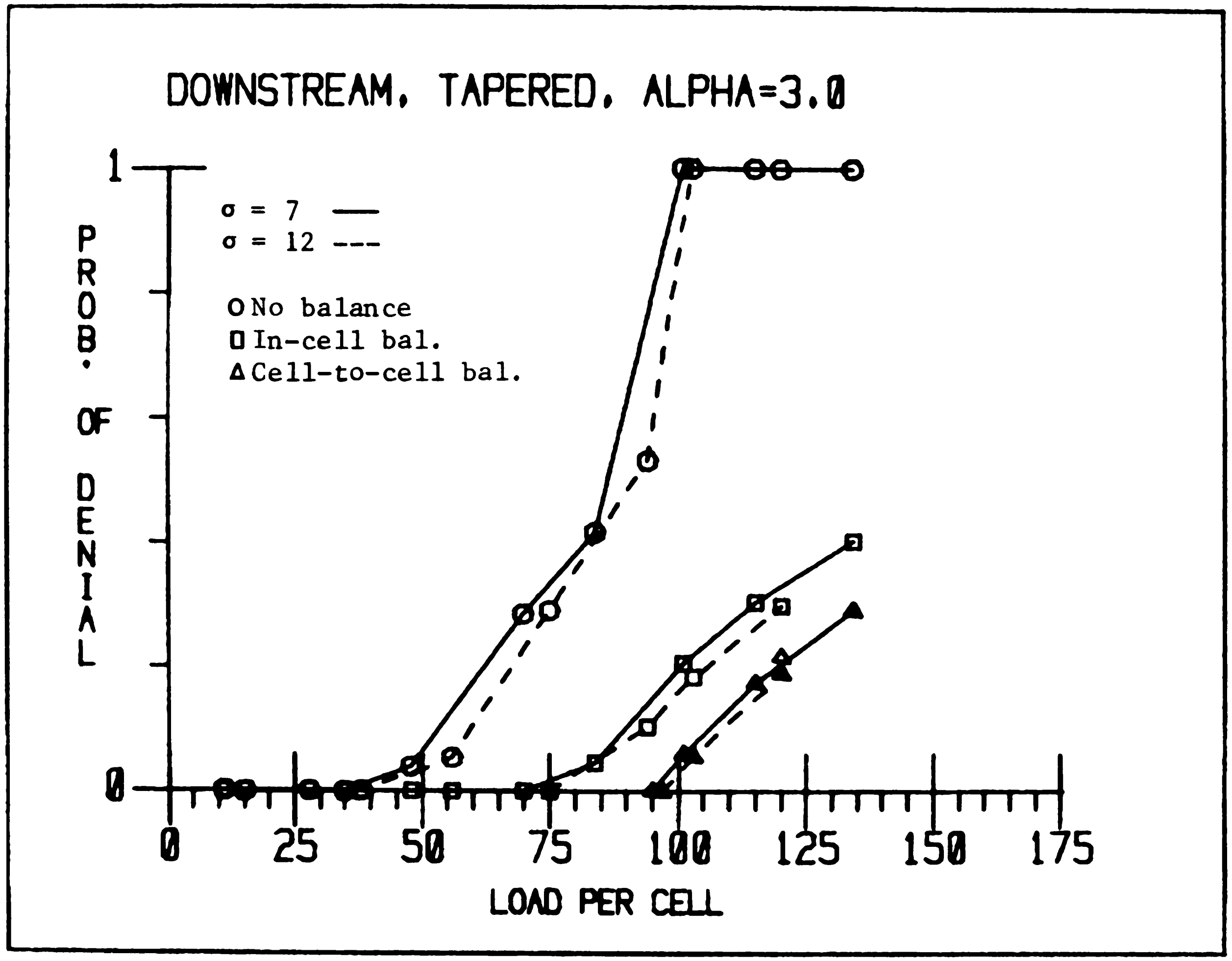

Figure 6.24 Denial statistics for the center cell, α = 3.0, tapered traffic distribution, downstream.

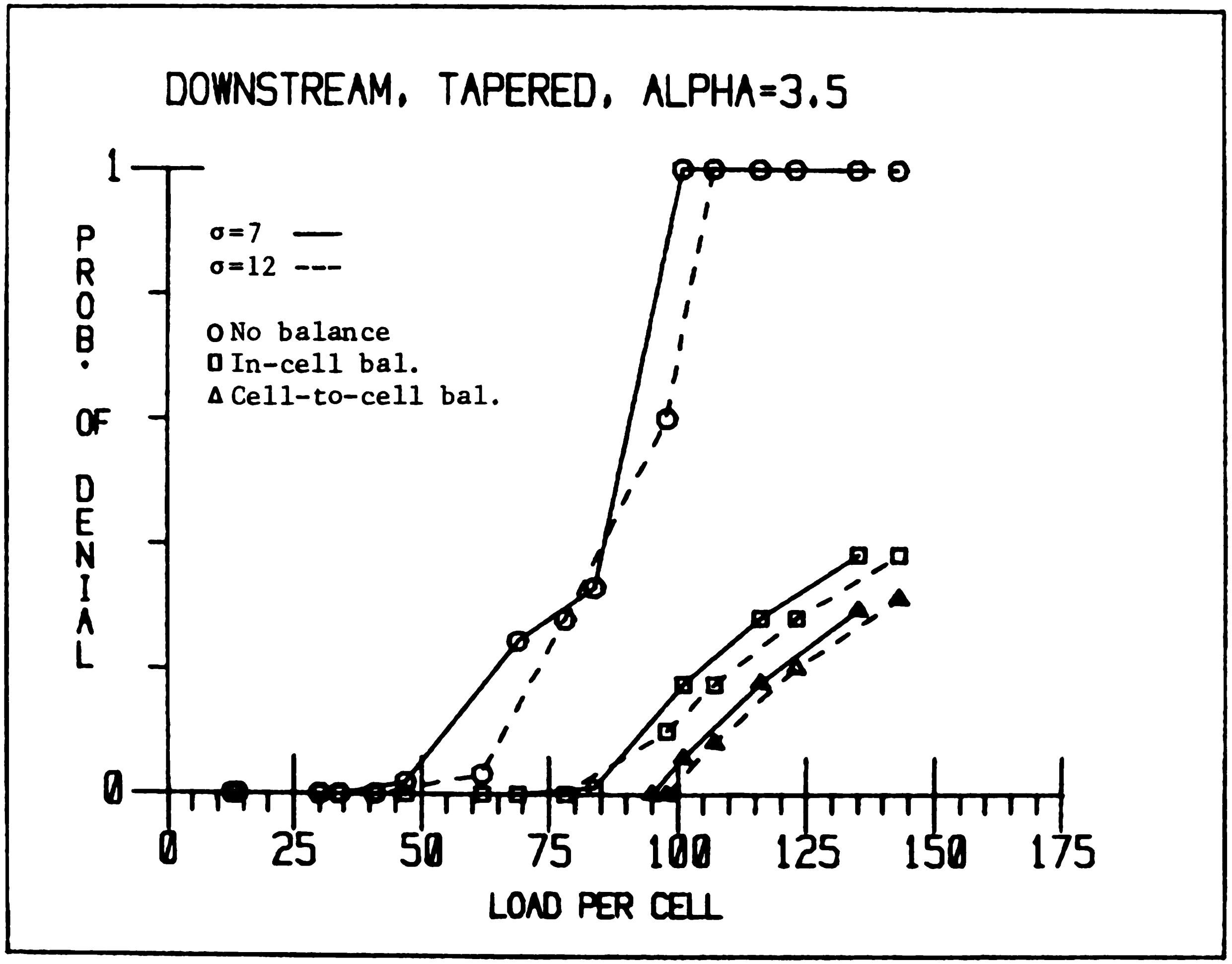

Figure 6.25 Denial statistics for the center cell, $\alpha = 3.5$, tapered traffic distribution, downstream.

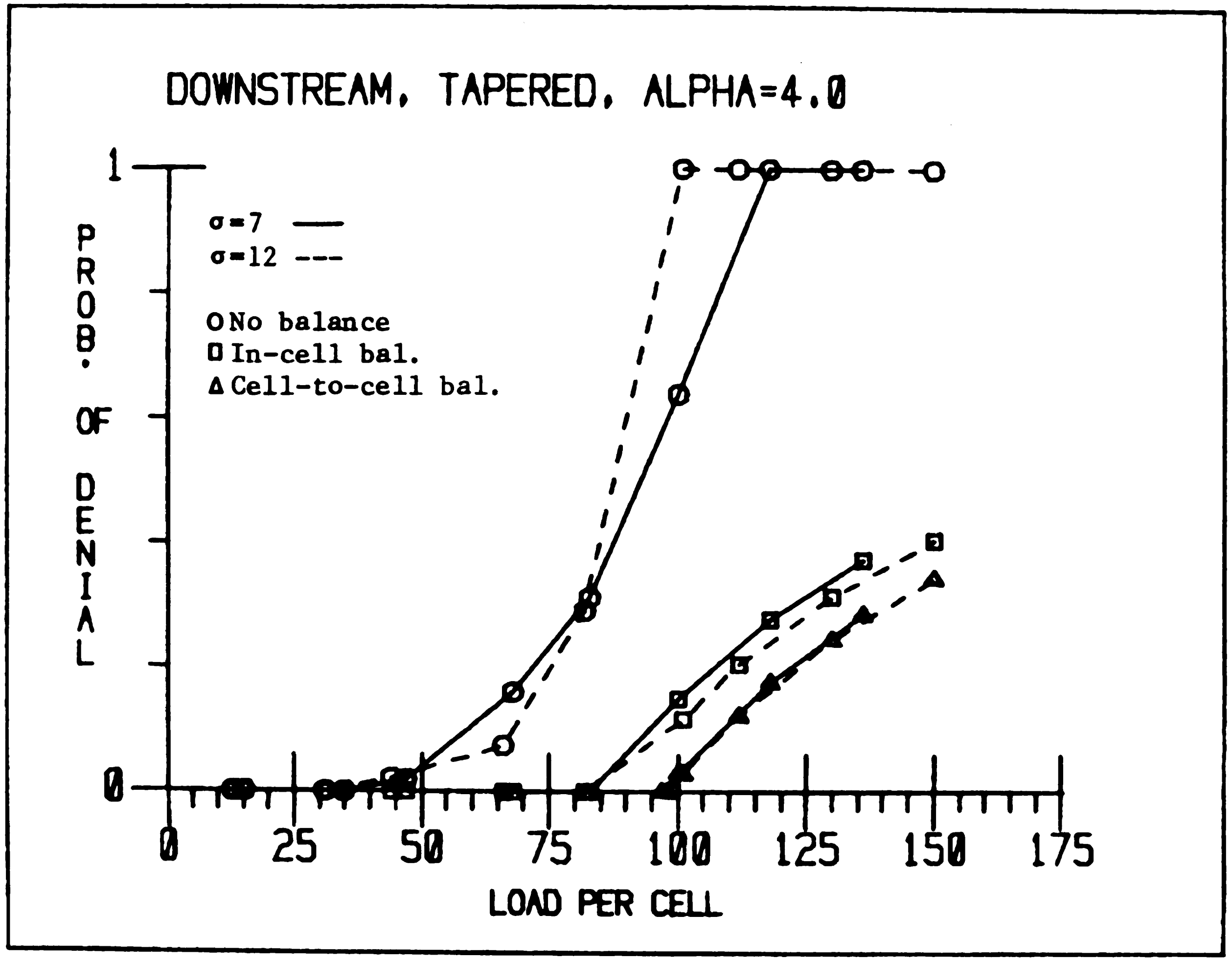

Figure 6.26 Denial statistics for the center cell, $\alpha = 4.0$, tapered traffic distribution, downstream.

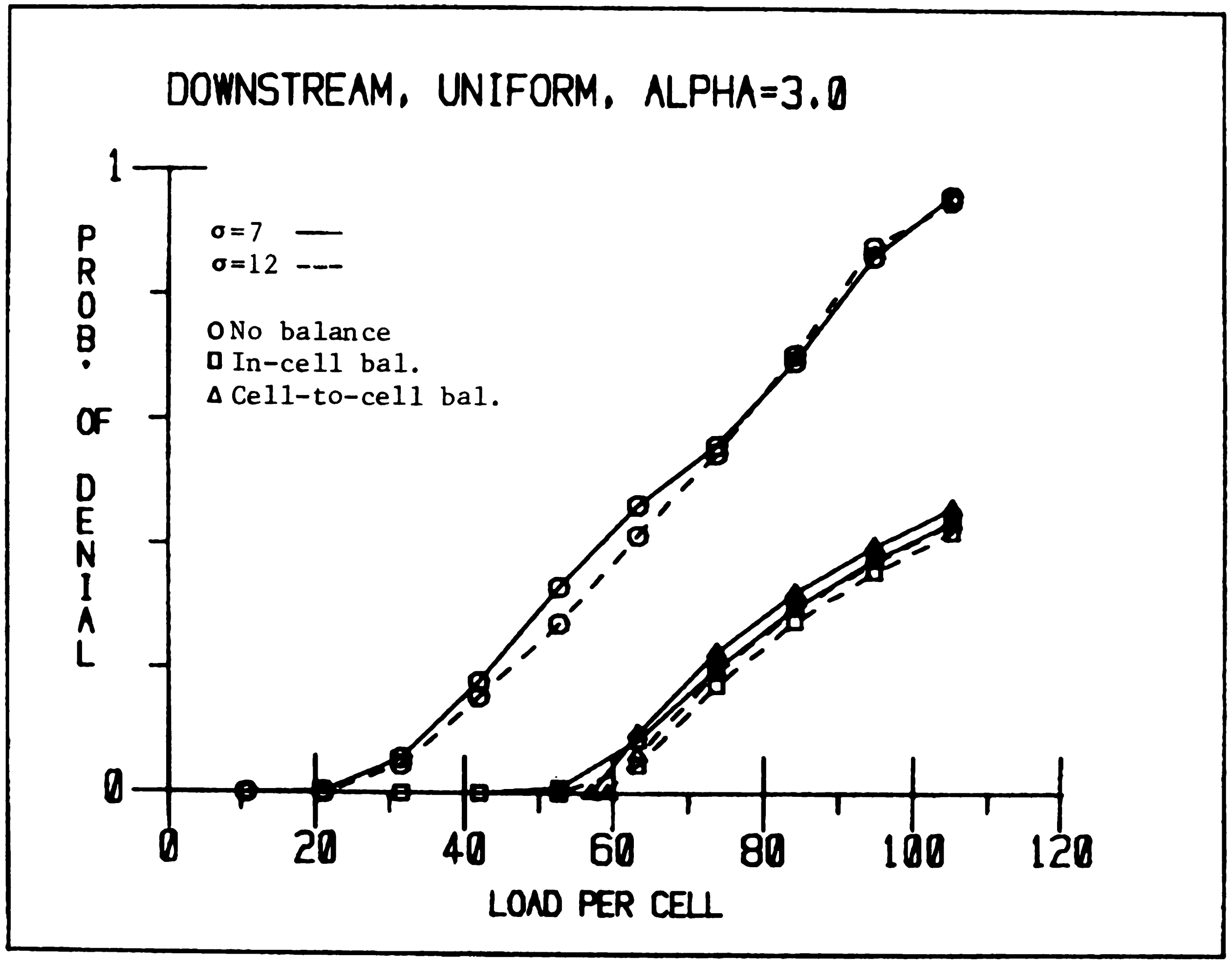

Figure 6.27 Denial statistics for the total system, α = 3.0, uniform traffic distribution, downstream.

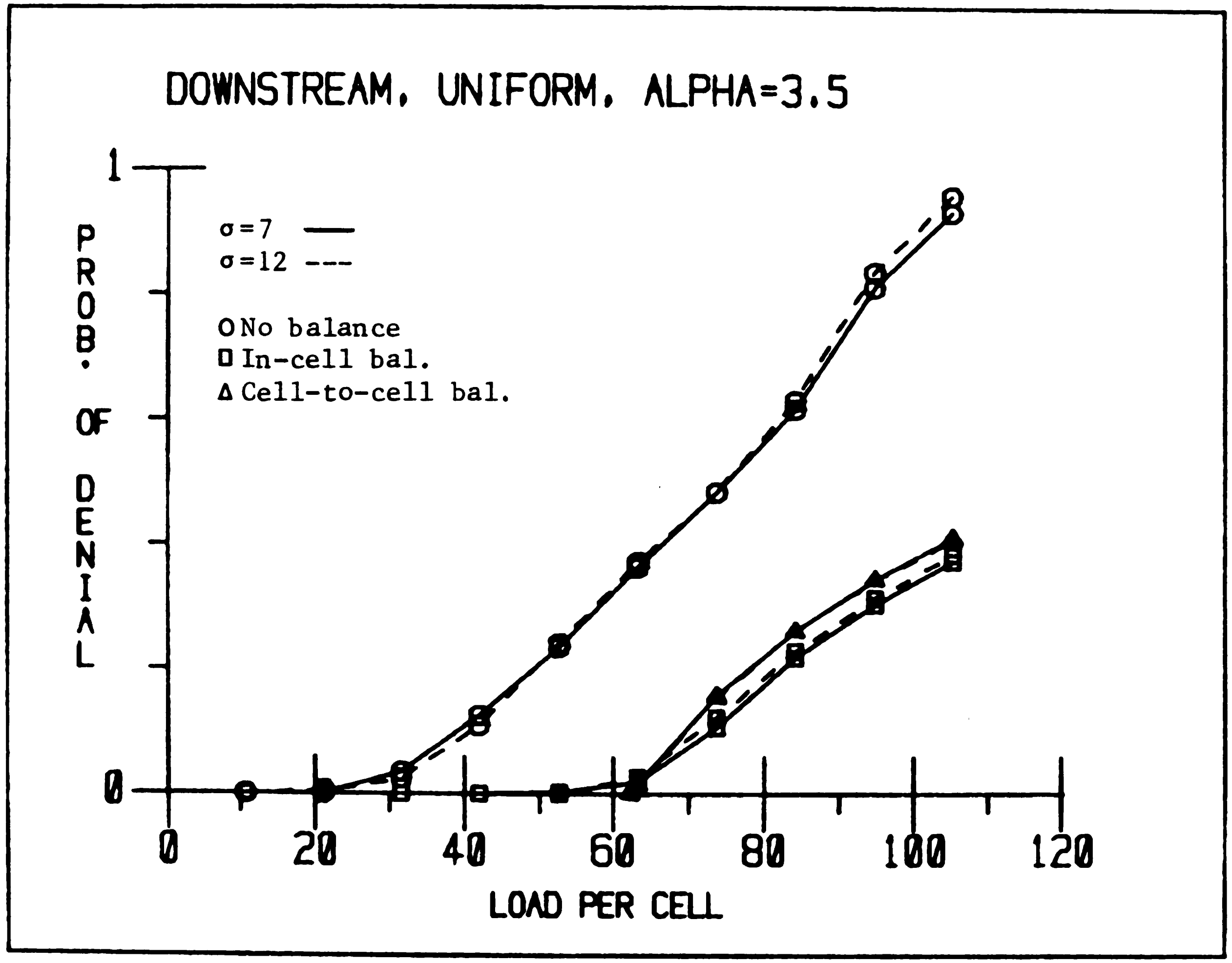

Figure 6.28 Denial statistics for the total system, $\alpha = 3.5$, uniform traffic distribution, downstream.

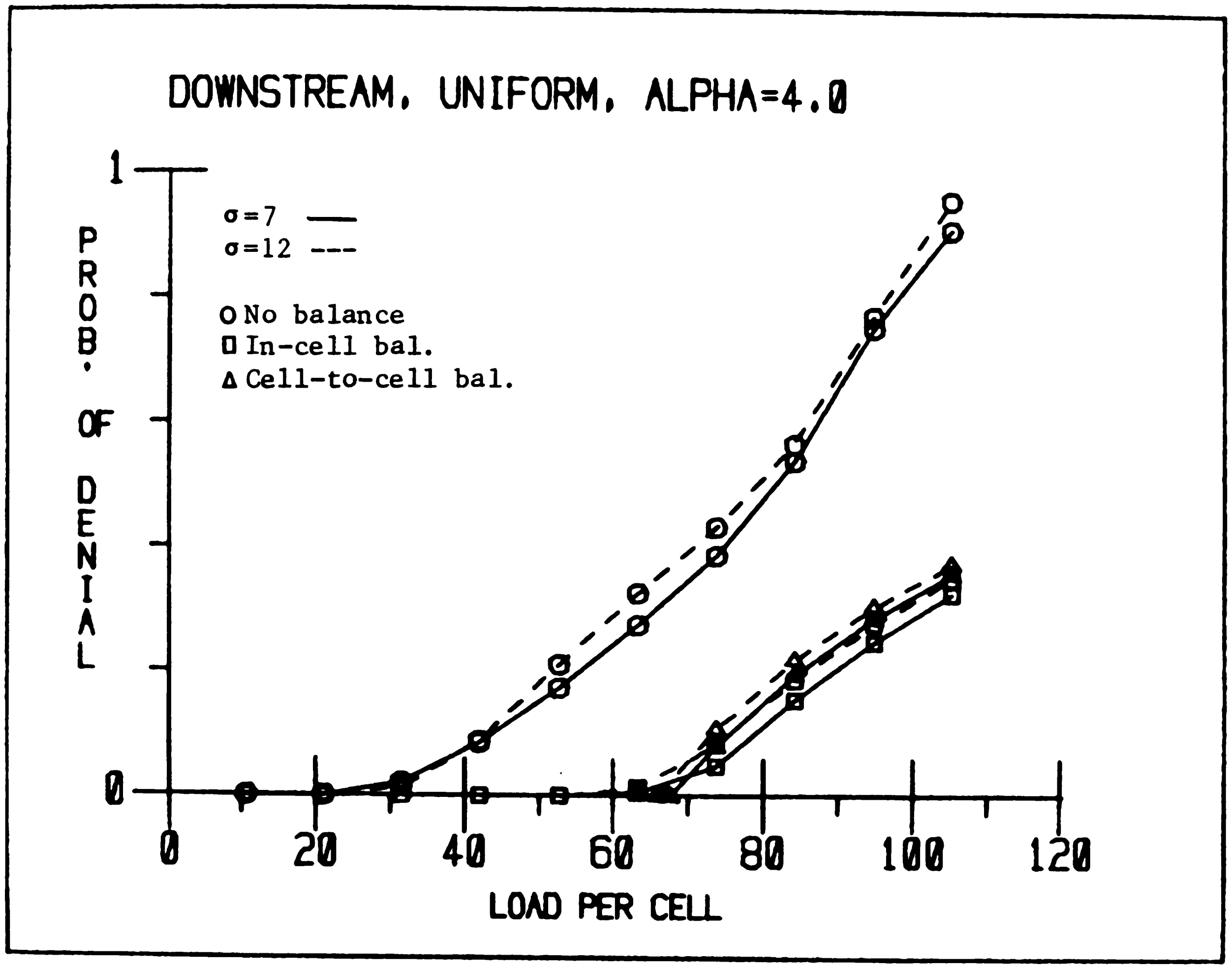

Figure 6.29 Denial statistics for the total system, $\alpha = 4.0$, uniform traffic distribution, downstream.

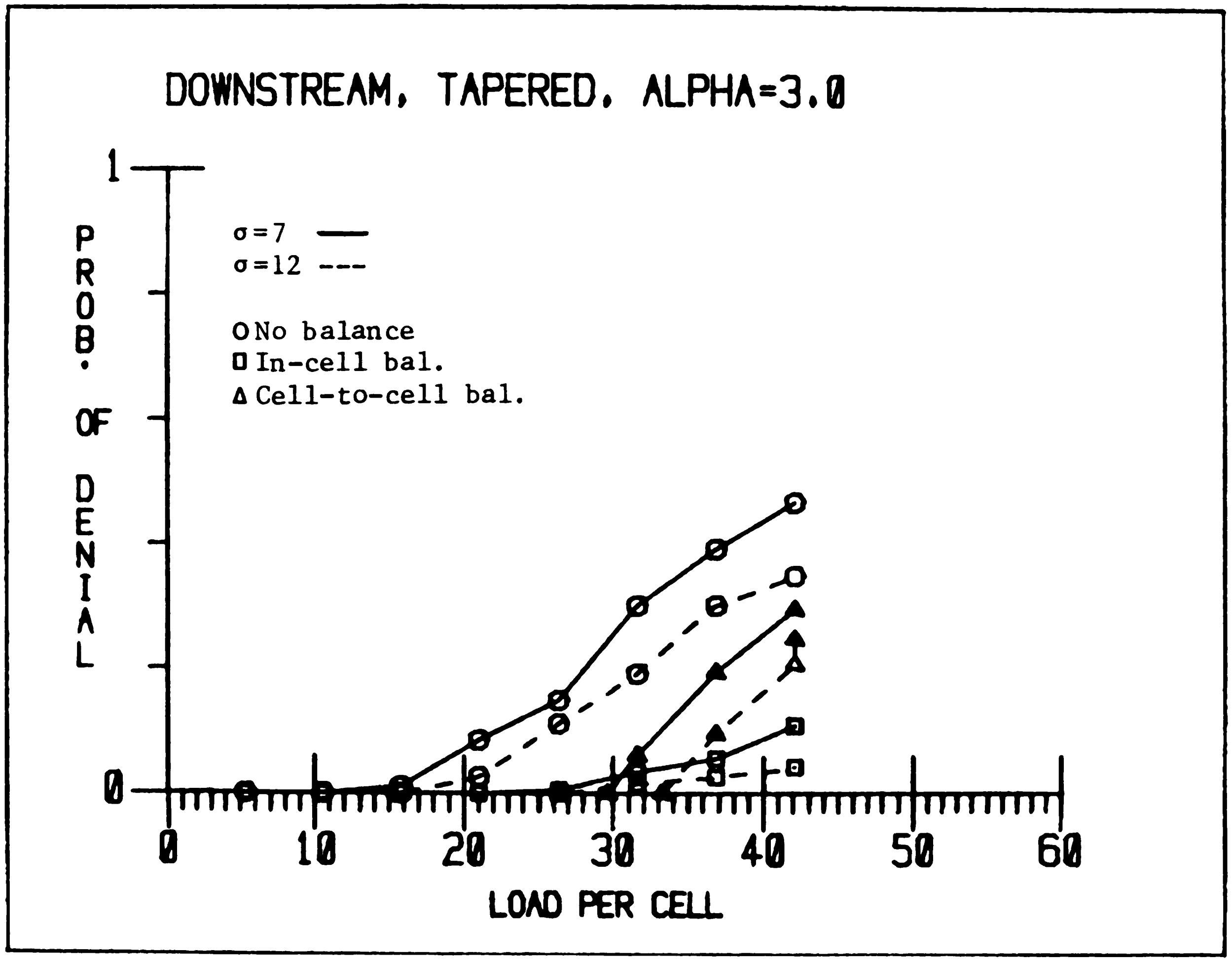

Figure 6.30 Denial statistics for the total system, $\alpha = 3.0$, tapered traffic distribution, downstream.

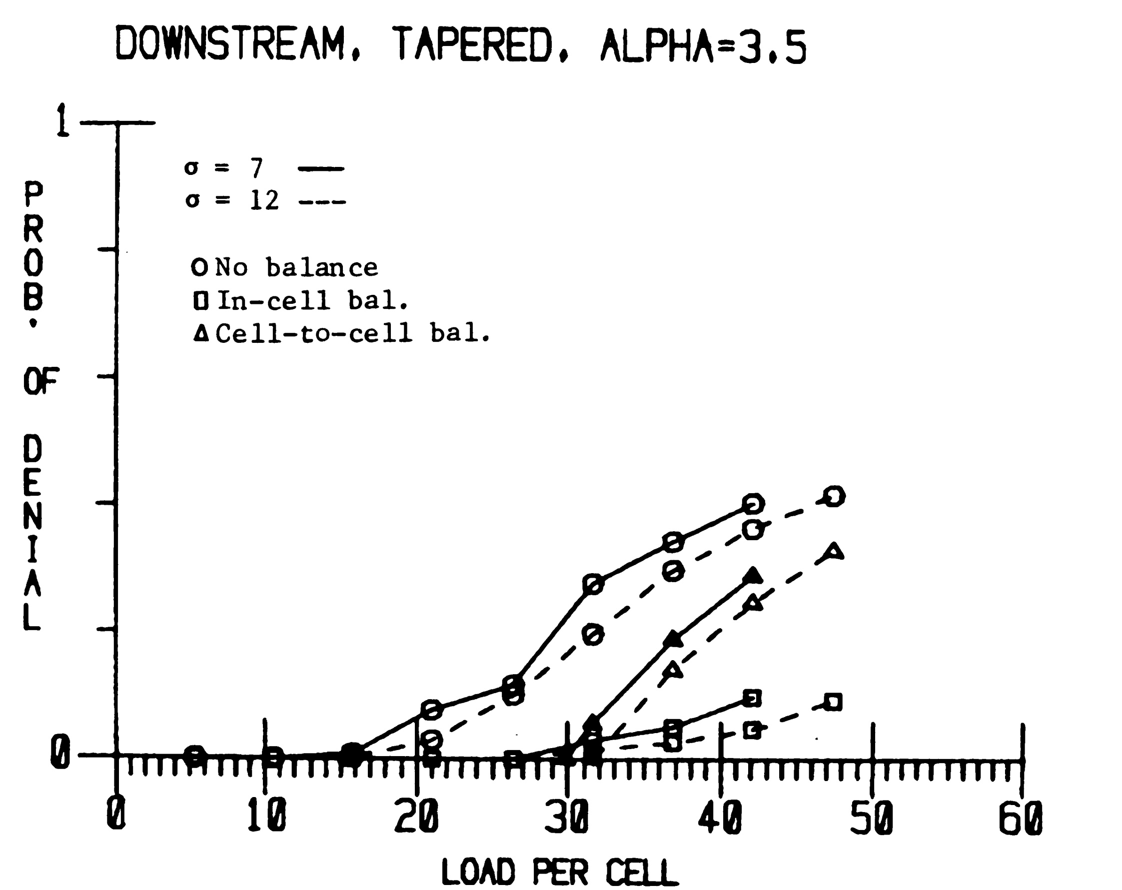

Figure 6.31 Denial statistics for the total system, $\alpha = 3.5$, tapered traffic distribution, downstream.

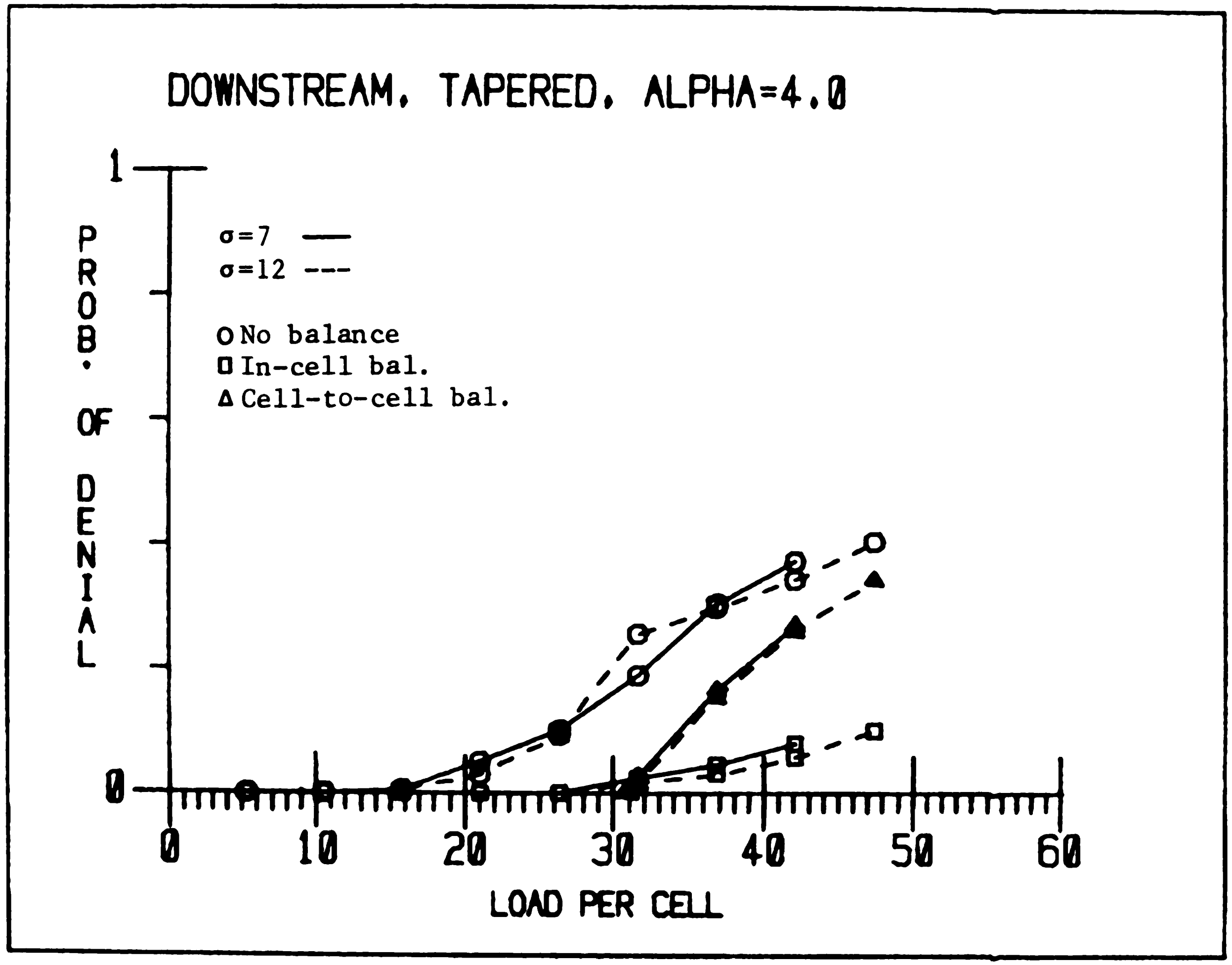

Figure 6.32 Denial statistics for the total system, α= 4.0, tapered traffic distribution, downstream.

contrary to the upstream case, the capacity of the system goes up as the value of α grows. This is because a more rapid attenuation law shrinks the size of the region near cell corners where the corner effect is manifested. This can be shown as follows: The "corner region" is the area in which a mobile receives about the same amount of power from several base stations (3 in the model with hexagonal cells.) Now if we consider a simplified model where there are only two cells in the system, a mobile located in the corner region receives about the same amount of power from the two base stations. Suppose a mobile is located at an effective distances of d_1^{ef} from one station and d_2^{ef} from the other. Also suppose that both of the base stations transmit an equal amount of power P. Then the corner region can be defined as an area in which

$$\left| \frac{P/(d_1^{ef})^\alpha}{P/(d_2^{ef})^\alpha} - 1 \right| \leq \epsilon, \tag{6-6}$$

where ϵ is small. Thus we have

$$(1-\epsilon)^{1/\alpha} \leq d_1^{ef}/d_2^{ef} \leq (1+\epsilon)^{1/\alpha}. \tag{6-7}$$

Now as grows, $(1 \pm \epsilon)^{1/\alpha}$ gets closer to 1; which means that for a larger α, d_1^{ef} and d_2^{ef} must be closer to each other so that the mobile can be considered to be located in the corner region. In other words, a larger shrinks the size of the corner regions.

Comparing the uniform case and the tapered case, when there is no balancing applied, the capacity of the system is higher for the uniform load case. It is also obvious that the tapered unbalanced case is more sensitive to variations in σ than the uniform case. When the total system is considered, the capacity for cases with $\sigma = 12$ is higher than cases with $\sigma = 7$ by up to 20%. This can be explained by the balancing effect due to an increase in σ explained in section 6.1. This effect causes the tapered case to resemble the uniform case more closely, when distribution of load in different cells is the determinning factor.

Considering the balanced case, results are identical for the upstream and downstream cases, when in-cell and cell-to-cell balancing are both applied. This is because, as was shown in chapter 4, the SIR's and thus the denial rates are the same for upstream and downstream cases when the system is fully balanced. For the uniform traffic distribution, the results of the two types of balancing are almost identical, as we found in the upstream case. Therefore in the uniform case there is almost no advantage in applying the cell-to-cell balancing algorithm for both upstream and downstream links. The improvement achieved by in-cell balancing, however, is considerable. We encountered improvements of 30% to more than 100% for the downstream case.

For the tapered traffic distribution, the upstream and downstream results are different with in-cell balancing only. Our results show improvement ratios over the non-balanced case of over 100% with in-cell balancing and a further 15% when cell-to-cell balancing is added. This latter improvement is at all levels of denial probability for the center cell, and at low levels of denial rate for the total system. Also comparing the uniform load and the tapered load cases, when full power control is applied, the capacity of the system is much higher for the uniform load than for a tapered one if the total system is considered. In the tapered case, when only in-cell balancing is applied, this higher denial rate does not increase as rapidly as the case with cell-to-cell balancing; and as load goes up, it gets closer to the denial rates of the uniform case. This effect which was also observed in the upstream case, is caused by the "matching effect" of the cell-to-cell balancing and the capacity sacrifice that it causes for the cells with lower loads.

In the balanced system, the effect of variations of α on the denial rates of the downstream link is very similar to the upstream case. As α decreases from 4 to 3 the difference is very small and not more than 15%. The absence of sensitivity to the variations of σ is noticeable in the downstream, balanced case also.

Improvements of up to 20% are observed as σ varies from 7 to 12. This is due to the balancing effect of the increase in α/σ ratio on the load distribution, as previously discussed.

6.3.2 *Dynamic Ranges of Transmitted Powers*

Figures 6.33 to 6.38 show the average dynamic range of powers (DRP^D) required for the transmitted signals to the mobiles, in order to achieve balance in the downstream case. Contrary to the upstream case, these ranges are different for the cases where only in-cell balancing is applied, and cases where cell-to-cell balancing is also applied. Results show that the downstream ranges are quite reasonable in terms of hardware realizability. This is because the corner effect is not a very severe effect and can easily be compensated by transmitting a few dB more power to the mobiles at the corners. For example a mobile that is located near the corner of three cells and receiving the same amount of power from 3 base stations, suffers three times as much interference as a mobile near one of the base stations. Therefore the strength of the signal transmitted to this mobile must be larger by a factor of 3 (about 5 dB.) Table 6.3 shows the required DRP^D values at full system capacity.

The results for the case where only in-cell balancing

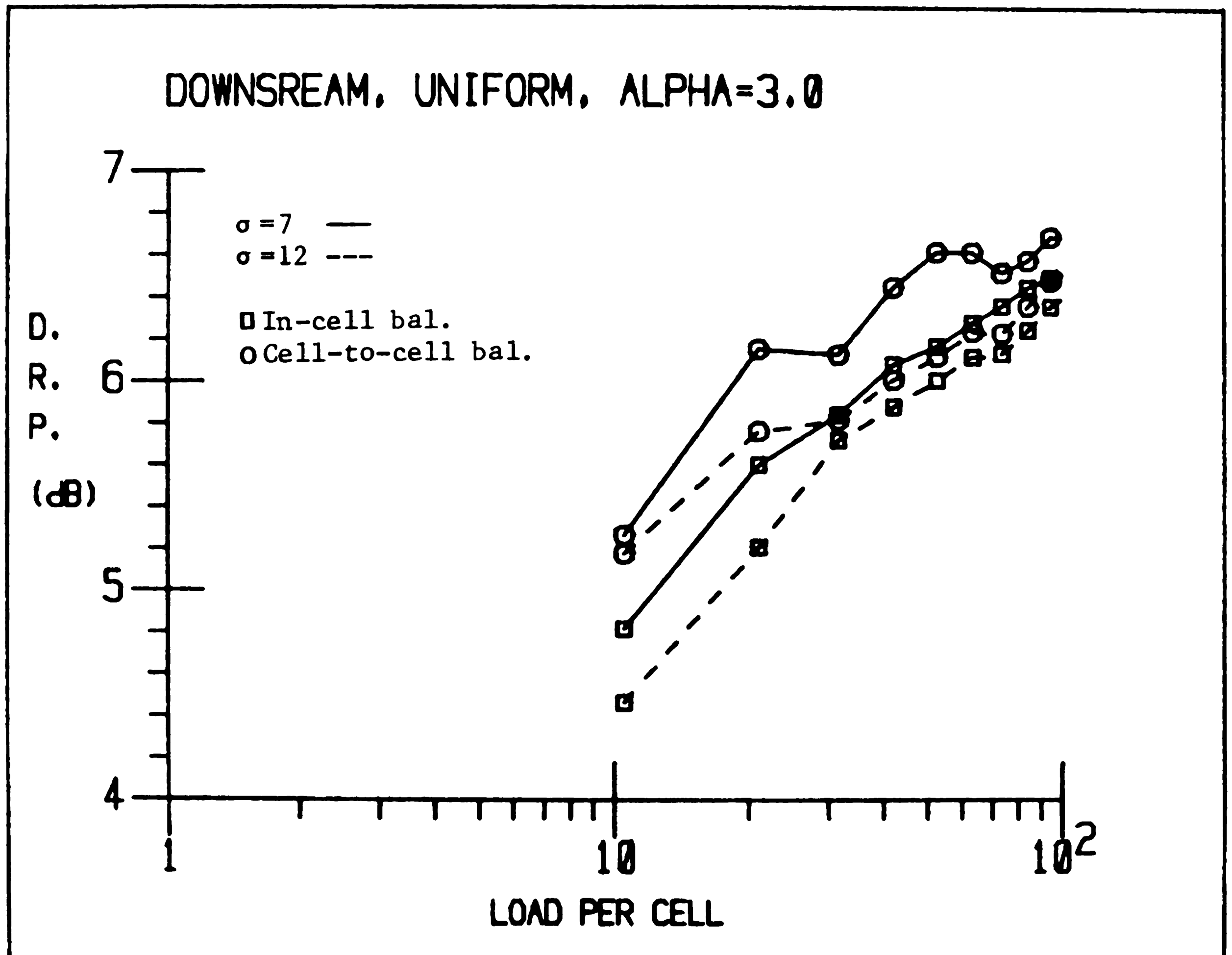

Figure 6.33 Average power control dynamic ranges required for downstream link balance, α=3.0, uniform traffic.

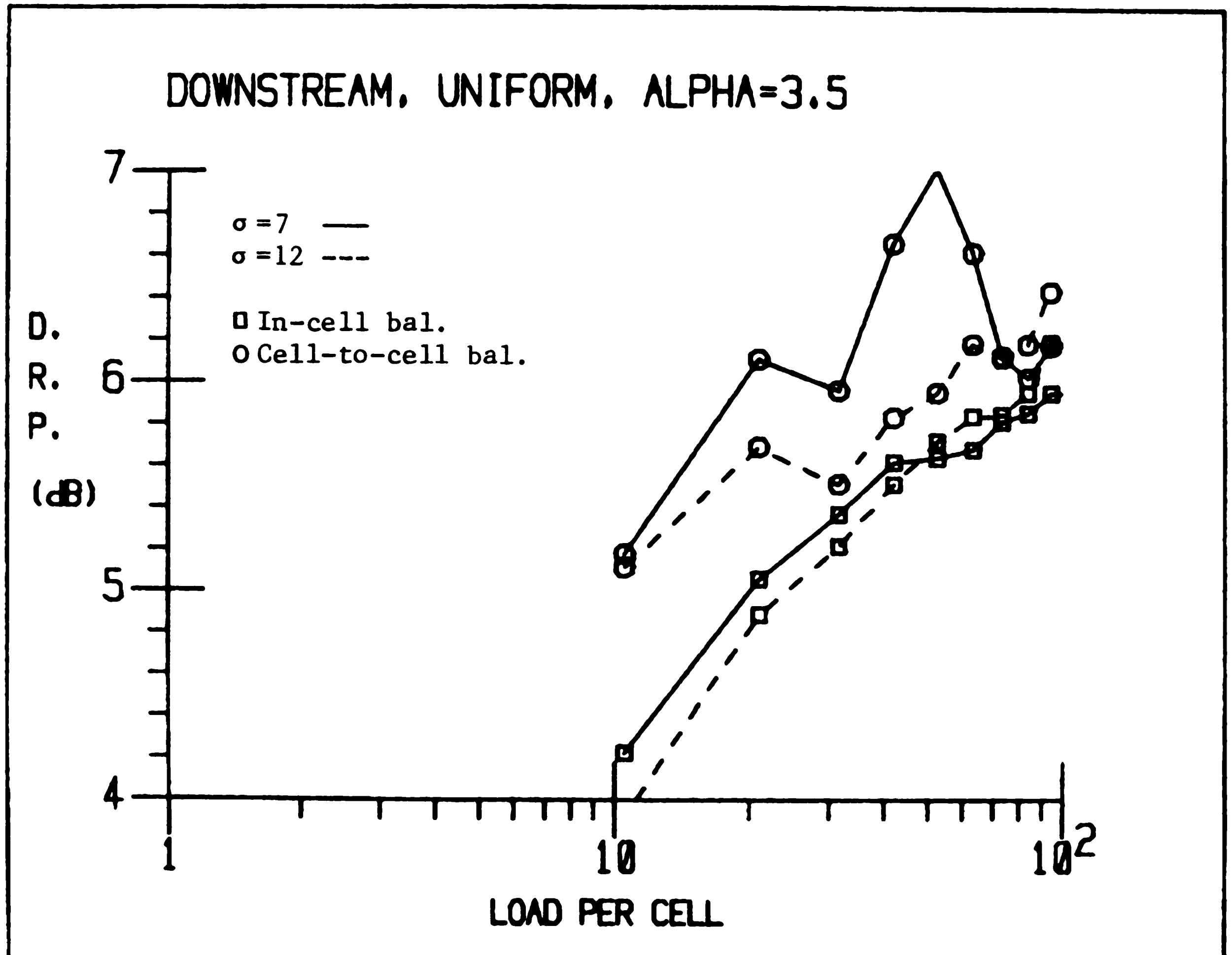

Figure 6.34 Average power control dynamic ranges required for downstream link balance, $\alpha=3.5$, uniform traffic.

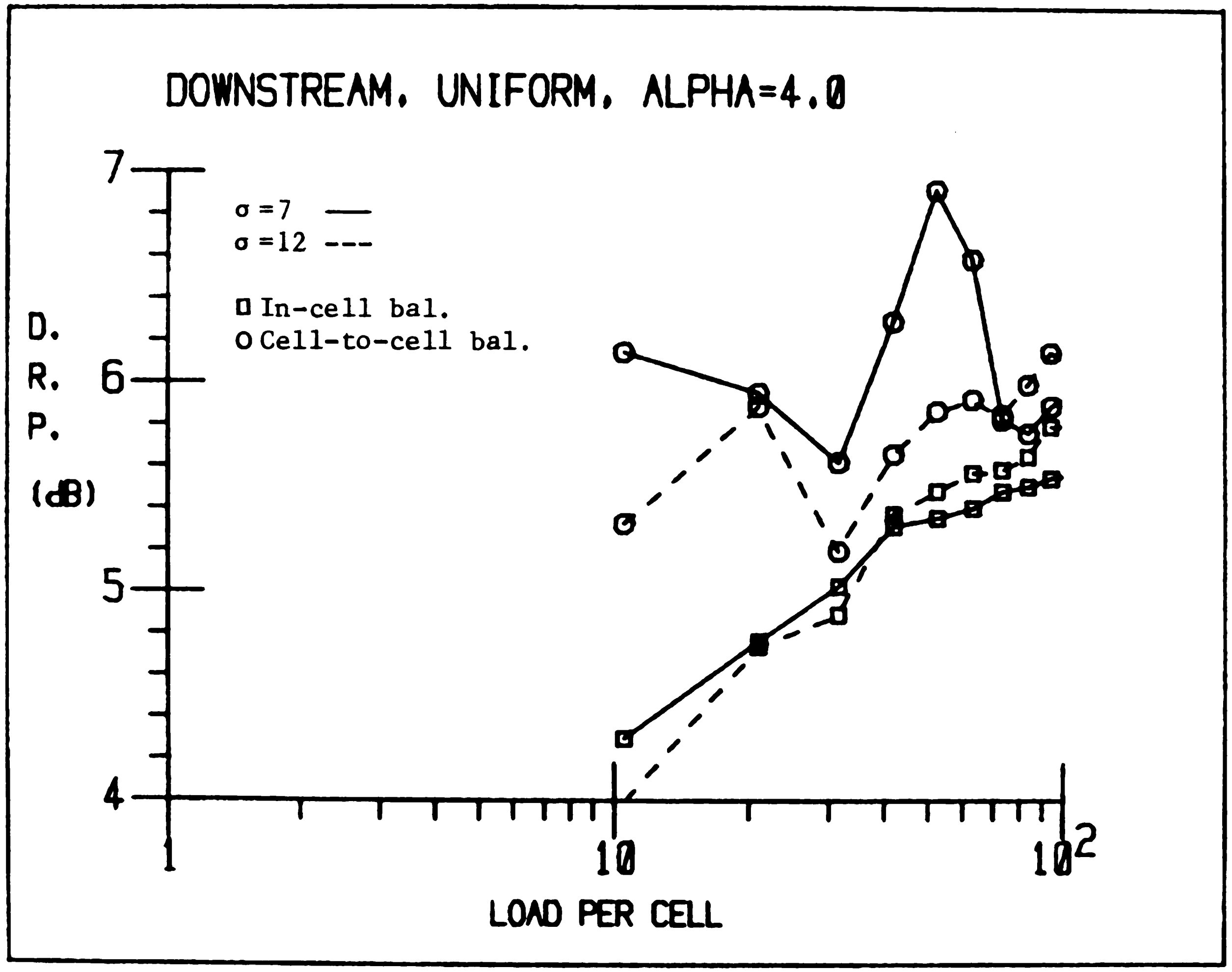

Figure 6.35 Average power control dynamic ranges required for downstream link balance, α=4.0, uniform traffic.

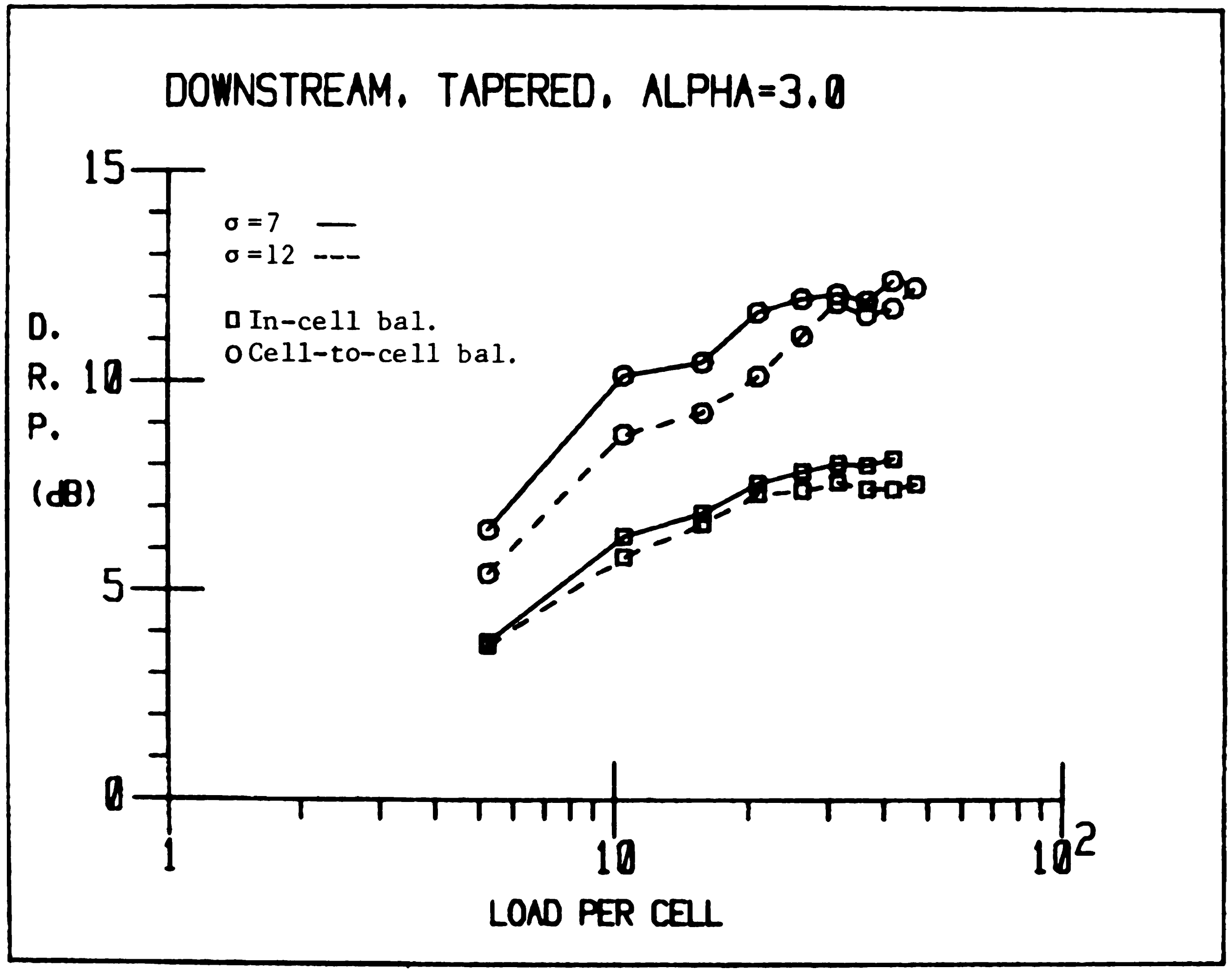

Figure 6.36 Average power control dynamic ranges required for downstream link balance, α=3.0, tapered traffic.

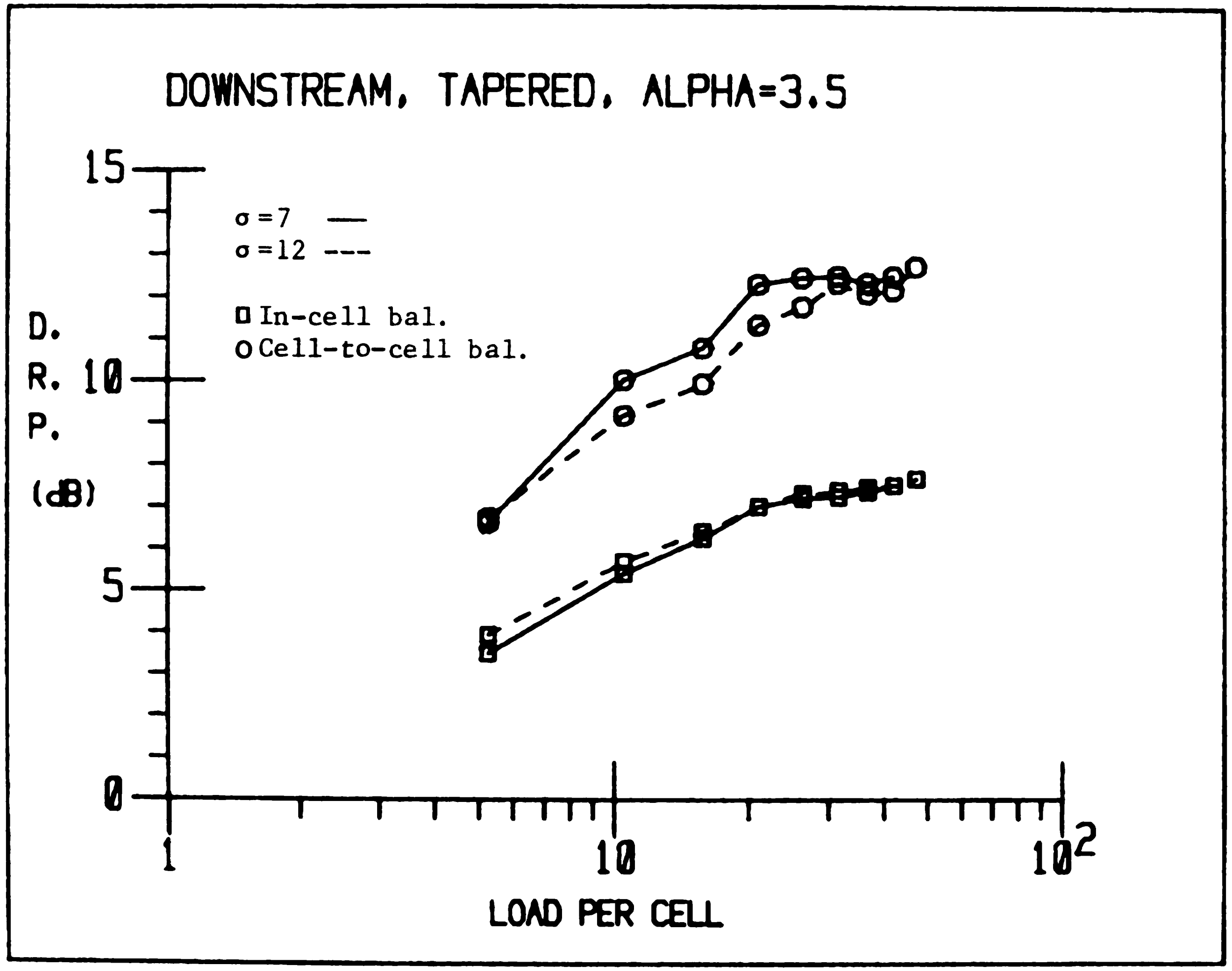

Figure 6.37 Average power control dynamic ranges required for downstream link balance, α=3.5, tapered traffic.

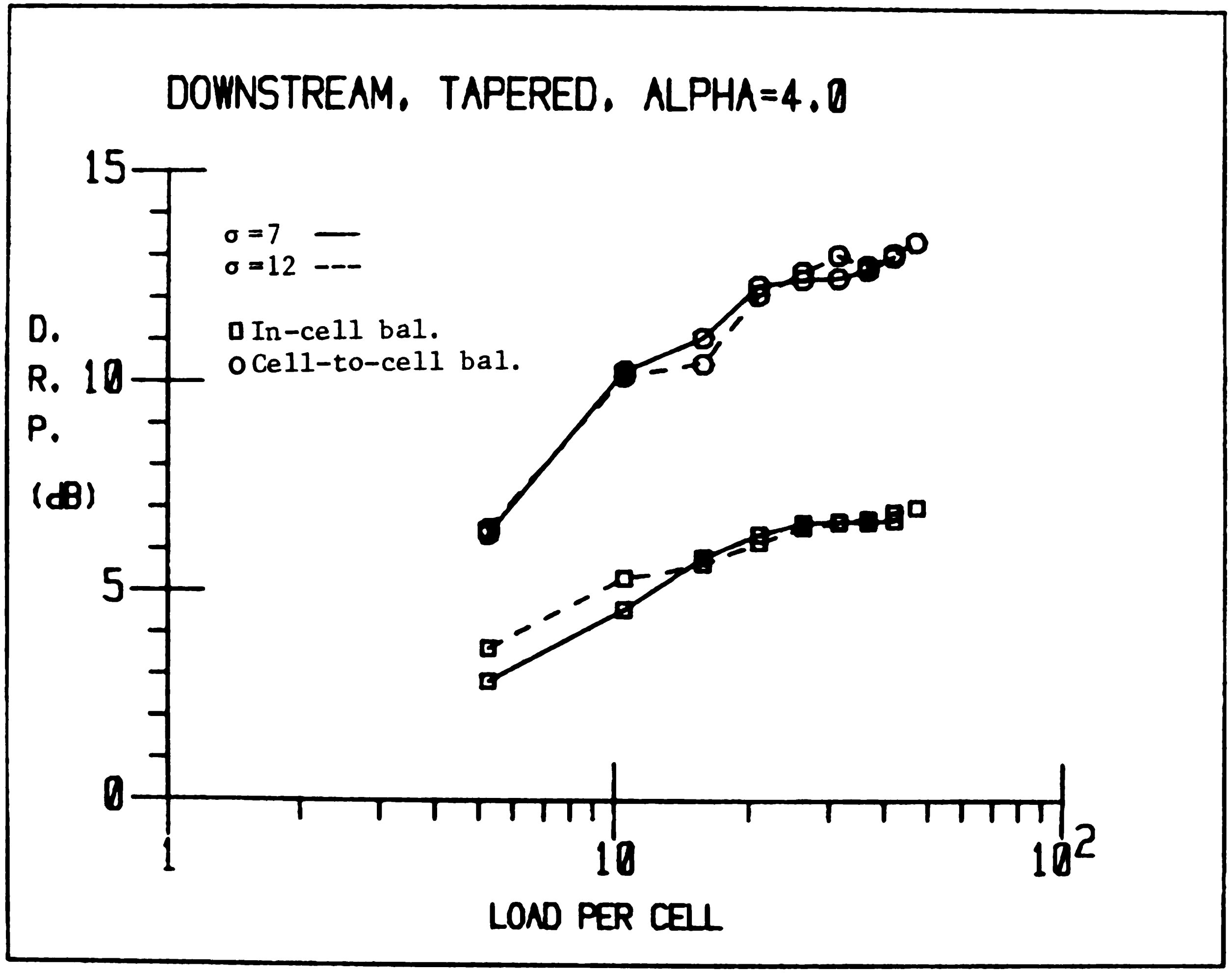

Figure 6.38 Average power control dynamic ranges required for downstream link balance, α=4.0, tapered traffic.

Table 6.3 Power control dynamic ranges required at full system capacity for the downstream link.

		UNIFORM		TAPERED	
		$\sigma=7$	$\sigma=12$	$\sigma=7$	$\sigma=12$
IN CELL	$\alpha=3$	6.2 dB	6.0 dB	7.9 dB	7.6 dB
	$\alpha=3.5$	5.65 dB	5.7 dB	7.2 dB	7.4 dB
	$\alpha=4$	5.4 dB	5.5 dB	6.7 dB	6.75 dB
CELL TO CELL	$\alpha=3$	6.6 dB	6.1 dB	12.0 dB	11.8 dB
	$\alpha=3.5$	6.9 dB	6.0 dB	12.4 dB	12.35dB
	$\alpha=4$	5.7 dB	5.9 dB	12.5 dB	13.1 dB

was applied are very close to 5 dB. The reason they go slightly above this value at higher loads is due to the fact that loads are not perfectly uniform from cell to cell and many corner mobiles may suffer more interference than the corner mobile in the above example, especially in the tapered traffic distributions. This non-uniformity becomes more noticeable when cell-to-cell balancing is applied also. In that case, the base stations in cells with heavier loads, transmit even more power per user and thus make the system less uniform as far as power transmissions are concerned. Thus a mobile located in a corner of a lightly loaded cell, neighboring one or two heavily loaded cells, needs a signal strength of much more than 5 dB higher than a mobile near the base station. This is the reason we see higher dynamic ranges when cell-to-cell balancing is applied.

Comparing the results for different values of α, the ranges go down slightly as α grows, when only in-cell balancing is applied. This is because the corner regions shrink as α gets larger. When cell-to-cell balancing is applied, however, the system becomes less sensitive to variations in α. Results also show very little sensitivity to variations in the value of σ, for the dynamic ranges.

6.4. *Signal-to-Interference Ratio*

Figures 6.39 to 6.41 show the decline of SIR in the cell-to-cell balanced system as the system average traffic load per cell grows. Results are given for both uniform and tapered distributions. The SIR values are of course the same for both the upstream and downstream cases, when cell-to-cell balancing is applied. These curves illustrate the principle of "graceful degradation" with increasing load, for which spread-spectrum systems are famous. We note that variations in the values of α and σ make very little difference to these results. Load distribution, however, has a significant effect on these values. A uniform load throughout the system results in higher SIR values than the tapered load. A difference of about 3 dB is observed for the two load distributions.

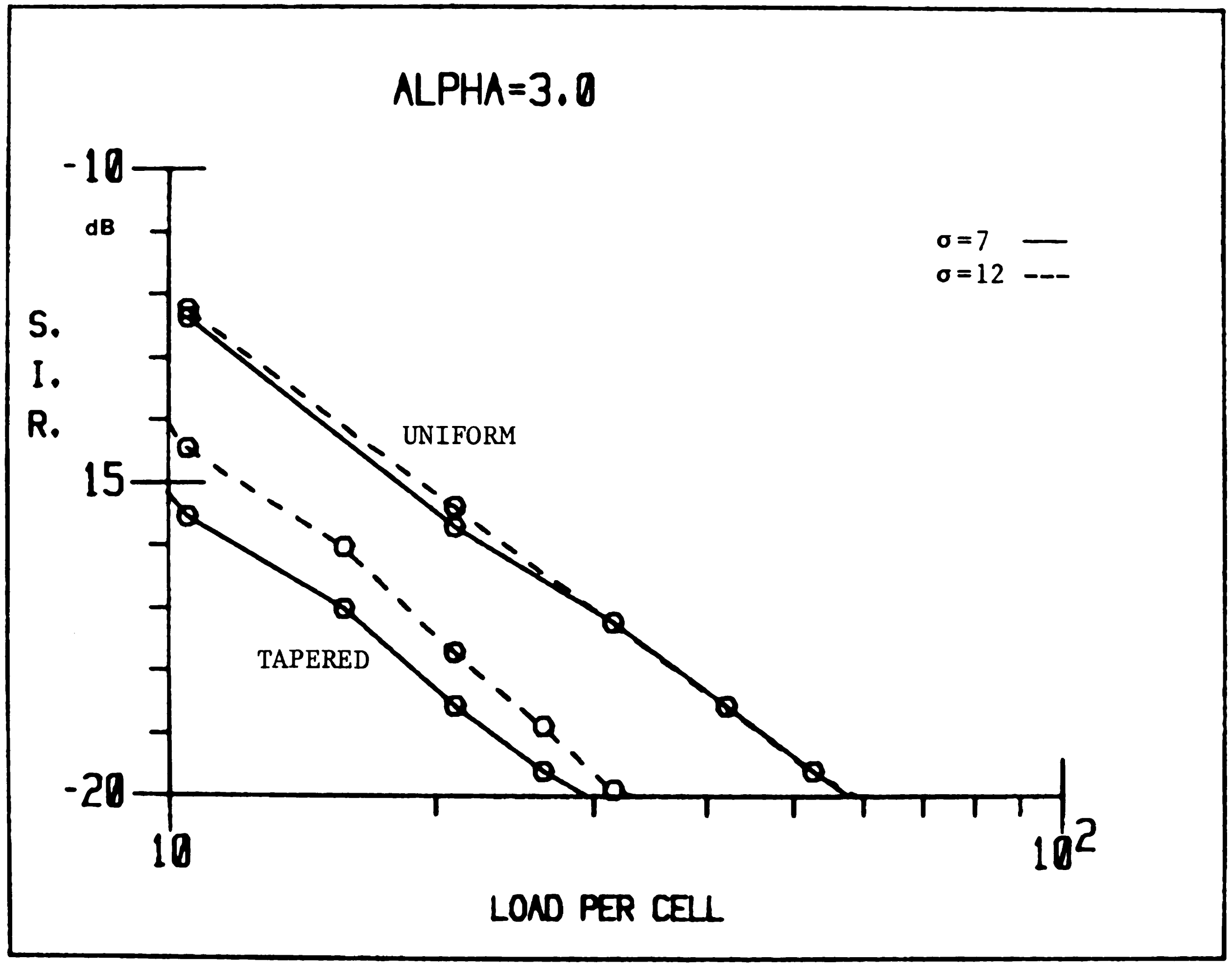

Figure 6.39 SIR versus average load per cell, α=3.0.

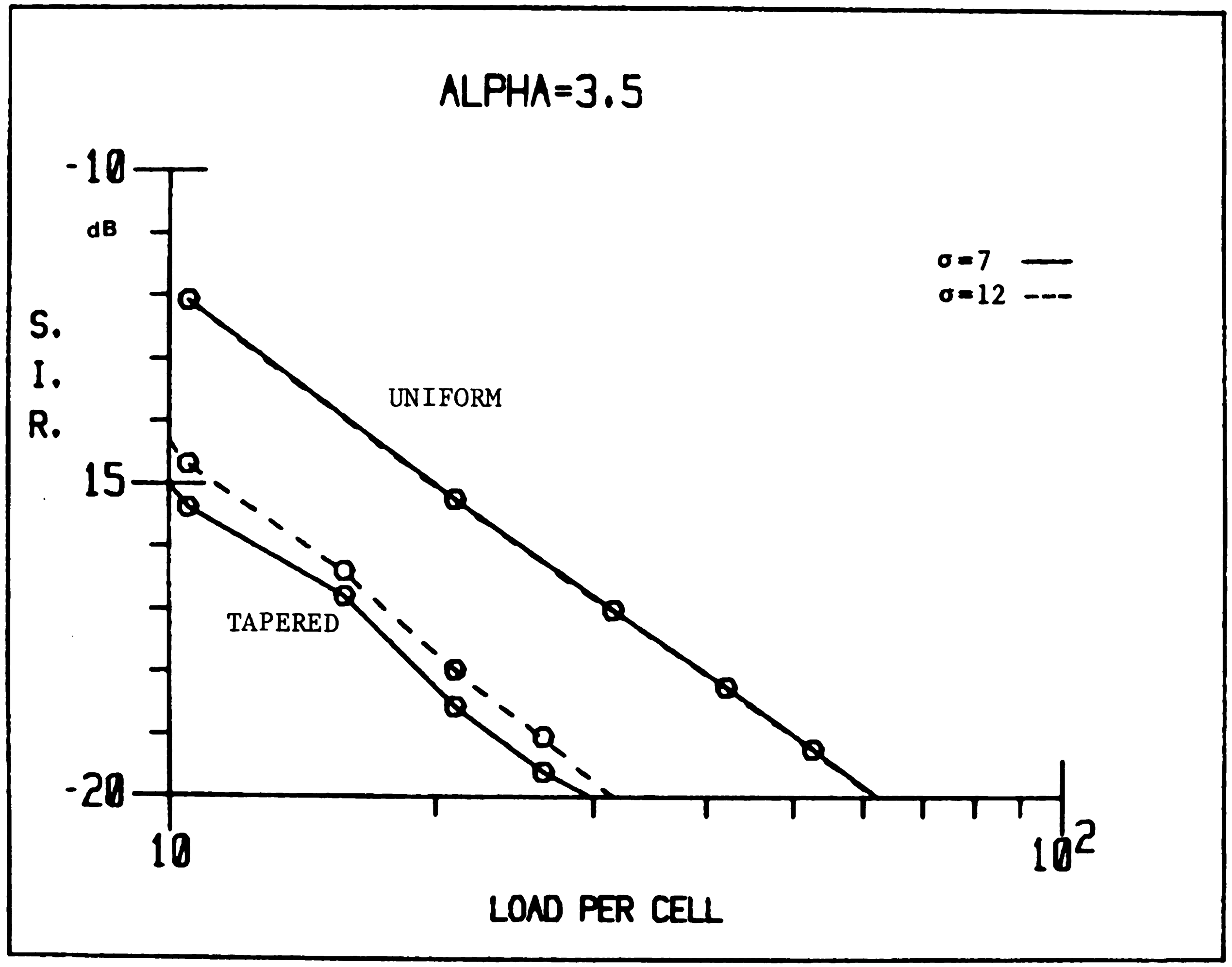

Figure 6.40 SIR versus average load per cell, α=3.5.

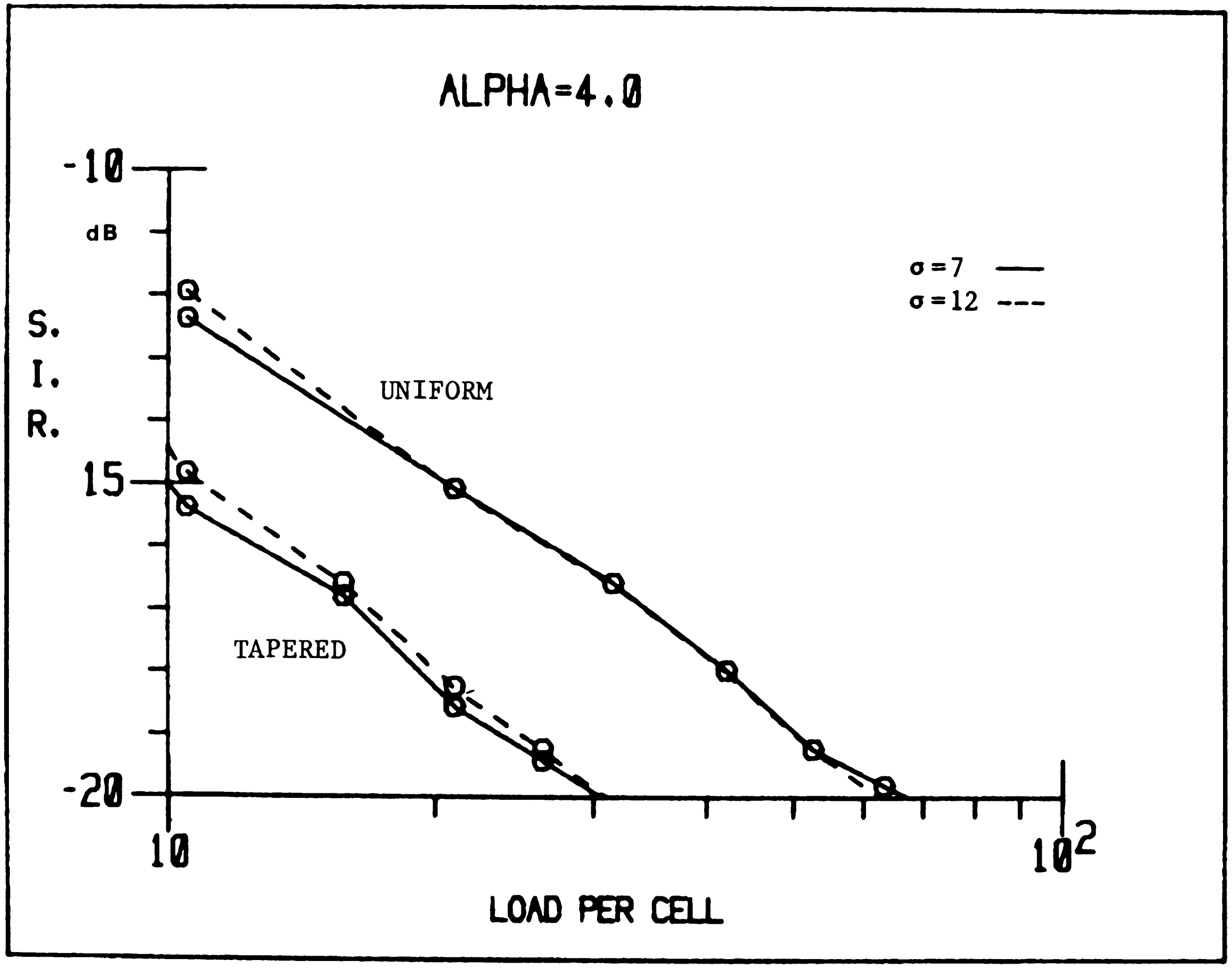

Figure 6.41 SIR versus average load per cell, α=4.0.

CHAPTER 7

CONCLUDING REMARKS

7.1 Conclusions

This work has presented analysis and simulation results of a power control system for spread-spectrum cellular mobile radio. We conclude that in-cell balancing is essential for satisfactory operation, and that cell-to-cell balancing may be desirable in cases where the traffic distribution is not uniform. Downstream balancing eliminates the so-called "corner-effect" and can easily be implemented with full dynamic range. Upstream balancing eliminates the so-called "near-far" effect, but probably can not be fully implemented. In our simulation the required dynamic range of transmitted powers by the mobiles took on values of more than 50 dB. This may be a difficult requirement to impose on a mobile transmitter.

This practical restriction provides a strong argument for the use of frequency-hopping modulation in such a system. Frequency-hopping is less sensitive to the near-far effect and thus when it is used, a power control scheme with a restricted dynamic range should operate nearly as well as one with full range. In frequency-hopping modulation, hard limiters may also be employed to compensate a restricted dynamic range.

We observed that the capacity of the systems shows a remarkably small sensitivity to environmental parameters such as rate of attenuation with distance (α) and shadow-fading standard deviation (σ). The dynamic range, however, is effected by these parameters. Results show that a higher α or σ require a considerably higher dynamic range.

The ratio α/σ was shown to have much significance in the operation of the system. A smaller α/σ results in a higher uniformity in the traffic distribution from cell to cell. This results in a higher capacity for the system and lessens the need for application of the cell-to-cell balancing algorithm.

7.2 *Recommendations for Further Study*

The research reported here has answered some questions regarding the interference management of the

system, while raising more questions. We conclude by discussing briefly some of the most pressing questions that need to be answered.

7.2.1 Restricted Power Control

Results presented in chapter 6 suggested that it may be difficult to apply power control with full dynamic range in the upstream link. Further study of the system using a restricted dynamic range is required to examine its effectiveness and practicality. Data on the resultant "outage" probability should be generated. It is also desirable to compare different modulation techniques, when such a restriction is imposed. The best alternative seems to be a frequency hopped scheme employing hard limiters together with power control with a restricted range.

7.2.2 Fading Model

The interference analysis presented here relies on the assumption that the median attenuation in a mobile environment may be assumed to be independent of Rayleigh rapid fading. This assumption is only based on the filtering effect of the human hearing response on the rapid fluctuations of this fading. It is important however, to investigate the effects of rapid fading on the

performance of the receiver. At typical data rates, each deep fade may cause hundreds of bits to be lost. This may cause a disruption in the proper performance of the receiver, such as loss of synchronization. The degree of such disturbances may vary depending upon the structure of the receiver, and on the presence of burst-error correction coding. Thus any such investigation would have to be on particular receiver design.

7.2.3 Interference Modeling

It is assumed in our analysis that interference between users may be modeled as white noise. This assumption is a more valid one when direct-sequence signaling is used. More careful analysis however, is needed for frequency-hopped schemes.

LIST OF REFERENCES

LIST OF REFERENCES

A1] J. M. Aein.
"Power balancing in systems employing frequency reuse."
Comsat Technical Review Vol. 3:2, Fall 1975, pp. 277-299.

A2] Gaston A. Arredondo.
"On trial: Bell's HCMTC."
Telephony, July 18,1977, p. 21.

B1] V. E. Benes.
Mathematical Theory of Connecting Networks and Telephone Traffic.
Academic Press, 1965.

C1] George R. Cooper, Ray W. Nettleton and David P. Grybos.
"Cellular land-mobile radio: Why spread spectrum?"
IEEE Communication Magazine Vol. 17:2, March 1979, pp. 17-24

C2] George R. Cooper and Ray W. Nettleton.
"A spread-spectrum technique for high-capacity mobile communications."
IEEE Transactions of Vehicular Technology, Special Issue on Emerging 900 MHz Technologies, Vol. VT-27:4, pp. 264-275.

C3] George R. Cooper and Ray W. Nettleton.
"Cellular mobile technology: The great multiplier"
IEEE Spectrum Vol. 20:6, June 1983, pp. 30-37.

C4] George R. Cooper and Raymond W. Nettleton.
"A spread spectrum technique for high capacity mobile communications."
Record of the 27th Vehicular Technology Conference, IEEE, March 16-18, 1977, pp. 98-103.

C5] George R. Cooper and C. D. McGillem.
Probabilistic Methods of Signal and System Analysis.
Holt, Rinehart and Winston, Inc., 1971.

C6] George R. Cooper.
Private conversation.
Unpublished Results.

C7] J. P. Costas.
"Poisson, shannon and the radio amateur."
Proceedings of the IRE 47(12), December 1959, pp. 2058-2068.

C8] D. C. Cox.
"Co-channel interference considerations in frequency reuse small-coverage-area radio systems."
IEEE Transactions on Communications COM-30:1, Part II, January 1982.

D1] Germund Dahlquist and Ake Bjorck.
Numerical Methods, Section 5-8.
Prentice-Hall, 1974.

D2] R. C. Dixon.
Spread-Spectrum Techniques.
Wiley, 1976.

G1] F. R. Gantmacher.
The Theory of Matrices.
Chelsea, 1959.

H1] George H. Hagn, Guest Editor.
IEE Transactions on Electromagnetic Compatability.
Vol. EMC-19:3, Agust 1977. Special Issue on Spectrum Management

I1] Sadao Ito and Yasushi Matsuzaka.
"800 MHz band land mobile telephone system - Overall view."
Review of the Electrical Communication Laboratories 25(11-12), November-December, 1977. Reprinted in *IEEE Transactions on Vehicular Technology* VT-27(4), November 1978.

J1] W. C. Jakes, editor.
Microwave Mobile Communications.
Wiley, 1974.

K1] R. S. Kennedy.
Fading Dispersive Communications Channels.
Wiley, 1969.

M1] James B. Mikulski.
"A system plan for a 900-MHz portable radio telephone."
IEEE Transactions on Vehicular Technology VT-26(1), February 1977, pp. 76-81.

N1] Ray W. Nettleton.
Spectral Efficiency in Cellular Land-Mobile Communications: A Spread Spectrum Approach.
Ph.D. Thesis, Purdue University, October 1978. Thesis supervisor: George R. Cooper.

P1] J. H. Park and C. Chayavadhanangkur.
"Effect of fading on FM reception with cochannel interference."
IEEE Transactions on Aerospace and Electronic Systems AES-13(2), March 1977, pp. 127-132.

P2] David R. Peterson.
Interference Power Balancing for Multiple Access Communication Systems.
Ph.D. Thesis, Purdue University, May 1976. Thesis Supervisor: George R. Cooper.

P3] M. B. Pursley and D. V. Sarwate.
"Performance evaluation for phase-coded spread-spectrum multiple-access communication, parts I and II."
IEEE Transactions on Communications COM-25, pp. 795-803, 1977.

S1] Leonard Schiff.
"Traffic capacity of three types of common-user mobile radio communication systems."
IEEE Transactions on Communication Technology COM-18(1), February 1970, pp. 12-21.

S2] Harold Staras and Leonard Schiff.
"A dynamic space division multiplex mobile radio system."
IEEE Transactions on Vehicular Technology VT-19(2), May 1970, pp. 206-212.

S3] Morton Stern and Victor Graziano.
"A new portable and mobile radio telephone system goes to Washington (and Baltimore)."
Telephony, July 18, 1977, p. 26.

T1] George L. Turin.
"The effects of multipath and fading on the performance of direct-sequence CDMA systems."
To be published.

W1] C. Weber, G. Huth and B. Batson.
"Performance considerations of CDMA systems."
IEEE Transactions on Vehicular Technology VT-30:1, pp. 3-10, February 1981.

W2] Gareth Williams.
Computational Linear Algebra with Models, section 6-7.
Allyn and Bacon, Inc., 1978.

Y1] W. Rae Young, Guest Editor.
The Bell System Technical Journal Vol. 58:1, January 1979.
Special Issue on the Advanced Mobile Phone Service (AMPS).

MICHIGAN STATE UNIVERSITY LIBRARIES
3 1293 03056 0530